UNIVERSITY OF PÉCS

Biological and Sport Biological Doctoral School

Bat related viral zoonoses in Algeria

PhD Thesis

ZEGHBIB SAFIA

PÉCS, 2022

UNIVERSITY OF PÉCS

Biological and Sport Biological Doctoral School

Bat related viral zoonoses in Algeria

PhD Thesis

Zeghbib Safia

Supervisor:

Prof. Dr. Ferenc Jakab
PhD, habil

Supervisor Leader of the doctoral school

PÉCS, 2022

Table of contents

Abbreviations

INFs – Interferons

ISGs – **interferon-stimulated** genes

HSPs – heat-shock proteins

STING – Stimulator of interferon genes

NiV – Nipah virus

SARS – severe acute respiratory syndrome

MERS – Middle East Respiratory Syndrome

SARS-CoV-2 – Severe Acute Respiratory Syndrome Coronavirus 2

ssRNA – single-stranded RNA

VPg – Viral Protein genome-linked

UTR – Untranslated Region

IRES – the internal ribosomal entry site

BtPVs – bat picornaviruses

CoVs – Coronaviruses

ORFs – Open Reading Frame

S – Spike

E – Envelope

M – Membrane

N – Nucleocapsid

NSP – Non-Structural Protein

RTC – Replication-Transcription Complex

sg mRNAs – sub-genomic messenger RNA

TRSs – Transcription Regulatory Sequences

TRS-B – Transcription Regulatory Sequences Body

TRS -L – Transcription Regulatory Sequences Body Leader

ERGIC – Endoplasmic Reticulum–Golgi Intermediate Compartment

HCoVs – Human coronaviruses

SL-CoV – Severe Acute Respiratory Syndrome Coronavirus Like

PBS – Phosphate Buffer Saline

PCR – Polymerase Chain Reaction

RT-PCR – Reverse Transcription Polymerase Chain Reaction

SOC – Super Optimal broth with Catabolite repression

IPTG – isopropyl-beta-D-thiogalactopyranoside

X-Gal – 5-Bromo-4-Chloro-3-Indolyl β-D-Galactopyranoside

EDTA – Ethylenediaminetetraacetic Acid

RdRp– RNA-dependent-RNA-polymerase

1. Introduction

1.1. General introduction

Remarkably, the chiropteran order is the second largest mammalian order, with 1423 recognized species and exceptional powered flight ability (Han et al., 2015). They are classified into two suborders, the *Yinpterochiroptera,* or megabats, and the *Yangchiroptera,* or microbats, which are characterized by different biology, ecology, and dietary characteristics. They have a broad, geographical distribution range, apart from the polar regions, extreme desert climates, and a few oceanic islands (Irving et al., 2021). Additionally, their long evolutionary history which can be traced back to 52.5 million years ago, allowed several viruses to co-evolve along with them, hence, making bats their natural reservoirs (Han et al., 2015). Strikingly, when compared to other mammals, they host far more zoonotic agents. Earlier, this was hypothetically explained by either immune variation during hibernation or the higher temperatures occurring during flight (fever-like state) leading to viral load reduction, consequently making them viral reservoirs. However, recent studies performed in vitro on bat cells propagated at high temperatures did not demonstrate any decrease in viral loads when compared with cells grown at 37º C (Irving et al., 2021). Moreover, supplementary studies highlight the tolerance regarding viral infection instead of viral load reduction. Recent investigations regarding bat innate and adaptive immune response, metabolism and mitochondrial dynamics, and the relationship between the metabolic and immune systems shed new light on how bats adjust the equilibrium between immune tolerance and host defense, which may contribute to their lengthy lifespans and diminished incidence rates of cancer, in addition to their exceptional status as an asymptomatic viral reservoir (Irving et al., 2021). The continuous expression of Interferons (INFs) and interferons-stimulated genes (ISGs), the elevated expression of heat-shock proteins (HSPs), and higher autophagy are examples of bat host defense. In parallel, immune tolerance is exemplified by suppressed inflammasome pathways and the dampening Stimulator interferon genes (STING) (Irving et al., 2021; Subudhi et al., 2019) (Fig 1).

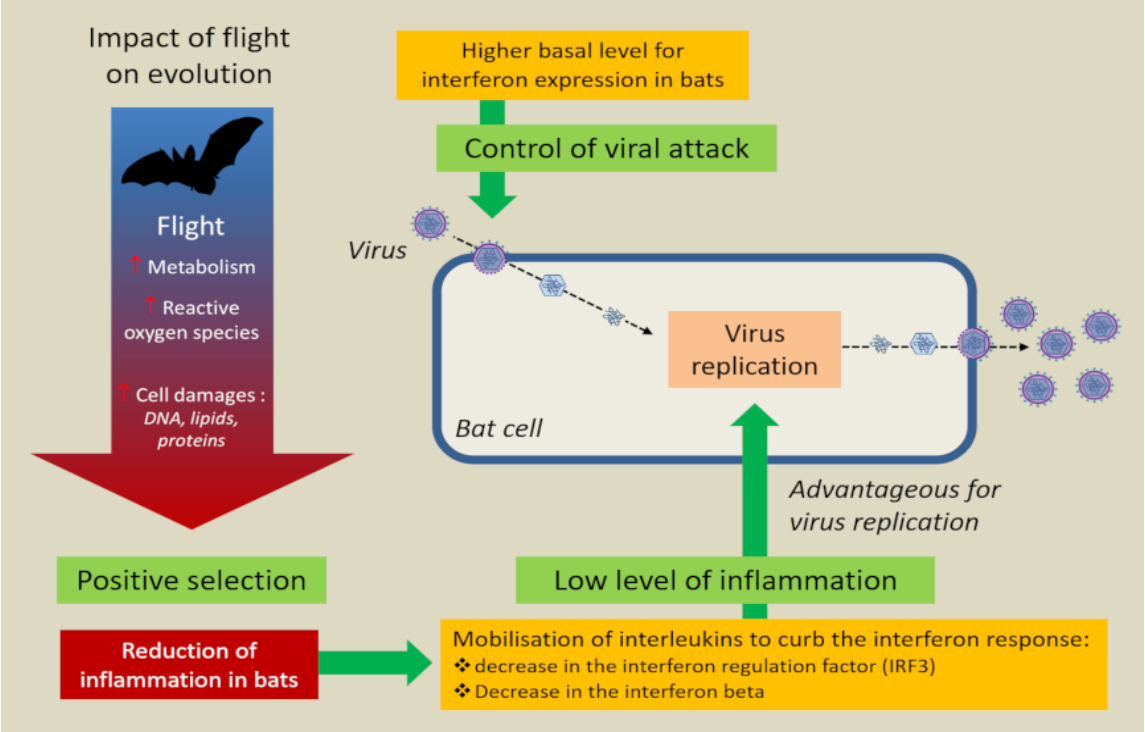

Figure 1. General idea referencing the tolerance towards viral infection among bats. Summary of the possible components of the development of tolerance to DNA damage and the distinctive immune response against viruses in bats. (LARCHER Gérald, 2020)

In the past several decades, zoonotic infectious diseases have increasingly become a global health concern. A zoonosis is defined as any disease naturally transmitted from vertebrate animals to humans, and it can be due to viral, fungal, or bacterial agents with different severity outcomes (Taylor et al., 2001). Additionally, as reported by the World Health Organization (WHO), 60% of the identified human pathogens originated from animals, and 75% of emerging and re-emerging animal diseases agents bear the potential to cross the species barrier. These spillover events trigger the appearance of new pathogenic variants (Bidaisee & Macpherson, 2014; Haider et al., 2020). Furthermore, the largest proportion of emerging and re-emerging infectious diseases develop from wildlife animals, in particular, those with a taxonomically diverse range of thousands of species, such as rodents and bats (Jones et al., 2008; Kreuder Johnson et al., 2015). Likewise, several drivers for disease emergence and re-emergence were identified and differed between socio-economic, environmental, and ecological factors (Olson et al., 2015; Semenza et al., 2016). To cite an example, expanding global human populations lead to animal's natural habitat alteration and increased contact rate among animals and humans (Hassell et al., 2017).

Whereas globalization, travel, and trading ensure resultant outbreaks are hard to control even when implementing well-established mitigation measures (Sabin et al., 2020) (Fig 2).

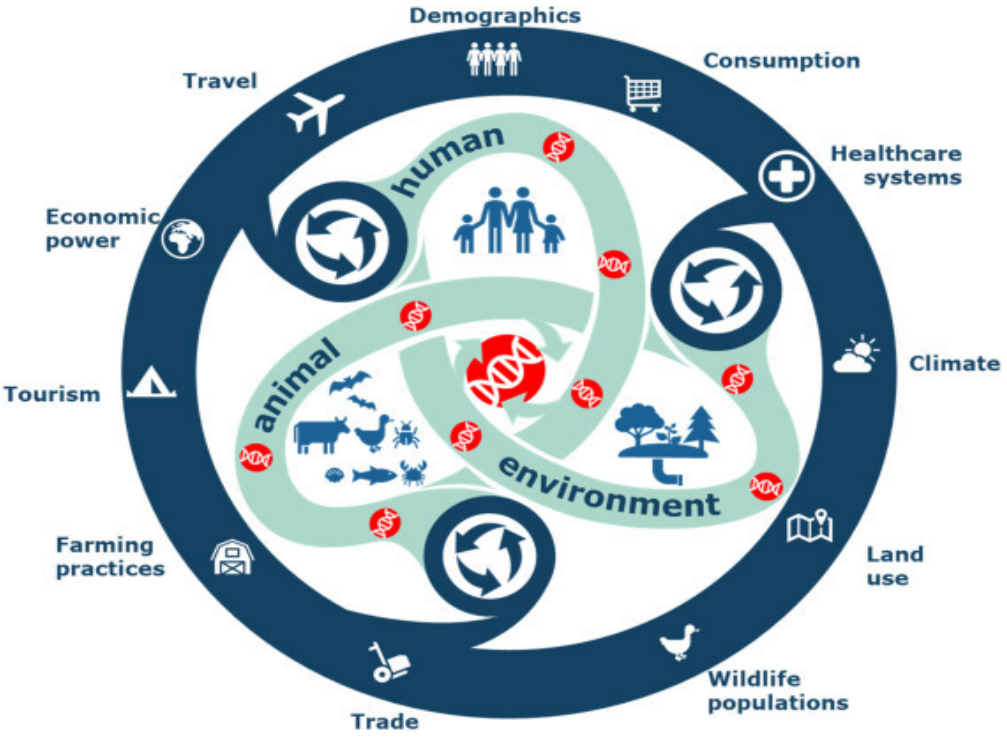

Figure 2. Summary of the main drivers regarding zoonotic disease emergence (Sikkema & Koopmans, 2021)

Perhaps it is not so unsurprising that several serious emerging viral diseases were linked to bats in recent decades. To cite an example, the Nipah virus (NiV) discovered among Pteropus fruit bats was responsible for the first Nipah outbreak declared in 1998, in Malaysia. Thereafter, a second NiV related outbreak was reported in Bangladesh between 2001 and 2005. The disease caused respiratory syndrome among pigs and encephalitis in humans with a mortality rate between 45 and 75%. The spillover to humans occurred either from the consumption of contaminated palm sap, or close contact with diseased pigs (intermediate host) following feeding on contaminated fruits (Han et al., 2015). Similarly, in consideration of the severe acute respiratory syndrome (SARS) outbreak declared in China in 2002, civet cats were first recognized as reservoir hosts. Nevertheless, following various investigations regarding diverse bat species, the Chinese horseshoe bats were considered as host reservoirs (Shi & Hu, 2008). The subsequent coronavirus outbreak specifically, the Middle East Respiratory Syndrome (MERS) was first reported in 2012, and supposedly originated among bats (Han et al., 2016). Lastly, in 2019, a new emergent coronavirus, viz *SARS-CoV-2,* caused an outbreak in Wuhan, China, and later, a worldwide

pandemic, with roughly 310 million infections and over 5.5 million fatalities as of January 11, 2022. Despite the unclear route by which *SARS-CoV-2* spilled over to humans, most hypotheses support the premise referencing bats as natural reservoirs (Prince et al., 2021; Temmam et al., 2021). Overall, numerous viruses are associated with bats starting with rabies (*Lyssaviridae*), first identified in the 1930s (Letko et al., 2020). Other viruses include *Astroviridae, Caliciviridae, Coronaviridae, Flaviviridae, Hepeviridae, Picornaviridae, Arenaviridae, Filoviridae, Hantaviridae, Nairoviridae, Orthomyxoviridae, Paramyxovirdae, Parvoviridae, Adenoviridae, Herpesviridae and Hepadnaviridae* (Chen et al., 2014). Nevertheless, several aspects such as zoonotic potential. spillovers events, evolution, and much more all remain poorly understood. Distinctively, intensive research needs to be performed to fill the knowledge gap and subsequently aid in the outbreak and pandemic preparedness efforts (Aarestrup et al., 2021; Simpson et al., 2020).

In Algeria, there is a vast bat diversity resulting from the various biotopes. Algeria has five different areas stretching from north to south which are distinguished by their climates: the Tell, including the plain territories characterized by a humid Mediterranean climate. The Tellian Atlas located between the sea and the high plains with a subhumid Mediterranean climate. The high plains and highlands domain englobing vast steppe plateaus has a semi-arid climate. The Saharan Atlas. The southern portion of this chain of mountains delimits the arid climate, and lastly the Sahara, and its massifs (Hoggar and Tassili), which represents more than four-fifths of the country and includes both dry and arid climates (Ahmim, 2018). The chiropteran order is represented by seven families engulfing the following species: *Rhinopomatidae (Rhinopoma cystops), Emballonuridae (Taphozous nudiventris), Rhinolophidae (Rhinolophus blasii, Rhinolophus Euryale, Rhinolophus ferrumequinum, Rhinolophus hipposideros, Rhinolophus mehelyi), Vespertilionidae (Eptesicus isabellinus, Myotis punicus, Myotis capaccinii, Myotis emarginatus, Myotis nattereri, Nyctalus leisleri, Nyctalus noctula, Otonycteris hemprichii, Pipistrellus kuhlii, Pipistrellus pipistrellus, Pipistrellus rueppellii, Hypsugo savii, Plecotus gaisleri), Molossidae (Tadarida aegyptiaca, Tadarida teniotis), Miniopteridae (Miniopterus schreibersii)* and lastly *Hipposideridae (Asellia tridens)*. However, in Algeria, despite their wide distribution and presence in urban areas including in close proximity to humans, bats are still poorly studied, especially as viral reservoirs. Astonishingly, with exception to our investigations regarding picornaviruses (Zeghbib et al., 2019) and coronaviruses (Zeghbib et al., 2021), no other references are available with regards to bat-related viral zoonoses.

1.2. Introduction to viruses included in the thesis

1.2.1. *Picornaviridae*

As of September 2020, the virus family counted 147 species grouped into 63 genera, and includes various well-known human and animal pathogens, triggering different symptoms ranging from mild febrile illness to severe diseases of the heart, liver, or the central nervous system. Conversely, many viruses are currently awaiting classification (Zell et al., 2017). Virions are small, spherical, non-enveloped viruses, with icosahedral symmetry. The common characteristic features for all family members include the following; three/four capsid proteins with β-barrel folding, polyprotein processing with cysteine proteinase encoded by the virus, and RNA-directed RNA polymerase replication with a YGDD sequence motif (Tuthill et al., 2010). The genetic makeup is a monopartite, linear, polyadenylated positive ssRNA, 6.7–10.1 kb in length, including a single ORF (except *Dicipivirus* genus which possesses two ORFs) encoding a large polyprotein, flanked on the 5′ end by 500-1200 nucleotide untranslated region (5′ UTR) and at the 3′ end by 30-650 nucleotide 3′ untranslated region (3′ UTR). The genome is organized as follow: VPg+5′-UTR-[(L-)1A-1B-1C-1D/2A-2B-2C/3A-3B-3C-3D]-3′-UTR-poly(A) (Fig 3). VPg is covalently attached to the 5′-end, and the 5′ UTR, of which, harbors clover-leaf replication signals and the internal ribosomal entry site (IRES). It is followed by leader proteins (L) present in some genera (e.g., *Mischivirus, Cardiovirus*) (Zell et al., 2017). The 1A-1B-1C-1D represents the P1 region corresponding to the capsid, however, many picornaviruses have three capsid proteins, since 1AB remains linked, while the P2 region consists of 2A-2B-2C. 2A is a viral protease involved in shutting off the host translation (Lewis-Rogers & Crandall, 2010), 2B causes membrane alteration among infected cells, and 2C interacts directly with the 3' of the negative strand in support of the subsequent synthesis of positive-strand RNA, hence, playing an important role in RNA replication (Banerjee & Dasgupta, 2001). Finally, the 3A-3B-3C-3D characterize the P3 region, in which 3A is incriminated in the hindrance of cellular functionality (such as protein secretion) in reference to efficient virus replication and also influences host immune response (Jackson & Belsham, 2021). 3B corresponds to the VPg which primes both positive and negative RNA strand synthesis and 3C is involved in the polyprotein processing and the initiation of viral RNA synthesis. Moreover, it can prompt the cleavage of some host cellular factors deemed essential for transcription and translation (Sun et al., 2016). Lastly, the 3D representing the RNA dependent RNA

polymerase is one of the major constituents in reference to the viral replication complex (Lin et al., 2009).

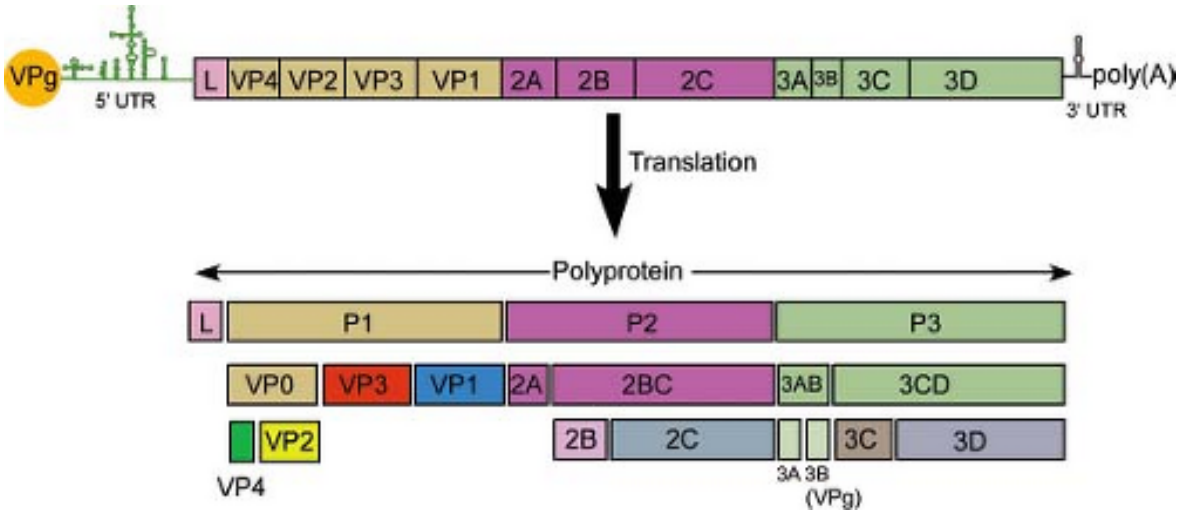

Figure 3. Picornavirus genome organization and polyprotein processing. (Themes, 2016)

To date, discovered bat picornaviruses (BtPVs) possess extreme genetic diversity and are either associated with the *Mischivirus, Hepatovirus, Crohivirus, Kunsagivirus, Sapelovirus, Kobuvirus, and Shanbavirus* genera or remain unassigned (King et al., 2018; Zell et al., 2017). Nevertheless, they persist in being neglected with limited available data, especially regarding their pathogenicity, zoonotic potential, and evolution. For instance, it was assumed *Mischivirus* genus was only related to bats and was classified in three species *Mischivirus A* and *Mischivirus B,* isolated from *M. schreibersii*, the *Mischivirus C* was detected in *Hipposideros gigas,* in addition to putative mischiviruses described from *Myotis myotis* and *Myotis oxygnathus* (Kemenesi et al., 2015; Lukashev et al., 2017; Wu et al., 2012). Nonetheless, it was later reportedly seen in a foxhound (*Mischivirus D*) (Norby et al., 2017) and the Asian house shrew *Suncus murinus* (*Mischivirus E*) (GenBank accession number MF352410). This suggests host-jumping events during their evolution and may highlight a zoonotic potential, therefore requiring serious investigation.

1.2.2. *Coronaviridae*

As of 2019, Coronaviruses (CoVs) are classified within the *Orthocoronavirinae* subfamily of the *Coronaviridae* family in the *Cornidovirineae* suborder of the *Nidovirales* order. They comprise four genera, *Alphacoronavirus, Betacoronavirus, Deltacoronavirus* and *Gammacoronavirus*. *Alphacoronavirus* (14 sub-genera) and *Betacoronavirus* (5 sub-

genera) generally infect mammals and are widely described as having originated from bats (P. J. Walker et al., 2019). Virions are spherical, 120–160 nm in size, including a helical capsid. They are named after the crown shape formed by spike proteins visualized when using electron microscopy. In terms of genetic complexity and genome size, *Coronaviridae* are the largest RNA viruses acknowledged thus far, with their 25-32 kb positive-strand RNA genome including 7-11 open reading frames (ORFs). The RNA is capped, polyadenylated, and organized as follows: 5′-UTR-replicase ORF1ab-S-E-M-N-UTR-3′. The 16 non-structural genes required for transcription and genome replication (ORF1ab) are located at the 5′ end and represent nearly 67% of the genome, whereas the structural genes (*S, E, M, N*) are located towards the 3′ end (Kumar et al., 2020). Accessory genes are interspersed between the essential genes. These accessory (niche-specific) genes were probably acquired via horizontal gene transfer and were likely lost with the evolution and divergence of different coronaviruses while adapting to new hosts (Chazal, 2021). In consideration of their replication mechanism, virions attach to the host cell through the interaction between the S1 region of the spike protein and its receptor. Subsequently, the virus accesses the host cell cytosol via the protease cleavage within the S2 portion of the protein and a consequent fusion of the viral and cellular membranes, resulting in the liberation of the viral genome into the cytoplasm. The next step is the direct translation of the replicase pp1a (NSP1-NSP11) and pp1ab (NSP12-NSP16) using ribosomal frameshifting from the rep1a ORF into the rep1b ORF. Following this, the replication-transcription complex (RTC) is formed, and the 3′ proximal genes (structural and accessory genes) are expressed from a nested set of capped and polyadenylated sub-genomic mRNAs (sg mRNAs). They share a common 3′ end with the genome in addition to a short 5′ leader sequence identical to the 5′- end of the genome. Note that the leader and body (coding region) sequences may be separated by more than twenty thousand nucleotides, however, they are linked through the discontinuous minus-strand RNA synthesis process under the regulation of the transcription regulatory sequences (TRSs), which are either TRS body (TRS-B) located upstream structural ORFs or just downstream of the leader sequence (TRS-L) (Chazal, 2021; V'kovski et al., 2021). Immediately afterward, the S, E, and M proteins are translated and inserted into the endoplasmic reticulum (ER). Following the secretory pathway, they reach the endoplasmic reticulum–Golgi intermediate compartment (ERGIC), where the N-encapsidated viral genomes bud into the ERGIC membranes encompassing the structural proteins forming mature virions. Lastly, they are translocated in vesicles to the cell surface and released by exocytosis. Interestingly, in numerous coronaviruses, the unassembled spike protein

transfers to the cell surface and triggers cell-cell fusion between infected cells and neighboring uninfected cells. This conducts the formation of giant polynucleated cells thereby allowing the spread and the humoral immune evasion of the virus (Fehr & Perlman, 2015). (Fig 4)

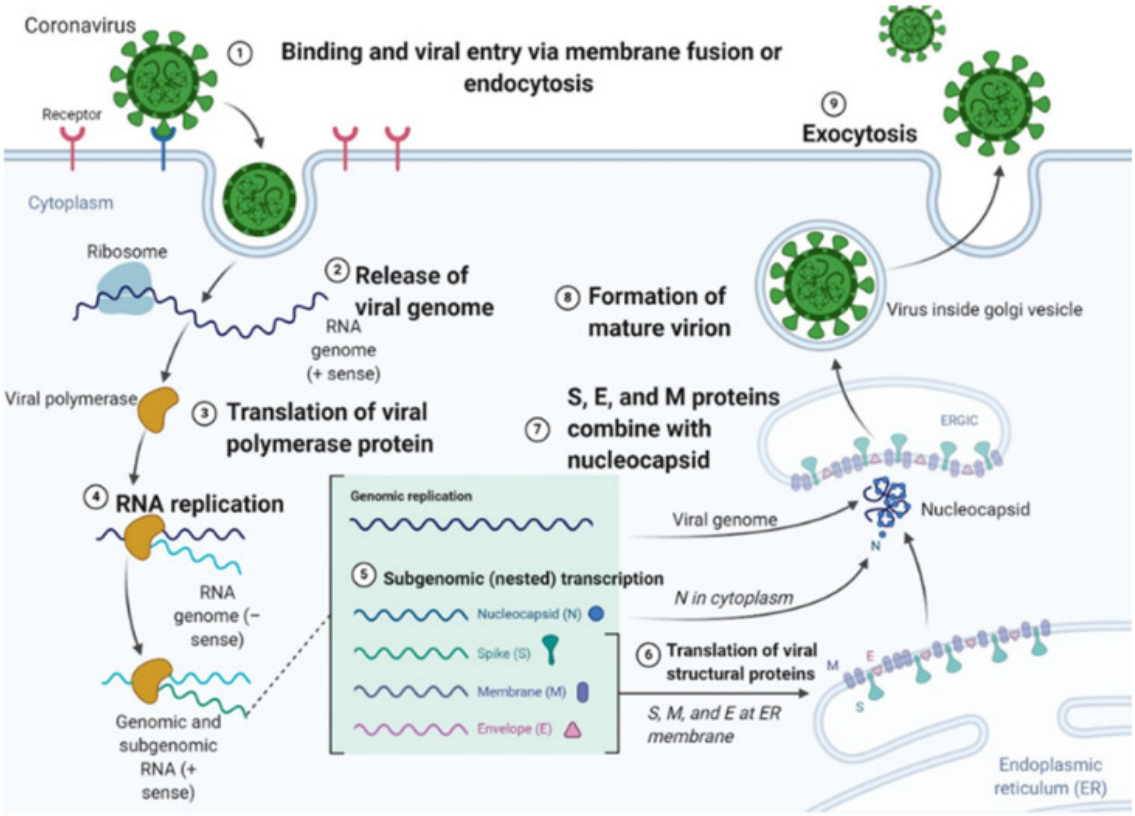

Figure 4. Coronavirus entry and replication with a human host (Batra et al., 2020).

Thus far, all known human coronaviruses (HCoVs) possess a zoonotic origin and they are linked directly or indirectly to bats. For instance, the detection of 229E-like bat CoVs in Hipposideros bats in Africa (Pfefferle et al., 2009), in addition to the subsequent identification of NL63-like CoVs in Triaenops bats (Tao et al., 2017) and American tricolored bat *(Perimyotis subflavus)* (Huynh et al., 2012), supports the evolution theory regarding HCoVs originating from ancestral bat coronaviruses. Similarly, following the SARS pandemic, the isolation of SARS-CoV-like (SL-CoV) virus from horseshoe bats reinforced the spillover hypothesis from bats, while the further detection of genetically diverse SL-CoV in different bat species worldwide highlighted once again, the enormous diversity of CoVs among bats and the complex mechanisms involved in their evolution (Hu et al., 2015; Z. Zhou et al., 2021).

2. Aims of the study

The first objective was revealing the viral diversity among Algerian bats and illustrating potential spillover risks:

- Bat sampling from caves located in close contact with humans
- Large scale characterization regarding viruses
- Accurate identification of viral RNA positive bats via DNA barcoding
- Evolutionary and comparative analyses

The second objective was the molecular investigation of the novel SARS-CoV-2 pandemic in Algeria:

- Identification of main transmission patterns in relation to the Algerian outbreak.
- Molecular tracing and highlighting missing unsampled data
- Description of Algerian characteristic nucleotide and amino acid mutations including their effect on the corresponding protein
- Statistical assessment of the effectiveness of the implemented mitigation measures

Overall, this thesis aims to fill the vast dearth of knowledge with respect to bat-related viruses including the novel SARS-CoV-2 pandemic in Algeria, and subsequently provide primary scaffold data for further investigations. All methods and research projects within this thesis are role models for future zoonotic infection research and outbreak response throughout the country.

3. Materials and methods

3.1. Sample collection

Samples were collected from several regions in Algeria **(**Fig 5). The sampling process was performed in different time frames, depending on either the appropriate collection season (bats) or the current SARS-CoV-2 pandemic diagnostic and surveillance purposes in the case of humans. Bats were sampled from two cities with the same warm Mediterranean climate: Béjaïa and Constantine (Sahabi Abed & Matzarakis, 2017).

In relation to SARS-CoV-2 analyses, human nasopharyngeal swab samples were primarily sent for sequencing to the Pasteur Institute in the nation's capital, Algiers, from the following cities: Algiers, Bouira, Blida, Tipaza, Tizi Ouzou, Sétif, and Bordj Bou Arreridj located in the north and east of Algeria and Adrar, El Oued and Laghouat located in the southern part of the country. Note that, Algeria has an area of 2,381,741 km^2, with a 2,400 km distance from east to west and 2,100 km from north to south. However, the Pasteur Institute is the only research center charged with the responsibility of epidemiologic surveillance regarding the SARS-CoV-2 pandemic.

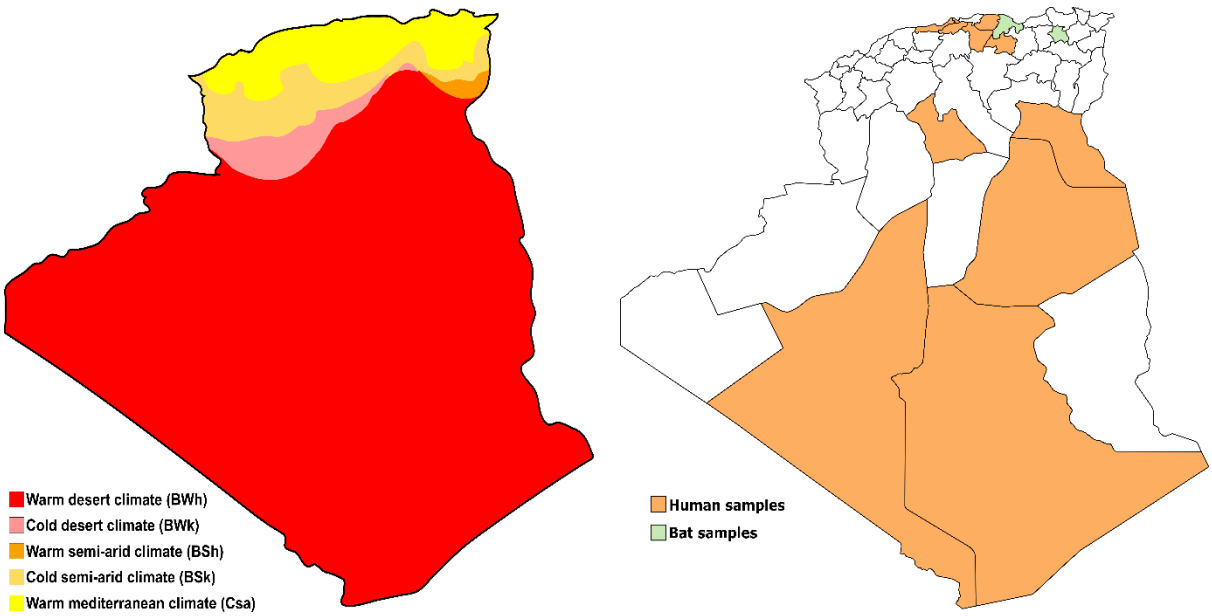

Figure 5. The sampling locations in Algeria; colored according to the sample's type. The different types of climates are demonstrated with a color gradient ranging from red for the warm desert climate to yellow corresponding to the warm Mediterranean climate.

3.1.1. Bat sampling

Between 2016 and 2018, sample collection was conducted in Béjaia, located on the Algerian coast, in two caves; the protected Jiri Gaisler cave in Aoukas and another cave

situated in the municipality of Melbou. Droppings were collected directly under roosting bats, either as individual guano or pooled samples (Figs 6A, 6B). In 2018, another sampling was performed in a cave located in the city of Constantine, municipality of Ibn-Ziad. Bats were captured using a fishing net and individually sampled using a perforated plastic box to collect the droppings directly from the animal. Additional fresh pooled guano samples were directly harvested from the terrain (Figs 6C, 6D). A total of 97 samples were collected in which they were transported in a dry shipper and stored at -80° C until further use.

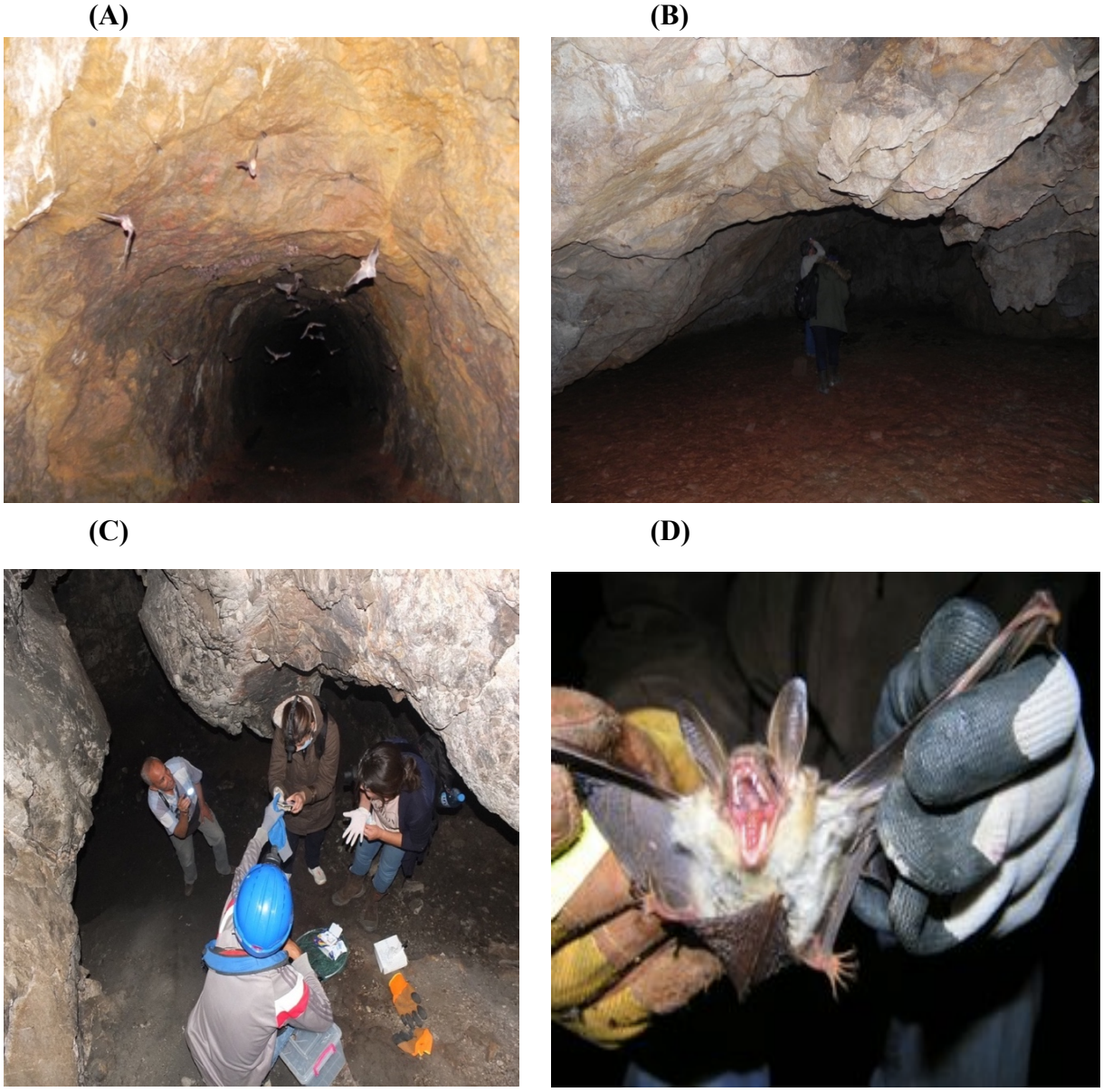

Figure 6. Bat sampling. (A) Flying and roosting bats in the Aouakas cave. (B) Fresh guano collection under a roosting bat in the Melbou cave. (C) Bat capture in Constantine using the fishing net and individual guano collection using the perforated plastic box. (D) *Myotis punicus* bat caught in Constantine's cave and individually sampled.

3.1.2. Human sampling

With regards to the recent SARS-CoV-2 pandemic, the nasopharyngeal samples were tested in the Pasteur institute Algeria as a part of a diagnostic and surveillance process, thereafter, sent to Pasteur France for sequencing. The 29 Algerian sequences were readily available on the GISAID database.

3.2. Bat guano samples preparation and nucleic acid extraction

In support of homogenization, 500 µl of 1X PBS and two pieces of 2.0-2.5 mm diameter glass beads (Kisker Biotech GmbH & CO., Germany) were added to each tube containing the guano sample and homogenized for 60 sec at maximum speed using a Minilys® personal homogenizer (Bertin Corp., USA). Following this, samples were centrifuged at 15,000 *g* for 10 min. Nucleic acid was extracted with strict adherence to the manufacturer's recommendations from 200 µl of supernatant using the GeneJET Viral DNA/RNA Purification Kit (Thermo Fisher Scientific., USA) or Genaid viral nucleic extraction kit II (Geneaid Biotech Ltd., Taiwan) dependent upon availability. The extracted nucleic acid was eluted in 50 µl of nuclease-free water, then stored at -80° C until further laboratory processes.

3.3. Polymerase Chain Reaction (PCR) methods

For the sake of viral-specific nucleic acid detection, molecular identification (barcoding), or full genome recovery, several oligonucleotides and PCR types were used. All PCR steps were previously optimized to obtain the best annealing temperature. Reverse transcription-polymerase chain reactions (RT-PCR) were achieved using the QIAGEN OneStep RT-PCR Kit (Qiagen, Germany) for short amplicons (≤ 1000 bp), whereas longer fragments (>1000 bp) were obtained with the SuperScript® III One-Step RT-PCR System with Platinum® Taq DNA Polymerase Kit (Thermo Fisher Scientific, USA). Conventional PCRs were performed using either the GoTaq® G2 Flexi DNA Polymerase Kit (Promega, USA) for short fragments, or the Phusion High-Fidelity DNA Polymerase (Thermo Fisher Scientific, USA) for long amplicons (>800 bp) amplification. Oligo-primers, the type of PCR, and the size of the final amplicons including, the corresponding references are all summarized in Table 1.

Table 1. Summary of the primer sets used for detection of *Coronaviridae* (CoV), *Picornaviridae* (PiV), bat DNA barcoding (COI), and picornavirus genome walking (PiV GW) with the PCR type and reference (Ref).

Primers	Amplicon size	PCR type	Ref
(CoV) FR26RV-N: 5'-GCCGGAGCTCTGCAGATATCNNNNNN-3' PC2S2: 5′ -TTATGGGTTGGGATTATC- 3′ PC2As1: 5′-TCATCACTCAGAATCATCA-3′ PCS: 5′-CTTATGGGTTGGGATTATCCTAAGTGTGA-3′ PCNAs: 5′-CACACAACACCTTCATCAGATAGAATCATCA- 3′	~440	Two-step nested RT-PCR	(de Souza Luna et al., 2007)
(COI) SFF_145F: 5′-GTHACHGCYCAYGCHTTYGTAATAAT-3′ SFF_351r: 5′-CTCCWGCRTGDGCWAGRTTTCC-3′	202	Normal PCR	(F. M. Walker et al., 2016)
(PiV) 3′ Race Primer 1/3′ Race: 5′-TGTTCTTGGCTCTGCTATTG-3′ Primer 2/3′ Race: 5′-GATAACAACCCCTTTCTCAA-3′	-	RACE-PCR	(Zeghbib et al., 2019)
(PiV) GW First 1800pb F: 5′-GATACACCTCCACCTCTT-3′ First 1800pb R: 5′-GCAAATGAAACCACAACTCT-3′ Second 2kb F: 5′-TACTATCCCCTTTATCTCTC-3′ Second 2kb R: 5′-TCTTCCTGTTTCTGTTGCTA-3′ Third 2kb F: 5′-ATGGATTTGAAGGATGAAGC-3′ Third 2kb R: 5′-GGCAGTTGACAGCAGTAA-3′	-	RT-PCR	(Zeghbib et al., 2019)

3.4. Cloning and Sanger Sequencing

Concerning bat coronaviruses, the resultant PCR amplicons were cloned into a pGEM-T Easy vector (Promega, USA) and subsequently, *Escherichia coli* JM109–competent cells (Promega, USA) were transformed with the recombinant plasmid in full adherence to the manufacturer's protocols. *Escherichia coli* was incubated for one hour and a half at 37º C while oscillating in the SOC medium prepared as follow: 0.5% Yeast Extract, 2% Tryptone, 10 mM NaCl, 2.5 mM KCl, 10 mM $MgCl_2$, 10 mM $MgSO_4$, 20 mM Glucose; the glucose was added after autoclaving the solution, then the solution was cooled down. Following this, the final solution was filtered using a 0.2 µm filter. Lastly, for the blue/white selection of the recombinant colonies, the transformed cells were plated on LB dishes containing 100µg/ml ampicillin, 0.5mM IPTG, and 40µg/ml X-Gal. Thereafter, the plates were incubated overnight at 37° C. Following this, positive clones represented as white colonies were

selected and amplified by colony PCR using pGEM-T Easy Vector-specific primers with full adherence to the manufacturer's instructions. The resultant products were purified using the Geneaid Gel/PCR DNA fragment kit (Geneaid Biotech Ltd, Taiwan) and a subsequent sequencing PCR was performed using the BigDye Terminator v1.1 Cycle Sequencing Kit (Applied Biosystems, USA). Samples were sequenced bidirectionally on an ABI Prism 310 DNA Sequencer (Applied Biosystems, USA).

3.5. Next-Generation sequencing with Ion Torrent PGM and Illumina

For metagenomic analysis and in order to increase viral reads, three viral enrichment methods were combined (Hall et al., 2014). The centrifugation of the homogenate at 12,000 *g* for 10 minutes at 4º C was the starting point, followed by a filtration using Sartorius filter tubes (Sartorius, Germany). Lastly, an enzymatic enrichment was performed in which a homemade buffer was initially prepared (1M Tris HCl, 100 mM $CaCl_2$, 30 mM $MgCl_2$, final pH=8). A mix of 200 µl sample and 0.66 µl Micrococcal nuclease (Thermo Fisher Scientific, USA), in addition to 2 µl Benzonase (Sigma-Aldrich., USA) and 7 µl from the homemade buffer prepared previously were incubated for 2 hours at 37º C and further processed for nucleic acid extraction using the Geneaid Virus DNA/RNA Extraction Kit (Geneaid Biotech Ltd, Taiwan). Nucleic acid samples were denatured at 95° C for 5 min in the presence of 10 µM random hexamer PCR primer (Djikeng et al., 2008). Reverse transcription was achieved with 30 U AMV reverse transcriptase (Promega), 100µM for each dNTP, and 5 × AMV RT buffer [composition; 250mM Tris-HCl (pH 8.3 @ 25° C), 250mM KCl, 50mM $MgCl_2$, 2.5mM spermidine and 50mM DTT], at 25º C for 10 min, followed by 42° C for 60 min, then 70º C for an additional 15 min. Next, 3 µl of the acquired cDNA was added to 22 µL PCR mixture to obtain a final volume of 25 µl and a concentration of 250 µM for the PCR primer (Djikeng et al., 2008), 100 µM for each dNTP, 1.5 mM $MgCl_2$, 1 × Taq DNA polymerase buffer, and 0.6 U of Taq DNA polymerase (Thermo Scientific, USA). The reaction conditions comprised of an initial denaturation step at 95° C for 3 min, followed by 40 cycles of amplification (95° C for 30 s, 48° C for 30 s, 72° C for 2 min) and ended at 72° C for 8 min. Subsequently, samples were cleaned using the Geneaid Gel PCR DNA fragment extraction kit (Geneaid, Taiwan). In consideration of Ion torrent sequencing, the concentration was measured with Qubit® 2.0 equipment using the Qubit® dsDNA BR Assay kit (Invitrogen). 8 µl of the previously prepared cDNA underwent an enzymatic fragmentation and adaptor ligation in full adherence to the manufacturer's recommendations

using the NEBNext® Fast DNA Fragmentation & Library Prep Set for Ion Torrent™ kit (New England Biolabs, USA). The IonTorrent Xpress barcode adapters were procured from Thermo Fisher Scientific, USA. Thereafter, cDNA libraries were measured using a Qubit® 2.0 as previously mentioned. To clonally amplify the resultant libraries, an emulsion PCR was carried out using the Ion PGM Template kit on a OneTouch v2 instrument (Life Technologies, USA) in full adherence to the manufacturer's protocol. Templated beads were enriched via an Ion OneTouch™ ES pipetting robot (Life Technologies, USA). The sequencing was achieved with the Ion Torrent PGM (Life Technologies, USA) with strict adherence to the 200 bp sequencing protocol on a 316 chip (Life Technologies, USA). Thereafter, CLC Genomics Workbench version 9.0 (http://www.clcbio.com) was employed for raw sequence readings, trimming, and quality control. The minimal read length parameter was fixed to 35. Taxonomic binning was achieved using the Diamond v0.8.3 against NCBI-NR (Buchfink et al., 2015). The resultant files were analyzed and visualized by MEGAN6 Community Edition (Huson et al., 2016). In parallel and in support of Illumina, sequencing libraries were prepared using the NEBNext Ultra II RNA Library Prep Kit for Illumina (New England Biolabs) in full adherence to the manufacturer's protocol. Both the concentration and the fragment size of the libraries were measured and examined using the Agilent TapeStation 4200 (Agilent Technologies) and Qubit 3.0 Fluorometer (Thermo Fisher Scientific). Library preparation was followed by sequencing on the Illumina NextSeq with 2 × 150 bp read length (Illumina).

3.6. Rapid Amplification of cDNA-Ends by Polymerase Chain Reaction (RACE-PCR)

Through the combination of nested RT-PCRs with a primer walking approach, a 3′ RACE protocol, and next-generation sequencing, the complete picornavirus genome was nearly obtained (Alkan et al., 2015). First, using a SuperScript III Reverse Transcriptase kit (Invitrogen, USA), a total volume of 25 µl per sample master mix was prepared: containing a 12.5 µl 2X Reaction Mix (a buffer containing 0.4 mM of each dNTP, and 3.2 mM $MgSO_4$), 4.5 µl of Nuclease Free Water, 1 µl of SuperScript™ III RT/Platinum™ Taq Mix and 0.5 µl of 37.5 µM Oligo dT-Anchor Primer from the 2nd Generation RACE kit (Roche, Switzerland) and 0.5 µl of 10 µM sequence-specific primer (1/3′ race) designed in Oligo Explorer 1.4 (http://www.genelink.com/tools/gl-oe.asp). The Cycling profile was comprised of the following steps: 45º C for 30 min and 94º C for 2 min. Subsequently, the program was

paused and the second set of primer consisting of 0.5 µl of 12.5 µM PCR Anchor Primer (Roche, Switzerland) and 0.5 µl of 10 µM from another sequence-specific primer (2/3′ race) were added, followed with additional cycling comprised of 94º C 30 sec, 42º C 30 sec, 68º C 20 min, 10 cycles: 94º C 30 sec, 42º C 30 sec, 68º C 5 min, 30 cycles: 94º C 30 sec, 48º C 30 sec, 68º C 3 min and final elongation at 68º C for 10 min. Lastly, the mixture was suspended at 4º C. Thus, gel electrophoresis was performed on a 1.2% agarose gel composed of 0.48g agarose, 40 ml 0.5 X Tris Borate EDTA (40 mM Tris-Cl; pH 8.3, 45 mM boric acid and 1mM EDTA) visualized under ultraviolet light. Subsequently, the band was sliced and cleaned using the Geneaid Gel PCR DNA fragment extraction kit (Geneaid, Taiwan). The purified nucleic acid was stored at -20º C until the next step in which Next-Generation Sequencing using Ion Torrent (Life Technologies, USA) was achieved. Finally, the CLC Genomics Workbench (http://www.clcbio.com/) was used for de novo sequence assembly and reference mapping.

3.7. Sequence data selection

3.7.1. *Picornaviridae*

As of May 2018, all known bat picornavirus sequences, representing either complete or partial coding sequences, were retrieved from GenBank, including the novel mischivirus sequence presented in our project. The BtPVs sequences were sampled from 26 bat species belonging to nine genera. Sequence's provenance hail almost entirely from Europe n = 35, Asia n = 25, Africa n = 9, and America n = 1. A total of 70 sequences were analyzed (three kobuvirus, nine mischivirus, one crohivirus, one kunsagivirus, one sapelovirus, four hepatovirus, one shanbavirus, and 50 unassigned viruses), including one amphibian ampivirus which was represented as an outgroup. The sampling location, collection date, and host genus were listed as indicated in GenBank sequence annotation, and/or the literature (Wu et al., 2016). Sequences with unknown hosts were discarded. To best represent mammalian host evolution, we downloaded both complete and partial mitochondrial cytochrome b gene (CYTB) (Agnarsson et al., 2011). In reference to the *Miniopterus schreibersii* bat, we obtained additional CYTB sequences from the Hungarian Natural History Museum in Budapest. All details regarding the analyzed sequences can be found in the supplementary materials section.

3.7.2. *Coronaviridae*

In consideration of bat coronaviruses, two datasets based on the helicase and RdRp genes were constructed respectively. The first dataset englobed the Algerian partial helicase sequence revealed by the metagenomic analysis in addition to 23 partial alphacoronavirus bat-related helicase genes. A betacoronavirus sequence was used as an outgroup (FJ588687). In parallel, the second dataset comprised 806 partial alpha and betacoronavirus bat-related RdRP sequences retrieved from GenBank and included five Algerian sequences. A delta coronavirus (KJ601780) was used to root the tree (accession numbers of used sequences can be found in supplementary materials).

Furthermore, regarding the ongoing SARS-CoV-2 pandemic investigations, a total of 95 sequences, including 29 Algerian genomes, were retrieved from the GISAID database (as of April 2021) (Shu & McCauley, 2017). 41 sequences originated from Africa, 27 sequences from Europe, 13 from America, 12 from Asia, and two sequences from Australia. Sampling dates ranged from 24 December 2019, through 4 March 2021. We used only 95 sequences to demonstrate the dispersion of the Algerian sequences within the phylogenetic tree, therefore, highlighting multiple introductions of the virus. The sequences were randomly chosen from the GISAID database. We selected sequences from the five continents, with most sequences from Europe since it's the main traffic destination. All sequences were sampled prior to 4 March 2021, and it is the last sampling date regarding the Algerian sequences (details referencing sequences used in this study are in the supplementary material).

3.8. Sequence editing, Temporal signal assessment, phylogenetic and phylogeographic analysis

3.8.1. *Picornaviridae*

Sequences were aligned by MAFFT using the L-INS-I parameter and manually inspected in MEGA 6 (Katoh et al., 2002; Tamura et al., 2013). Sequence length adjustment was acquired using the GeneDoc (Nicholas & Nicholas, 1997). The size ranged between 1,419–1,838 bp regarding the P1 region, 1,724–2,082 bp representative of the P2 region, and 343–1,404 bp in reference to the RdRp. Host sequences were not modified.

Before applying the datasets for phylogenetic reconstruction, we implemented the finest substitution model selection using Mega 6. The GTR + G substitution model was applied for phylogenetic construction based on the 3Dpol gene from Mischiviruses and their hosts. Additionally, the same substitution model was used to create a tree from the P1 region

of all BtPVs. Likewise, the GTR + G + I substation model was used to implement phylogeny based on the P2 region and 3Dpol gene of all BtPVs and their hosts. An amphibian picornavirus Ampivirus A sequence was used to root the viral phylogenies (Zell et al., 2017), while the *Furipterus horrens* CYTB sequence was used as a representative of the host tree outgroup. Non-molecular clock Bayesian phylogenetic trees were constructed using MrBayes v3.2.4 software (Ronquist et al., 2012). Each analysis operated for 10 million generations (25% were discarded as burn-in) and sampled every 1,000 generations, and the resultant trees were then visually edited using iTOL (Letunic & Bork, 2016). Thereafter, the viral non-molecular clock phylogenetic trees were subjected to a temporal signal assessment for time-calibrated phylogenies reconstruction. By definition, inferring molecular phylogenies on a natural timescale of months, years, or even days from sequences sampled at different time points, given that the investigated sequences endure a quantifiable amount of nucleotide or amino acid, results in changes between sampling time (heterochronous). The signal is measured based on a regression method of root-to-tip distances against dates of sampling regarding viral Bayesian trees using TempEst (Rambaut et al., 2016).

3.8.2. *Coronaviridae*

With respect to bat's Hel and RdRp datasets, sequences were aligned in the MAFFT web server using the default parameters (Katoh et al., 2002). Next, they were inspected using GeneDoc (Nicholas & Nicholas, 1997). Thereafter, both maximum likelihood phylogenetic trees were constructed in IQTREE webserver under the TIM2+F+I+G4 model with ultrafast bootstrapping for branch supports estimation (Hoang et al., 2018; Nguyen et al., 2015). Finally, the resultant trees were edited using the iTOL web server (Letunic & Bork, 2016).

In regards to SARS-CoV-2, first, a maximum likelihood phylogenetic tree was implemented using the IQTREE webserver under the GTR+I substitution model, with ultrafast bootstrapping following the best substitution model selection (Hoang et al., 2018; Nguyen et al., 2015). Considering the Algerian border closure since mid-March 2020, a dataset comprising only the Algerian sequences (18 complete genomes and 11 partial sequences) was analyzed as mentioned above under a GTR+I substitution model. The resultant Maximum Likelihood Trees were used as an input file in TempEst for temporal signal evaluation as formerly discussed (Rambaut et al., 2016). Subsequently, the tip-dated phylogenetic trees were generated using the Beast v1.10.4 package and the GTR+I substitution model under a lognormal uncorrelated relaxed clock model assuming an independent evolutionary rate upon the branches. This implies a sudden change of the

evolutionary rate across branches, much like going from fast to slow or vice-versa (Drummond et al., 2006; Suchard et al., 2018). Considering population size and growth, the parametric coalescent exponential growth model supposing an exponential increase in the population was used as a prior, for both the entire dataset and the Algeria dataset (Drummond, 2005). An additional non-parametric Skyline plot model supposing different effective population sizes for each coalescent interval was applied as a prior regarding the Algerian dataset (Lai et al., 2020). The Markov Chain Monte Carlo chains (MCMC) were operational for 100 million generations and sampled every 10,000 generations, with 10% discarded as burn-in. Subsequently, the effective sampling sizes (ESS > 200) were examined using the TRACER v1.6.0 (Rambaut et al., 2018). In parallel, the date of the most recent common ancestor (MRCA) regarding the pandemic in addition to the evolutionary rate were estimated for both datasets. Furthermore, the Maximum clade credibility trees (MCC) (trees with the highest posterior score) which summarize the results of the Bayesian phylogenetic inference were annotated employing the TreeAnnotator v1.10.4 and visualized in FigTree v1.4.4 (Drummond & Rambaut, 2007). Moreover, both a discrete and a continuous phylogeographic analysis were implemented using Beast v1.10.4 (Drummond & Rambaut, 2007). In the Bayesian framework, the first approach combines the continuous-time Markov chain (CTMC), a Bayesian stochastic search variable selection (BSSVS) which permits the exchange rates among the CTMC to be zero with some prior probabilities, and a standard symmetric substitution model regarding the discrete diffusion process. The latter specifies a discrete state ancestral reconstruction using a standard continuous-time Markov chain (CTMC) in which the transition rates between locations are reversible (Ebranati et al., 2019). Subsequently, a Bayes factor test that identifies the most parsimonious phylogeographic diffusion scenario of viral families across a set of discrete locations (countries, cities, and municipalities) was realized (Dellicour et al., 2021). Rates with a BF of > 3 were considered significant. The samples' spatial data/locations of isolation were used to infer the discrete geographical spreading patterns regarding the virus in Algeria as formerly described. On the other hand, the continuous diffusion model based on The Brownian diffusion assuming a homogeneous dispersal rate over the phylogeny, which can infer ancestral states based on coordinates (latitude and longitude) was also applied (Lemey et al., 2010). This model combines the inference of the evolutionary relationship among the sampled sequences and geographic locations of the unsampled common ancestors, thus producing a more realistic reconstruction of the spatial spreading history regarding the sampled population (Nahata et al., 2021). Thereafter, SpreaD3 v0.9.7 software was used to visualize the transmission routes

and calculate the Bayes Factor (BF). To achieve this, the MCC trees and the discrete analysis's log file were used, respectively (Bielejec et al., 2011).

3.9. Pairwise genetic distance

The evolutionary distance between a pair of sequences is estimated by either the number of nucleotide or amino acid changes among them. This was applied for PiV RdRp nucleotide and amino acid sequences, using the MegAlign Pro program (DNASTAR v15.2.0) with uncorrected pairwise distances as a metric. Similarly, in MEGA v6, P distance was employed for the same purpose. It's simply calculated by dividing the number of nucleotide differences by the total number of nucleotides compared (Tamura et al., 2013).

3.10. Phylogeny-trait association analysis

This analysis was performed in consideration of the *Picornaviridae* family. Basically, it is the exploration of the degree to which neighboring taxa in a phylogenetic tree share a characteristic interest (location, species) than expected by chance. This was performed using the association index (AI) which considers the shape of the phylogeny by measuring the imbalance of internal phylogeny nodes and the parsimony score (PS) which estimates phylogeny-trait correlation. Moreover, larger monophyletic clades with the same trait among their tips should be the result of strong phylogeny–trait associations. This attribute is measured with the maximum monophyletic clade (MC) index. All the previously mentioned statistics are available in the BaTS package. Mischiviruses and all BtPiVs (based on the 3Dpol gene) were inspected using BaTS software. Both exhibited significant bunching due to the following characteristic states of interest: bat host genus, species, or sampling location. This analysis compared the posterior distribution of trees regarding our data formerly mentioned, to a null distribution of 1000 trait-randomized trees. The values obtained and the results were interpreted in accordance with Parker and colleagues (Parker et al., 2008). Prior to this, the trace files generated by MrBayes were analyzed in Tracer v1.6 (Rambaut et al., 2018) to discard the burn-in trees.

3.11. Virus-host co-evolution analysis

The co-evolution between Picornaviruses and their corresponding chiropteran hosts was examined using the approach of host and parasite phylogenetic trees reconciliation via event-cost methods. Put differently, the virus phylogenetic tree is mapped onto the host tree,

using the maximum parsimony method, in which reconstruction is desired in such a way it minimalizes the total cost of occurring events. The evolution may occur because of Co-speciation, duplication, host switches, loss, and failure to diverge events. Less likely events acquire larger costs. To estimate the virus-host co-divergence scope, we simultaneously analyzed picornaviruses (RdRp) and their hosts' phylogenies along with mischiviruses and their hosts' phylogenies, all in the operational use of Jane v4.0 (Conow et al., 2010). It deduces the nature and frequency of different evolutionary events by determining the congruence with the least costly reconstructions of the host-parasite connection using tree topologies. Thus, the parameters for the entire event costs (co-speciation, duplication, host switch, loss, and failure to diverge) were set to 0, then 1, and after co-speciation, equal to 0 and other events equal to 1 with a population size equal to 100 and 100 generations for both datasets mentioned above. Before proceeding to the reconciliation analysis, a script was created using the R program to convert nexus files to the appropriate Jane format (R Core Team, 2020). Lastly, Tanglegrams for all bat PVs and their hosts, in addition to mishiviruses and their hosts, were created using Dendroscope v3 (Huson & Scornavacca, 2012).

3.12. Selection pressure and mutation analyses

This was performed regarding the SARS-CoV-2 sequences which originated from Algeria. First, the pairwise selective pressure at the protein level was evaluated for each of the following genes: *ORF1a*, *ORF1b*, *S*, *E*, *M*, *N*, *ORF3a,* and *ORF8,* by estimating the ω ratio representing the rate of the non-synonymous mutation (Ka/dn) to the synonymous mutations (Ks/ds), according to Nei and Gojobori, using SNAP v2.1.1 (Bromberg & Rost, 2007; Masatoshi Nei & Takashi Gojobori, 1986; Z. Yang & Bielawski, 2000). When several non-synonymous mutations which promote changes with physiochemically different amino acids occur, they show a tendency to be deleterious to the protein. Thus, they are improbable to become fixed in the population leading to an adverse selection resulting in $Ka < Ks$ ($\omega < 1$). Contrariwise, when advantageous non-synonymous substitutions strike, they are likely to become fixed in the population, thus, amino acid changes in the protein are enhanced ($\omega > 1$). Finally, if a neutral selection is promoted $Ka=Ks$ ($\omega=1$). Furthermore, the Algerian sequences were subjugated to the genome detective coronavirus typing tool and the CoVsurver mutations App implemented in the GISAID database to highlight variations in the mutational pattern, both on the amino-acid and nucleotide levels among them (Cleemput et al., 2020; Elbe & Buckland-Merrett, 2017). Subsequently, the Cov-glue webserver was

used to assess the effect of the amino-acid replacement on the corresponding protein according to Hanada and colleague's amino acid classification, and in reliance on Grantham distance based on three properties; composition, polarity, and molecular volume, in addition to the Miyata distance which is founded on two physicochemical properties; the volume and the polarity (Grantham, 1974; Hanada et al., 2006; Miyata et al., 1979; Singer et al., 2020). Results were interpreted accordingly: regarding the Grantham distance, the substitution is considered conservative if the score is from 0-50, moderately conservative if it is between 51-100, moderately radical in the case of 101-150, and finally, a radical substitution is characterized by a score above 151. Regarding Miyata's distance, it ranged between 0.06 and 5.13 from the most similar to the most divergent pairs, respectively. Consequently, the effects of mutations on protein function and disease relation were explored using the PredictSNP webserver which combines several prediction tools (https://loschmidt.chemi.muni.cz/predictsnp/, accessed on 1 August 2021). Results were interpreted according to Bendl and colleagues (Adzhubei et al., 2013; Bendl et al., 2014; Capriotti & Fariselli, 2017; Ng & Henikoff, 2003).

3.13. Recombination analysis

GENECONV, BOOTSCAN, GENCONV, SISCAN, and MAXCHI methods implemented in the RDP4 software were used to effectively detect recombination events (Martin et al., 2015). Prior to this, all nucleotide sequences of interest were aligned. Subsequently, recombination events, parental and recombinant sequences as well as putative breakpoints all underwent analysis using default parameters. Regarding the bat picornaviruses, an additional method was used to assess the recombination; the generation of phylogenetic trees from various regions of the genomes (P1, P2, and 3Dpol genes), and the examination of discordances in their structures.

3.14. Statistical analysis

Spearman coefficient was used among the *Picornaviridae* family to estimate the strength of the correlation among picornavirus diversity represented by the number of picornaviruses detected clusters and the number of *Picornavirus* species tallied four each host genus. On the other hand, in sketching an overview regarding the pandemic evolution in Algeria, the cumulative number of the infected recovered and death cases were collected from the Johns Hopkins University Center for Systems Science and Engineering (2 May

2021) (Dong et al., 2020). Thereafter, the linear, exponential, and logarithmic trend lines were compared, and the best model was chosen based on the R^2 values. Subsequently, the correlation coefficient was calculated between the density and the number of confirmed cases. Before this, the cumulative confirmed cases for each of the 48 Algerian cities were collected from the official Algerian Ministry of Health website (*Algerian Ministry of Health*, 2020). The population density data regarding all Algerian cities was retrieved from the Wikipedia website ("Pandémie de Covid-19 en Algérie," 2021). Lastly, the value interpretation was as follows: 0.00–0.39 "weak" correlation, 0.40–0.59 "moderate", 0.60–0.79 "strong", and 0.80–1.0 "robust".

3.15. Haplotype network analysis

This was conducted only for the SARS-CoV-2 species. A dataset comprising 84 sequences, including the Algerian complete genomes, was subjected to recombination detection analysis using RDP 4 software as formerly described. Next, the DnaSP v6.12.03 package was applied to estimate insertions or deletions (InDels), recombination, and to generate a Haplotype nexus file, which will be used further (Rozas et al., 2017)**.** Subsequently, the appropriate input file for POPART software was generated according to the user manual. Thereafter, Haplotype network analysis based on the country of origin regarding viral sequences was performed via the median-joining network method with default setting (epsilon=0) (Bandelt et al., 1999; Leigh & Bryant, 2015).

4. Results

To depict an overview regarding virus discovery in Algeria, different samples varying between reservoir hosts and definitive hosts were investigated. Overall, samples included 29 human nasopharyngeal swabs and 97 bat fecal samples from four different species. As a primary result, we present the conceptual baseline regarding future zoonotic virus research and the genomic epidemiological toolkit for outbreak mitigation in support of future research in Algeria. Results are additionally detailed in each section.

4.1. Bat samples

Among the 97 samples, metagenomic libraries were prepared from 35 samples. The results revealed the presence of *Picornavirus* with 1179 reads in a *Miniopterus schreibersii* bat. Furthermore, PCR screening for *Coronaviridae* uncloaked 8 positive samples, however, sequences could be obtained from only 5 samples. Additionally, the combination of metagenomics and *Coronaviridae* PCR test unveiled the co-circulation of alpha and betacoronaviruses in a *Rhinolophus ferrumequinum.* Nevertheless, all positive samples undergo DNA barcoding to identify the virus-host species. Details considering all performed analyses are additionally described for each virus family.

4.1.1. *Picornaviridae*

Understanding viruses and their hosts' coevolution is critical towards demonstrating the evolutionary pattern and understanding potential disease emergence factors (Lukashov & Goudsmit, 2001; Sharp & Simmonds, 2011). Therefore, numerous phylogenetic and systematic evolutionary analyses were conducted regarding the *Picornaviridae* family, since the virus members of this family are continuously being discovered (Farkas et al., 2015; Hughes, 2004). However, the virus-host coevolution patterns for this group are poorly known. In this study, we define the first picornavirus from Algerian bats and include this new sequence in a detailed co-evolutionary analysis focusing on bat picornaviruses. The novel virus was detected from a *M. schreibersii* bat, according to bat DNA barcoding. Based on genome sequence identity, the novel characterized sequence (MG888045) clustered within the *Mischivirus* genus. Nearly the entire genome (6961 nt) was obtained (some 1,400 bp are missing, 5′ UTR and the beginning of the L protein). This exhibits the typical PV characteristic genome organization regarding UTR [L-P1(VP0, VP3, VP1)-P2(2 A, 2B, 2Chel)-P3(3 A, 3BVPg, 3Cpro and 3Dpol)] UTR-poly(A). Moreover, the conservative

motifs were very similar to the Hungarian Mischivirus B described by Kemenesi and colleagues (Kemenesi et al., 2015). Genome organization, in addition to hypothetical cleavage sites and conserved motifs, according to the first start codon in the obtained sequence are shown in Fig 7.

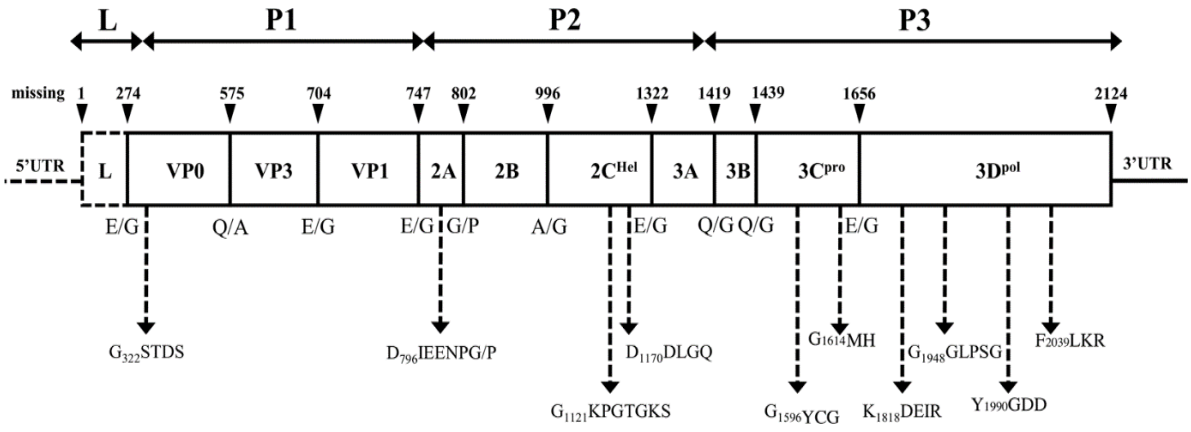

Figure 7. Schematic representation of the novel Algerian BatPV genome organization. 3′ UTR, P1, P2, and P3 regions are included. Additionally, the putative cleavage sites and the conserved motifs are depicted.

Furthermore, in accordance with the Blast results, the novel Algerian sequence shared 85% of nucleotide identity with the Hungarian virus and 73% identity with the Chinese strain. Likewise, it shared between 91–94% identity with shorter sequences available from the Bulgarian tentative mischiviruses. The phylogenetic analysis established using RNA-dependent RNA polymerase gene (RdRp) of mischivirus sequences (Fig 8) demonstrated how the novel Algerian BtPV formed a monophyletic clade together with the Hungarian Mischivirus B sequences (Kemenesi et al., 2015); in addition to the Bulgarian and Romanian tentative Mischivirus (Lukashev et al., 2017), and also including the Chinese Mischivirus A (Wu et al., 2012). In parallel, the regression analysis implemented in TempEst software to assess the temporal signal within the mischivirus dataset exhibited no association between sampling times and root-to-tip genetic distances, subsequently excluding any molecular clock dating ($R^2 = 0.0829$). Furthermore, the phylogeny-trait association analysis tests (AI = 0.028, PS = 2) statistically supported the clustering of bat mischivirus (n = 16) when considering the host genus ($p < 0.05$). The null hypothesis of no association between phylogeny and host species was retained based on the association index test (AI = 0.38, $p = 0.065$). However, it was rejected when considering the parsimony score test (PS = 3, $p = 0$). The MC statistic supported the association for both *Miniopterus* (MC = 12, $p = 0.001$) and *Hipposideros* (MC = 3, $p = 0.001$) genera, in addition to the *M. schreibersii* species

(MC = 12, p = 0.001). Similarly, the association index (AI = 0.029, p = 0.003) implied a strong phylogeny-trait association when examining the continent sampling, while the parsimony score (PS = 3, p = 0.23) exhibited no significant relationship. Additionally, since the majority of samples originated from Europe, the MC parameter supported the association between the phylogeny and the character-trait Europe (MC = 10, p = 0.009). Unsurprisingly, individual traits (single countries, species) consistently provided non-significant results.

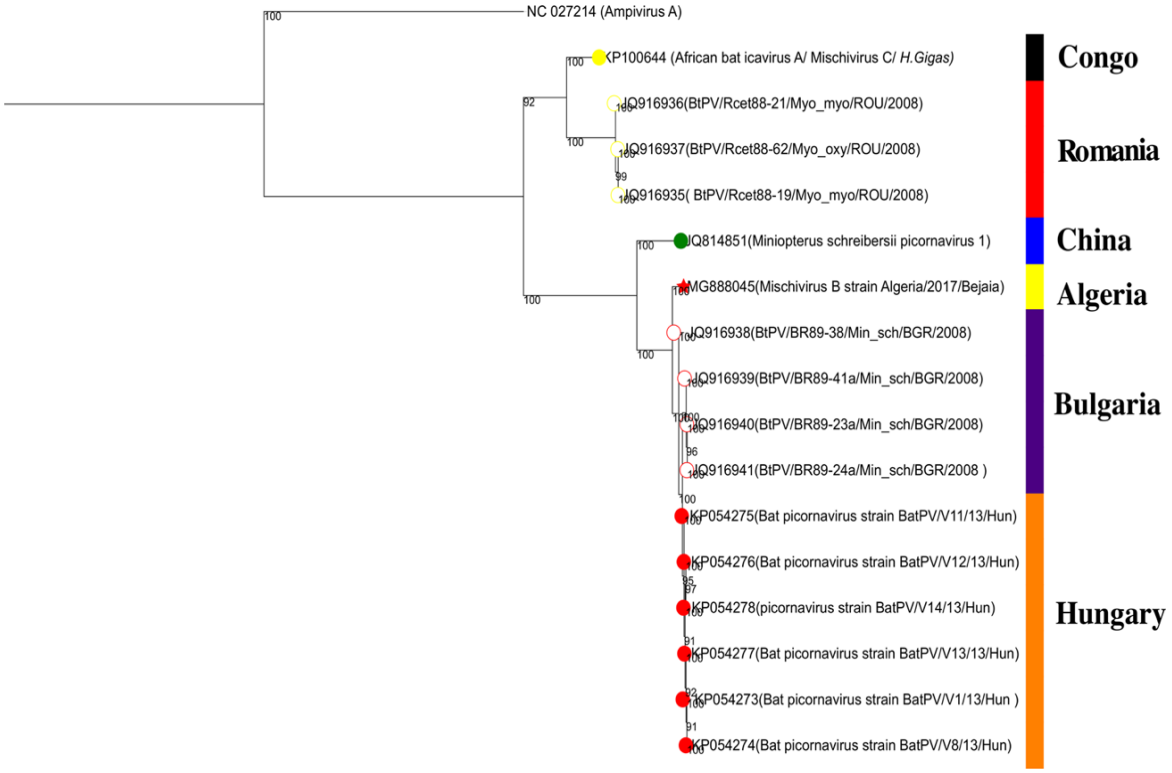

Figure 8. Bayesian phylogenetic tree of mischiviruses based on RdRp full and partial genes. The analysis was achieved using MrBayes. 3.2.4. ten million generations were performed. Posterior probabilities are indicated at the nodes. Branch symbols indicate Mischivirus species. Yellow color: Mischivirus C species, green: Mischivirus A species, red: Mischivirus B species. Solid circles indicate ICTV classified viruses, empty circles indicate the unclassified viruses, and the new Algerian Mischivirus is represented with a star.

Moreover, in a dataset comprising ICTV classified mischiviruses and the novel Algerian sequence, topological similarities were observed between mischiviruses and their hosts' phylogenies, indicating, at first, a co-divergence evolutionary scenario. However, this was not supported by the reconciliation analysis using Jane, based on the least costly event (data not included). When extending the dataset to all putative and classified mischiviruses, incongruence between mischiviruses and their host's phylogenetic trees were observed, while the reconciliation analysis revealed how host-jumping events were involved in the evolution of mischiviruses (Fig 9)

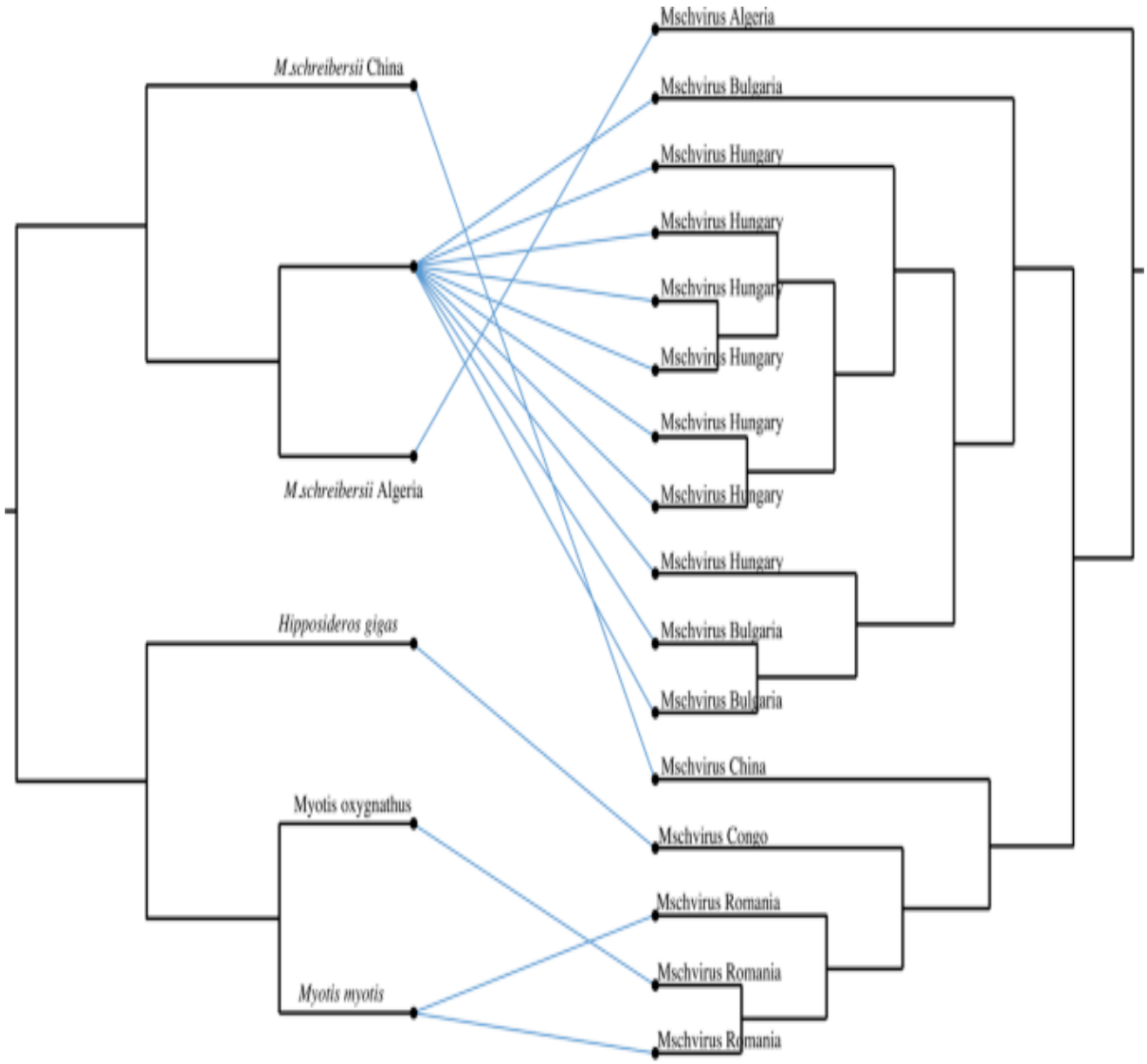

	Co-spetiation	duplication	Host switch	loss	Failure to diverge	cost
other events = 1	0	9	6	0	0	15
other events = 0"	0	9	6	0	0	0
< other events	3	9	3	0	0	12

Figure 9. Tanglegram and Jane result from all mischiviruses and their hosts.

From another perspective, an extensive phylogenetic analysis englobing all available bat picornaviruses (Fig 10) demonstrated both host genus and sampling locations clustering in some areas of the tree, whereas in other areas it was scattered. In regard to bat mischiviruses, they clustered according to host genus, and sampling location for each virus

species (Fig 8). Same as the mischiviruses dataset, when assessing the temporal signal for all bat picornaviruses tip dating, phylogenetic analysis was excluded ($R^2 = 0.0218$).

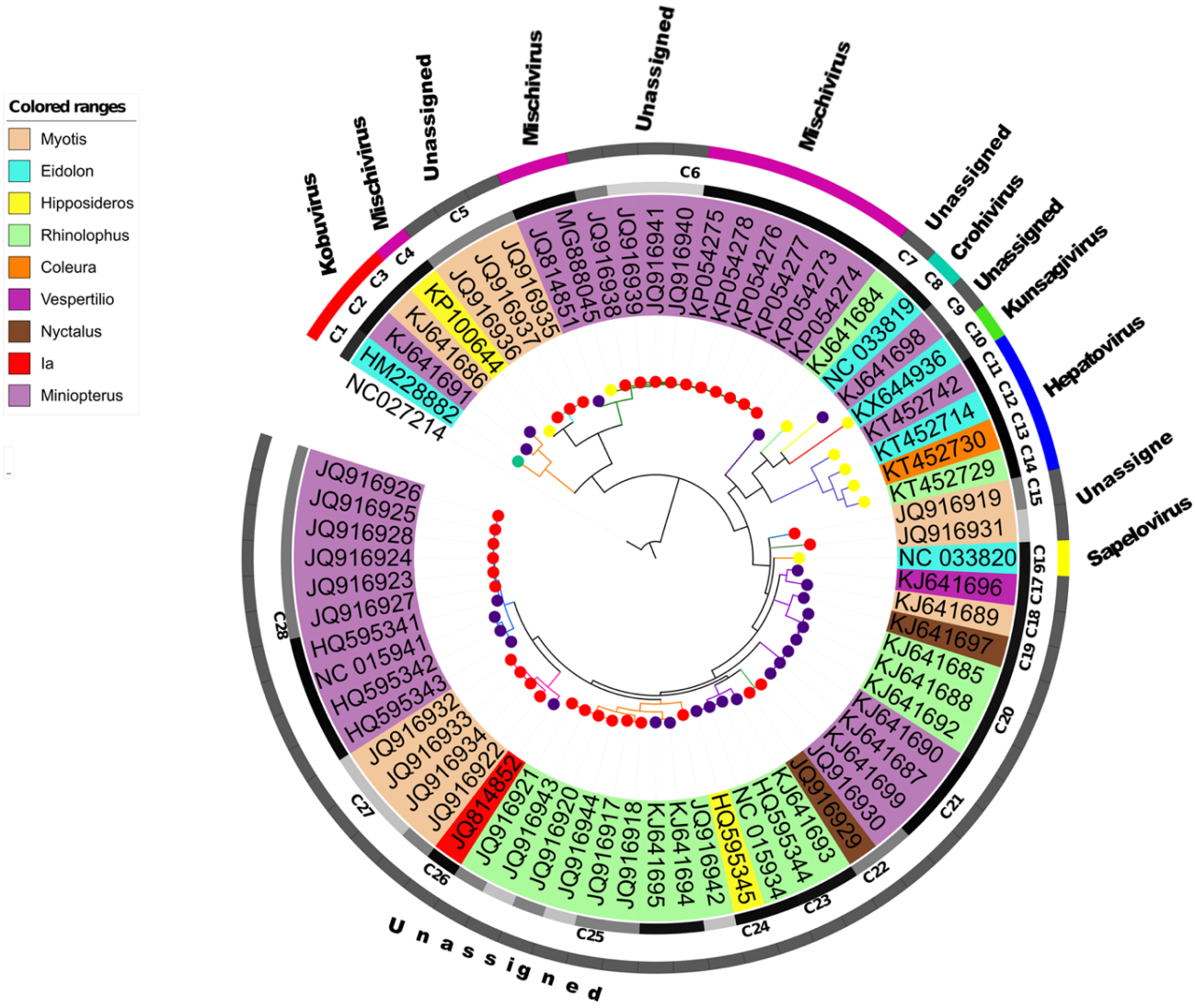

Figure 10. A Bayesian analysis of all bat picornaviruses based on 70 RdRp sequences, rooted using ampivirus A sequence (NC027214). Branch lengths indicate the number of substitutions per site. Genus-specific clusters are colored, based on bat genus. Solid circles represent Large-scale sampling locations, red for Europe, purple for Asia, yellow for Africa, and chartreuse for America. The bar encircling the tree represents the RdRp length range, sequences <500 bp are colored in light grey, sequences between 700 bp and 900 bp in dark grey, and black for sequences >1,000 bp. ICTV virus classification is indicated, if and when available.

Additionally, when performing the Bayesian Tip-association Significance testing analysis (BaTS) for all BtPVs ($n = 69$), AI and PS provided associations support ($p < 0.05$) when considering host genus (AI = 2.25, PS = 21), host species (AI = 3.47, PS = 32), and large-scale sampling area (AI = 0.60, PS = 15). Additionally, the MC statistics characteristic of each geographical location, host genus, and host species respectively indicated the continents Europe (MC = 10), Africa (MC = 4), and Asia (MC = 5), in addition to the host

genera Miniopterus (MC = 12), Myotis (MC = 4), and Rhinolophus (MC = 9), also the species *M. schreibersii, M. myotis, R. euryale, M. magnate, R. sinicus* and *M. fuliginosus* were not randomly distributed on the tips of the corresponding phylogenetic tree ($p < 0.05$). 28 different bat genus-specific clusters were identified based on the phylogenetic analyses (Fig 10): three bat genera in *Kubovirus* species, three in Mischivirus, one in Crohivirus, one in Shanbavirus, one in Kunsagivirus, one in Sapelovirus, four in Hepatovirus, and 14 clusters in different unassigned viruses. Likewise, we counted six PV phylogenetic clusters regarding the Miniopterus genus, five for Myotis, five for Rhinolophus, five for Eidolon, two for Hipposideros, two for Nyctalus, one for Coleura, and one for Ia. Since these BtPVs are associated with different host species and sampling locations, the number of RdRp sequences and/or host species tallied for each cluster vary. Strikingly, several of the clusters are composed of a single BtPV sequence. A very strong correlation was observed among the number of BtPV specific clusters and both its species richness ($r = 0.94$; $p = 0.0001$), and geographical sampling area ($r = 0.84$; $p = 0.002$). Obviously, accurate classification is dependent upon the length of the viral sequences, nonetheless, even short BtPv RdRp sequences permitted us to acquire a primary classification of the unassigned sequences. Complementary to this, the result of pairwise genetic distances reflected the vast diversity within BtPV. For instance, the mean nucleotide divergence between sequences from cluster C5 (*Myotis*) and C4 (*Hipposideros*) imply their close relatedness, thereby the unclassified sequences from C5 may belong to the genus *Mischivirus* (Table 2 and Fig 10). Notably, different virus species may be isolated from the same bat genus, thus explaining the percentage of differences observed among sequences belonging to the same host genus. By way of illustration, mean nucleotide and amino-acid divergence observed within the same genus were 36% and 54.8% for Miniopterus; 45.6% and 60.3% for Myotis; 40% and 45.7% for Rhinolophus; 55.3% and 78.5% for Hipposideros; 44% and 52.3% for Nyctalus; 58.7% and 75.5% for Eidolon.

Table 2. The numbers of nucleotide and amino-acid differences within and between clusters are shown in percentage with standard error obtained by 1,000 bootstraps. Abbreviations: [a] distances were calculated among sequences >700 bp; n/c: clusters which have a single sequence; [b] mischivirus clusters are indicated in italic bold.

Cluster b	Host genus	Mean within clusters amino-acid pairwise distances	Mean within clusters nucleotide pairwise distances	Mean between clusters nucleotide distances from the closest group a	Mean between clusters amino-acid distances from the closest group
C1	*Eidolon*	n/c	n/c	38.8% (0.018) C2	47.7% (0.06) C2
C2	*Miniopterus*	n/c	n/c	38.8% (0.018) C1	47.7% (0.06) C1
C3	*Myotis*	n/c	n/c	27.8% (0.021) C2	40% (0.06) C2
C4	***Hipposideros***	**n/c**	***n/c***	**52.6% (0.021) C3**	**70.8% (0.05) C3**
C5	*Myotis*	2.1% (0.014)	1.3% (0.003)	25.1% (0.016) C4	29.2% (0.05) C4
C6	***Miniopterus***	***13.3% (0.023)***	***8.4% (0.006)***	**39.9% (0.016) C5**	**57.8% (0.06) C4**
C7	*Rhinolophus*	n/c	n/c	54.5% (0.018) C3	58.5% (0.06) C3
C8	*Eidolon*	n/c	n/c	55.9% (0.019) C5	73.8% (0.05) C5
C9	*Miniopterus*	n/c	n/c	50.1% (0.019) C8	60% (0.06) C8
C10	*Eidolon*	n/c	n/c	56.2% (0.018) C9	72.3% (0.05) C9
C11	*Miniopterus*	n/c	n/c	55.6% (0.018) C7	61.9% (0.05) C8
C12	*Eidolon*	n/c	n/c	36.4% (0.018) C11	43.1% (0.06) C11
C13	*Coleura*	n/c	n/c	35% (0.019) C12	33.8% (0.06) C12
C14	*Rhinolophus*	n/c	n/c	31.1% (0.019) C13	30.8% (0.06) C13
C15	*Myotis*	n/c	n/c	50.5% (0.019) C4	70% (0.05) C11
C16	*Eidolon*	n/c	n/c	43% (0.019) C15	60.8% (0.05) C15
C17	*Vespertilio*	n/c	n/c	37.4% (0.019) C16	50.8% (0.06) C16
C18	*Myotis*	n/c	n/c	30.1% (0.018) C17	41.5% (0.06) C17
C19	*Nyctalus*	n/c	n/c	35.5% (0.018) C17	44.6% (0.05) C17
C20	*Rhinolophus*	10.3% (0.030)	4.1% (0.006)	28.8% (00.17) C19	35.9% (0.05) C19
C21	*Miniopterus*	27.4% (0.032)	19.1% (0.01)	40.7% (0.016) C15	54.2% (0.05) C20
C22	*Nyctalus*	n/c	n/c	28.1% (0.014) C21	43.1% (0.05) C21
C23	*Rhinolophus*	13.3% (0.032)	12.8% (0.01)	37% (0.016) C21	43.6% (0.05) C17
C24	*Hipposideros*	n/c	n/c	6.4% (0.005) C23	43.1% (0.06) C17
C25	*Rhinolophus*	23.5% (0.030)	18.7% (0.01)	35.3% (0.018) C24	44.8% (0.05) C23
C26	*Ia*	n/c	n/c	35.4% (0.017) C25	44.6% (0.06) C19
C27	*Myotis*	n/c	n/c	22.4% (0.018) C26	29.6% (0.05) C26
C28	*Miniopterus*	11.5% (0.026)	9.5% (0.007)	29,2% (0.019) C27	37.7% (0.05) C27

Despite what preceded, Jane analysis displayed increased duplication and host switch events than when compared with co-divergence events, independently of co-divergence costs (Table 3). The least costly events represented the best evolutionary scenario. The analysis helped us to determine hypothetic donors and receptors in cross-species transmission events. Further inconsistency was observed above all BtPVs, and their hosts' phylogenies indicated their evolution through more host-jumping events than co-speciation events (fig 11).

Table 3. Reconciliation analysis for all bat PVs. Co-phylogenetic reconciliation analysis (Jane) of all bat PVs sequences and their hosts displaying the frequency of different evolutionary scenarios. Abbreviation: least costly events (cost = 0).

	Co-speciation	Duplication	Host switch	Loss	Failure to diverge	Cost
Co-speciation = other events = 1	2	27	39	4	1	73
Co-speciation = other events = 0[a]	0	27	41	5	1	0
Co-speciation < other events	5	25	38	4	1	68

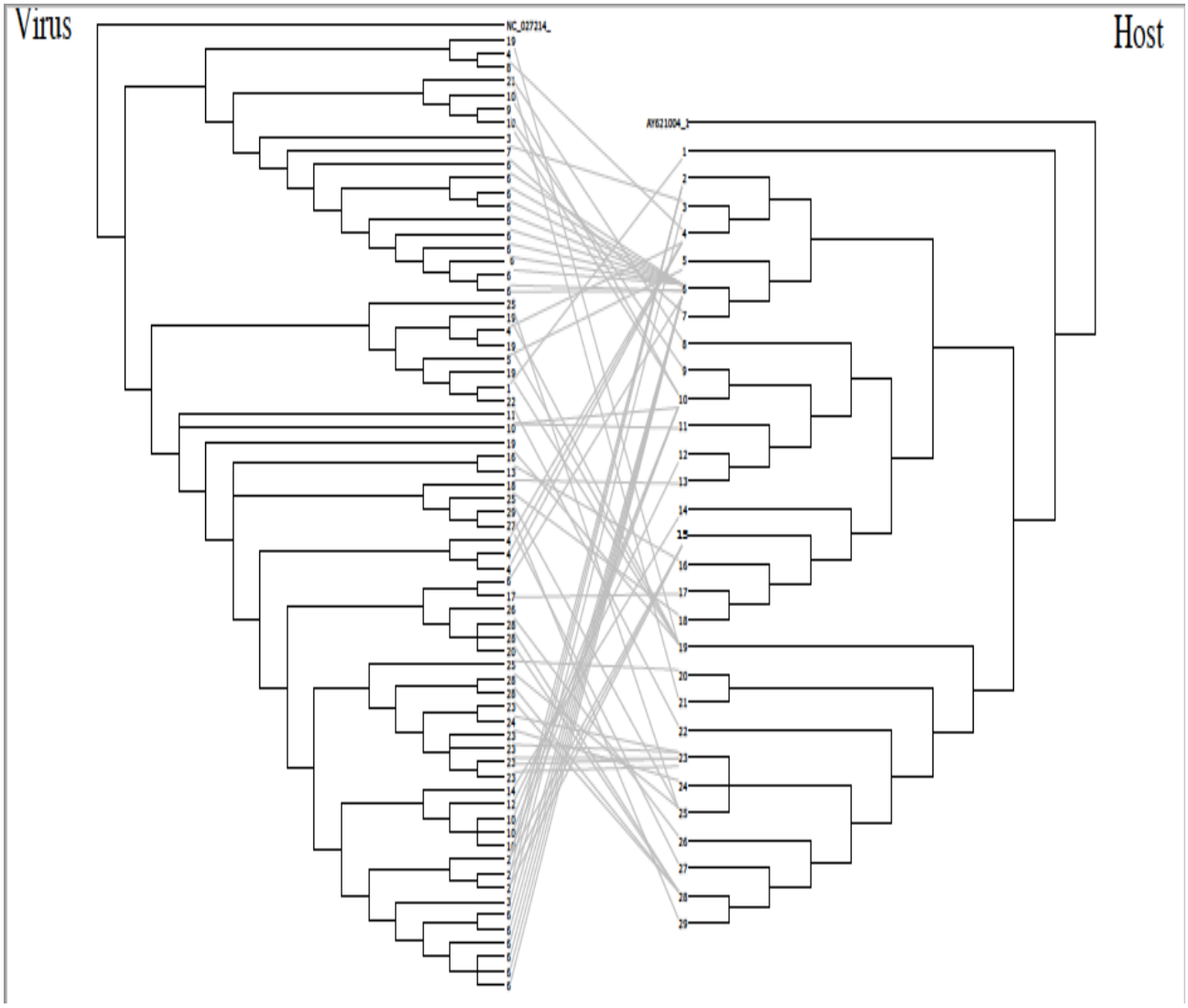

Figure 11. Tanglegram for all bat picornaviruses and their hosts. NC_027214 Ampivirus A Virus phylogeny outgroup, AY621004 *Furipterus horrens* host phylogeny outgroup, each number on the host tree indicates a bat species while the same number on the virus tree indicates the bat species related viruses. *1: Coleura afra, 2: Miniopterus magnater, 3: Miniopterus schreibersii, 4: Miniopterus fuliginosus, 5: Miniopterus manavi, 6: M. schreibersii Hungary, 7: M.schreibersii Algeria, 8: Myotis ricketti, 9: Myotis oxygnathus, 10: Myotis myotis, 11: Myotis bechsteini, 12: Myottis dasycneme, 13: Myotis altarium, 14: Ia io, 15: Pipistrellus abramus, 16: Vespertilio superans, 17: Nyctalus noctule, 18: Nyctalus plancyi, 19: Eidolon helvum, 20: Hipposideros armiger, 21: Hipposideros gigas, 22: Rhinolophus landeri, 23: Rhinolophus euryale, 24: Rhinolophus blasii, 25: Rhinolophus ferrumequinum, 26: Rhinolophus hipposideros, 27: Rhinolophus affinis, 28: Rhinolophus sinicus, 29: Rhinolophus Lepidus.*

Furthermore, to assess recombination among bat picornaviruses, two methods were used. First, phylogenetic tree inference based on P1, P2, and 3Dpol regions of BtPVs genomes displayed discordances in their structures indicating potential recombination events (Fig. 12a–c). Complementary to this, recombination analysis using the RDP 4 demonstrated that out of the 69 detected recombination, only 11 unique putative events were identified with two or more methods and were, therefore, considered significant (Table 4).

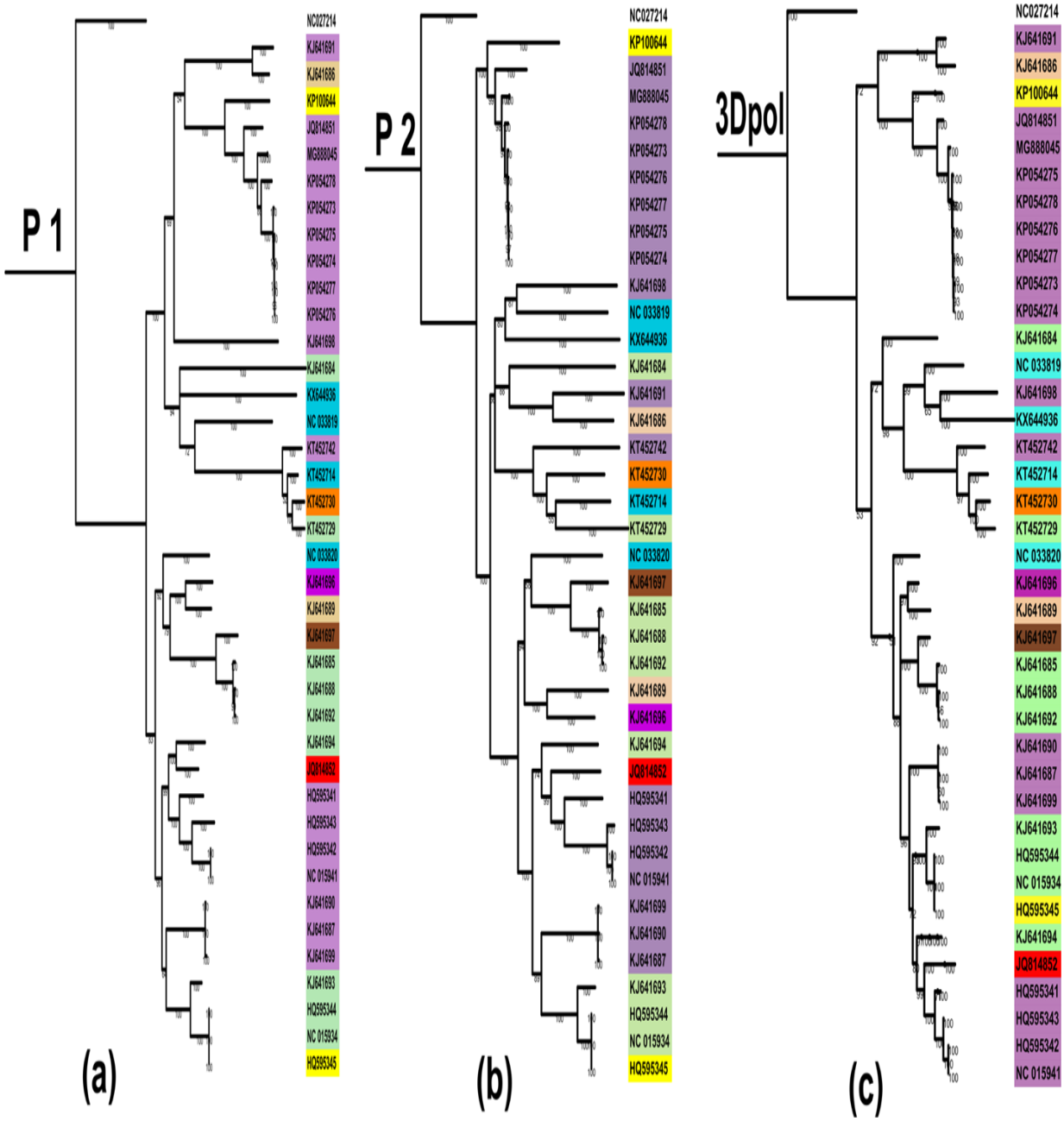

Figure 12. (a) Bayesian phylogenetic reconstruction of the P1 region for all BtPVs genomes included in this study. **(b)** Bayesian phylogenetic reconstruction of the P2 region for all BtPVs genomes included in this study. **(c)** Bayesian phylogenetic reconstruction of the RdRp region for all BtPVs genomes included in this study. Ampivirus A sequence (NC027214) was used as an outgroup for the three viral phylogenetic trees. Genus-specific clusters are colored, based on bat genus. Recombination may be reflected in tree structure incongruities between phylogenetic trees **(a–c).**

Table 4. Summary of recombination events detected by six algorithms within the Recombination Detection Program RDP4. RS: recombinant sequence. Beg: begin. ND: not detected.

RS	Breakpoint position in recombinant sequence		Parental sequence(s)		Score for the detection methods in RDP (P value)					
	Beg	End	Major	Minor	RDP	GENECONV	Bootscan	Maxchi	Chimaera	SISscan
HQ595342	81	24	HQ595343	KJ641694	0.05	ND	ND	ND	ND	> 0.05
KP100644	228	329	MG888045	Unknown	ND	ND	ND	> 0.05	> 0.05	ND
KJ641696	847	015	KJ641697	NC_027214	0.05	ND	ND	ND	ND	ND
KP054278	703	850	Unknown	KP054276	ND	ND	> 0.05	> 0.05	> 0.05	> 0.05
HQ595341	32	15	NC_015941	KJ641693	ND	ND	ND	> 0.05	> 0.05	> 0.05
KT452729	04	85	KT452730	KT452714	> 0.05	> 0.05	> 0.05	> 0.05	> 0.05	> 0.05
KT452742	232	579	Unknown	KT452730	> 0.05	> 0.05	ND	> 0.05	> 0.05	> 0.05
KT452714	407	509	KT452742	Unknown	ND	ND	> 0.05	> 0.05	ND	> 0.05
HQ595341	972	185	KJ641694	NC_033820	ND	ND	ND	> 0.05	ND	> 0.05
KP100644	090	185	KP054278	Unknown	ND	ND	ND	> 0.05	ND	> 0.05
HQ595343		615	JQ916923	NC_015941	> 0.05	> 0.05	ND	> 0.05	> 0.05	> 0.05

4.1.2. *Coronaviridae*

It is well-established bats serve as reservoir hosts regarding Coronaviruses, with relatively high commonalities and a striking genetic diversity, thus being responsible for the potential emergence of novel human coronaviruses (HCoVs) when proximity among humans and bats occurs (Ar Gouilh et al., 2018). Among the six sequenced bat-related coronaviruses, four pertained to the *Alphacoronavirus* genus and were detected in the following species: *Miniopterus schreibersii*, *Plecotus gaisleri, Rhinolophus ferrumequinum,* and *Myotis punicus*. Notably, Betacoronaviruses were spotted in *Rhinolophus ferrumequinum* and *Myotis punicus*. The sequence's length ranged between 259 and 875 bases' pair. Additional details regarding the sample's name, the related virus, and host, in addition to the detection and sequencing methodology, are summarized in Table 5. The nucleotide blast demonstrated the sequence MN701038 shared 96.37% identity with

an alphacoronavirus isolated from *Miniopterus fuliginosus* in China (KJ473799). Similarly, the sequence MN823618 had 92.89% identity on the nucleotide level with a betacoronavirus isolated from a *Rhinolophus ferrumequinum* bat in France (KY423411) and co-circulated with an alphacoronavirus. The later sequence was obtained from the helicase gene and shared 82.54% identity with a Chinese alphacoronavirus sequence found in the same host (EF434378). Similarly, 94.78% nucleotide identity was observed between MN701039 and a French alphacoronavirus sequence detected in *Rhinolophus ferrumequinum* (KY423475). Furthermore, 84.90% identity was noticed on the nucleotide level among MN823619 and KY423411 previously mentioned. Finally, the Alphacoronavirus sequence MN823620 achieved 97.96% nucleotide identity with the Algerian sequence MN701038 and 96.17% with the Chinese sequence KJ473799 recovered from the same host species.

Table 5. Coronavirus positive samples with their corresponding sampling location, genus, host species detection and sequencing method, the target gene, and sequence's length.

Seq ID	Sampling location	CoV Genus	Host	Detection/ Sequencing	Gene	Sequence length (bp)	Accession number
11	Constantine	Alpha	*Myotis punicus*	RT-PCR/Sanger	RdRp	413	MN701038
12	Constantine	Alpha Beta	*Rhinolophus ferrumequinum*	Metagenomics/ NGS RT-PCR/Sanger	Hel RdRp	875 259	OL468025 MN823618
15	Constantine	Alpha	*Plecotus gaisleri*	RT-PCR/Sanger	RdRp	346	MN701039
16	Constantine	Bets	*Myotis punicus*	RT-PCR/Sanger	RdRp	392	MN823619
23	Bejaia	Alpha	*Miniopterus schreibersii*	RT-PCR/Sanger	RdRp	393	MN823620

Interestingly, the phylogenetic analysis based on the helicase gene demonstrated the belonging of the Alpha_CoV/Algeria (OL468025) to the decacovirus subgenus. This sequence was cocirculating with MN823618 betacoronavirus in a *Rhinolophus ferrumequinum*. It formed a monophyletic clade with EF434378 recovered from the same host in China and MK720946 Rhinolophus bat coronavirus HKU32 obtained from *Rhinolophus sinicus* in Hong Kong (Fig 13). The phylogenetic tree based on the RdRp gene and englobing 806 sequences including our Algerian sequences demonstrated the clustering of MN823619 and MN823618 (bootstrap=100) with Z558550 SARS-like coronavirus isolated from *Rhinolophus ferrumequinum* in Korea (bootstrap=100) and were related to KP876546 SARS-like coronavirus detected in *Rhinolophus affinis* in China (Fig 14).

Similarly, MN701038 clustered with MZ558551and MZ558551 alphacoronaviruses isolated from mixed bat colonies in Croatia (bootstrap 95 % and 100 %, respectively) and was related to the Algeria sequence MN823620 described above (bootstrap 100). Based on the phylogeny, these sequences are related to Miniopterus bat coronavirus HKU8. Lastly, the MN701039 sequence clustered within the unclassified coronaviridae group together with the Kenyan sequence MH170123 isolated from a Rhinolophus bat.

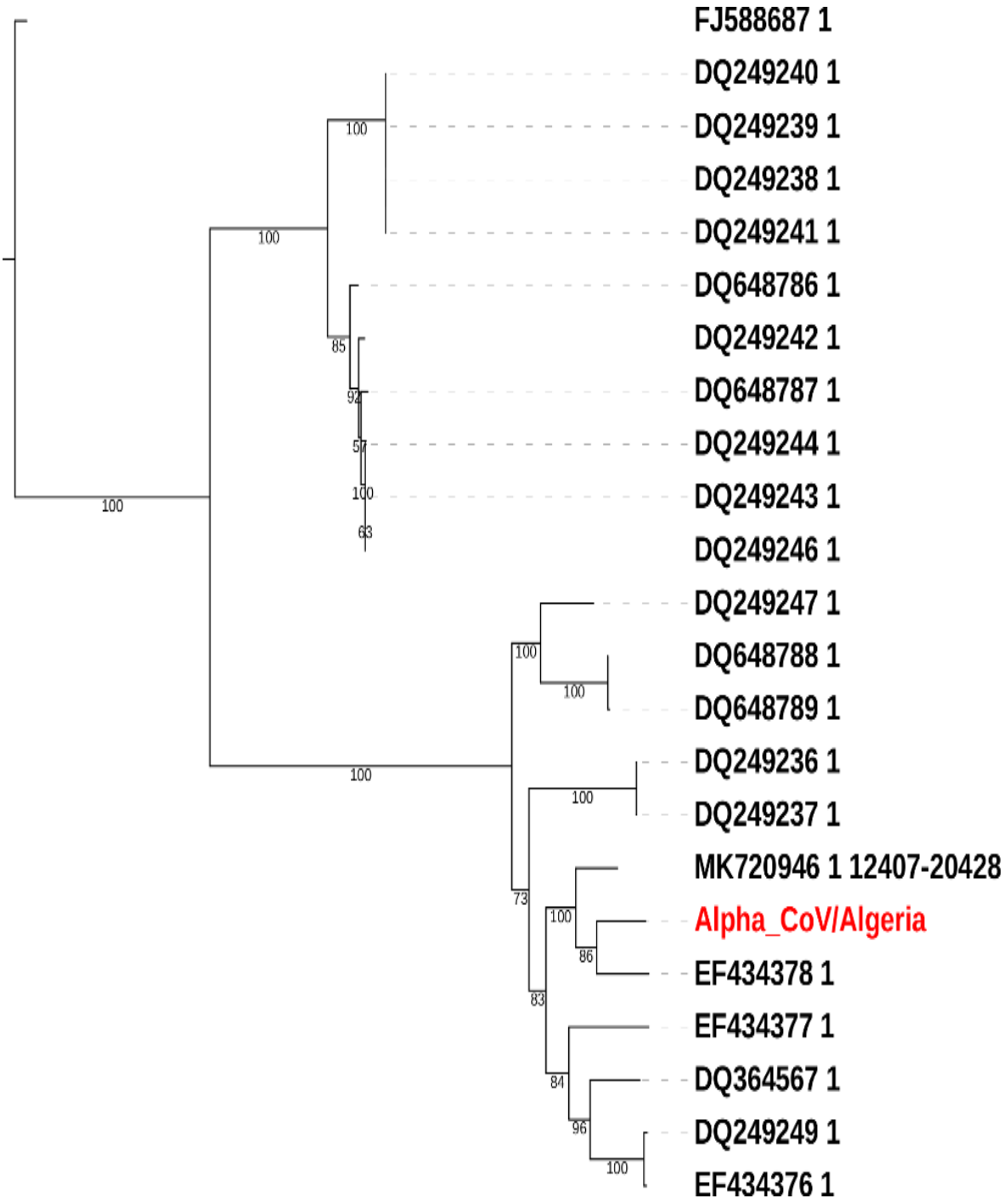

Figure 13. Maximum likelihood phylogenetic tree based on twenty-four partial helicase sequences. SARS-CoV FJ588687 was used as an outgroup. The Algerian sequence is indicated in red. Bootstrap values are mentioned at each node.

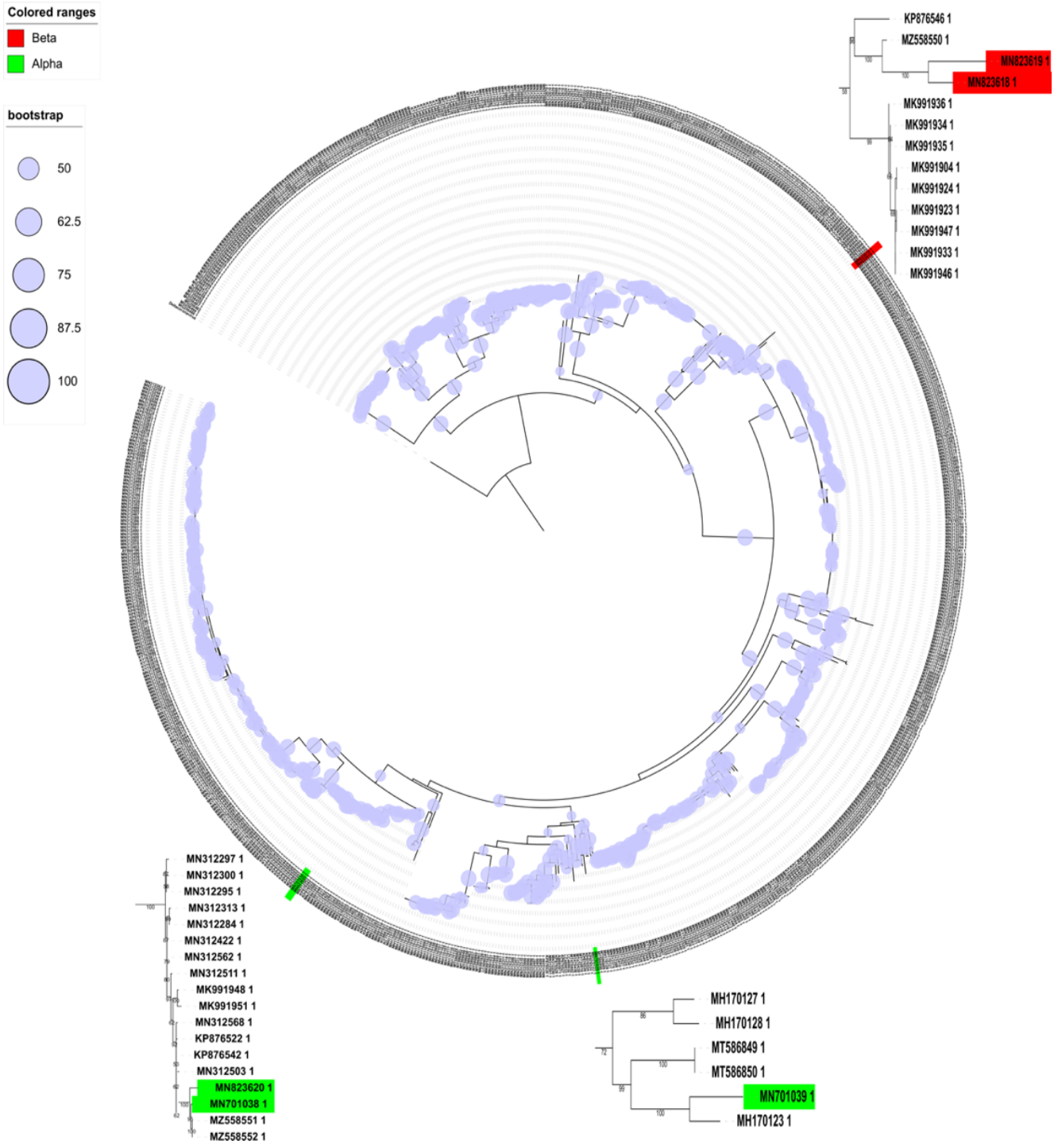

Figure 14. Maximum likelihood phylogenetic tree based on eight hundred six partial RdRp bat-related sequences demonstrating the clustering of the novel detected Algerian coronaviruses. Bootstrap values are indicated at each node with a circle, the size is proportional to the bootstrap value. The Algerian alpahacoronaviruses are indicated in green, whereas the Algerian betacoronaviruses are in red**.**

4.2. Human samples

4.2.1. *SARS-CoV-2*

In order to examine the spread of SARS-CoV-2 in Algeria, we performed an exhaustive analysis of all the complete and partial 29 SARS-CoV-2 sequences available from Algeria in addition to 66 sequences sampled worldwide. First, when inspecting the exponential and Skyline coalescent priors, the former prior was less suitable for the Algerian dataset, thus, only results under the Skyline plot model were considered for downstream analysis. The estimated MRCA regarding the Algerian pandemic was 28 January 2020 [29 October 2019 and 29 February 2020] and the SARS-CoV-2 evolutionary rate for the global pandemic was 5.4043 × 10^{-4} substitution/site/year [5.2458 × 10^{-4}, 8.2507 × 10^{-4}]. Furthermore, based on the maximum clade credibility tree (MCC) (Fig 15), multiple introductions were blatant via the interspersion of the Algerian sequences within the phylogenetic tree. This indicates multiple origins of the SARS-CoV-2 pandemic in Algeria.

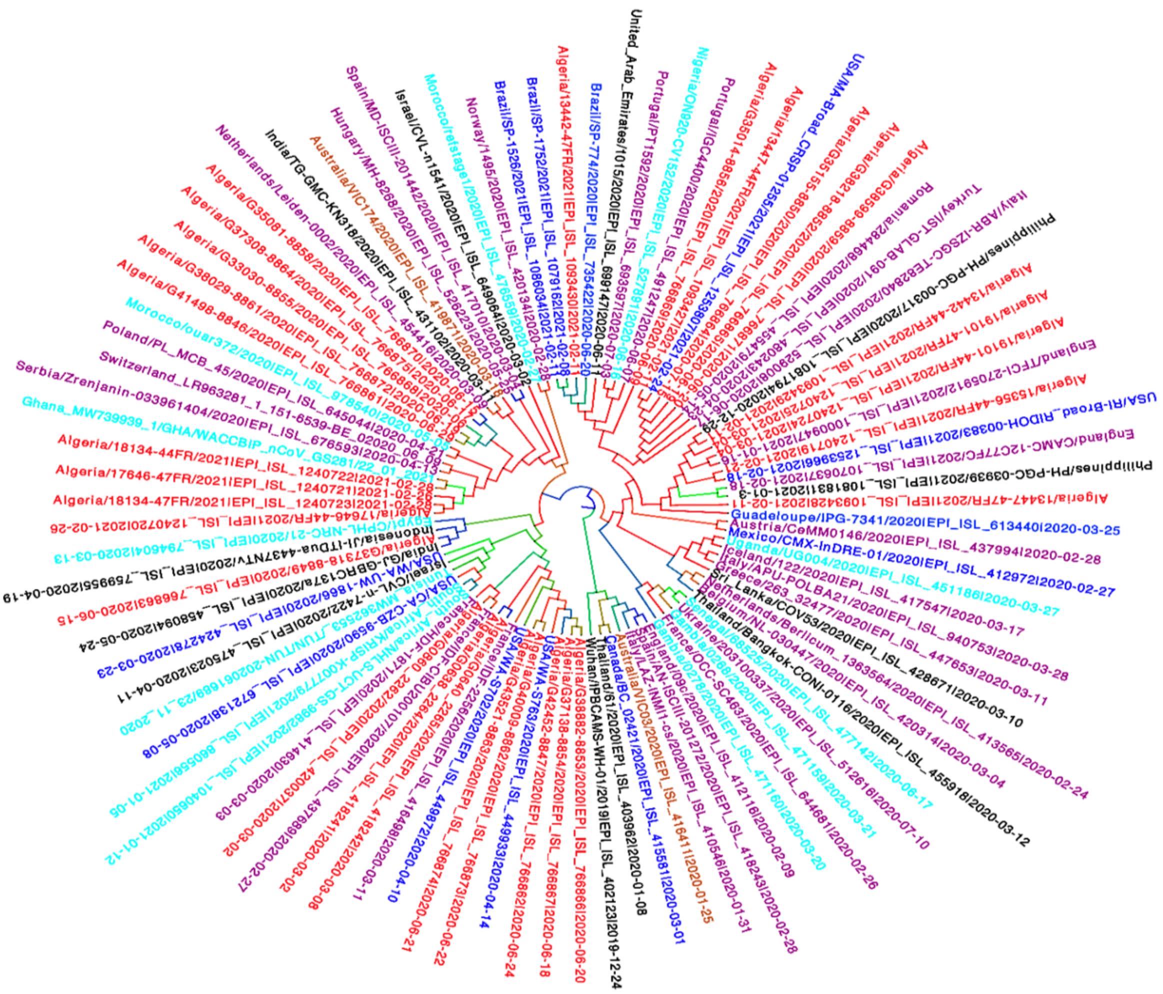

Figure 15. Bayesian phylogenetic trees implemented using BEAST v1.10.4 based on ninety-five genomes sampled worldwide. Colors indicate sampling locations. Blue represents sequences from America; Purple indicates sequences from Europe; Black shows sequences from Asia; Cyan for sequences from Africa; sequences from Australia are labeled in orange and sequences from Algeria are indicated in red.

While considering the Algeria complete lockdown starting from mid-March 2020, all transmissions occurring following this date are either local or a result of Algerian repatriation. Nevertheless, the impact of domestic travel during the pandemic spread can be clearly ascertained (Fig 16). For instance, hCoV-19/Algeria/18134-44FR/2021|EPI_ISL_1240722|2021-02-28 (Ain Salah) formed sister taxa together with hCoV-19/Algeria/17646-44FR/2021|EPI_ISL_1240720|2021-02-26 (Ouargla) supported with high posterior probability (PP = 98%). Interestingly, these sequences, rather than clustering with sequences from the same provenance, formed a monophyletic clade with sequences from Algiers (PP = 1).

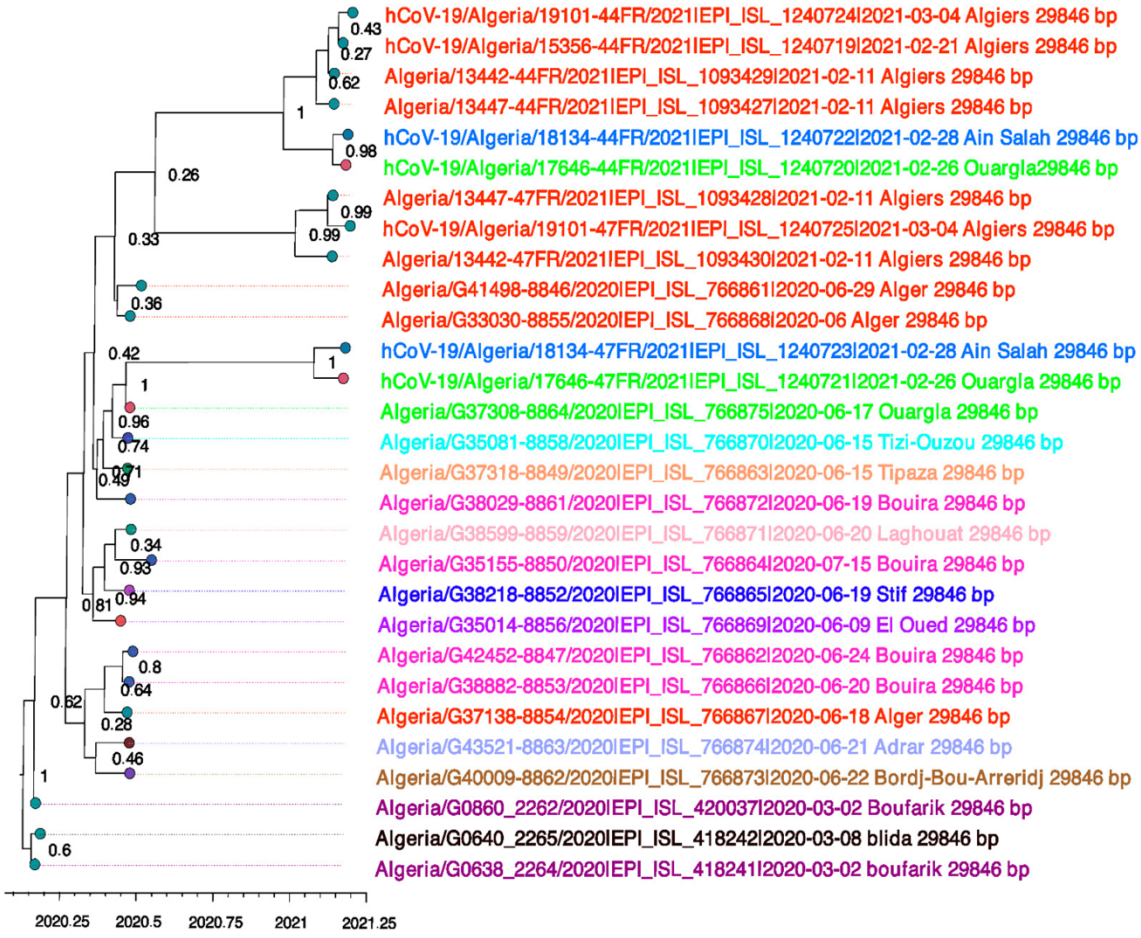

Figure 16. Maximum clade credibility tree. A Bayesian phylogenetic tree was reconstructed using twenty-nine Algerian genomes. Posterior probabilities are indicated at each tree node. Branches are time-scaled in decimal years. Sequences are colored according to their sampling location.

Moreover, to highlight the diffusion route regarding the SARS-CoV-2 in Algeria, both discrete and continuous approaches were used. As for discrete phylogeographic analysis, while relying on the Bayesian stochastic search variable selection/BSSVS and Bayes factor calculation, 14.1 non-zero-rates between cities were identified [95% HPD = 14–16], of

which, 12 migration rates were well-supported (BF > 3) (Fig 17A). The transmission started from Boufarik towards Blida and Bouira, then from Bouira to Adrar, Algiers, Setif, Ouargla, El Oued, and Tipaza, after which, from Ourgla to Tizi Ouzou. Setif to Laghouat, subsequently from Adrar to Bordj Bou Arreridj, and finally, from Bouira to Ouargla and Ouargla to Ain Salah (Fig 17B). In parallel, based on the reconstruction of the ancestral viral location coordinates assumed from the latitude and longitude of the sampling locations, a continuous dispersion model was employed to acquire a more detailed overview of the diffusion process. The estimated diffusion rate was 1620.3 km/year. The root coordinates corresponded to Bouinan in Blida. Furthermore, the transmission route started from Blida to Boufarik and back to Blida, following this, Bouira to El-Oued, Tizi Ouzou, and Tipaza, then from Bouira to Sétif, Laghouat, and Adrar, thereafter Bouira and Algiers towards Ouargla, and from Ouargla to Ain-Salah (Fig 17C)

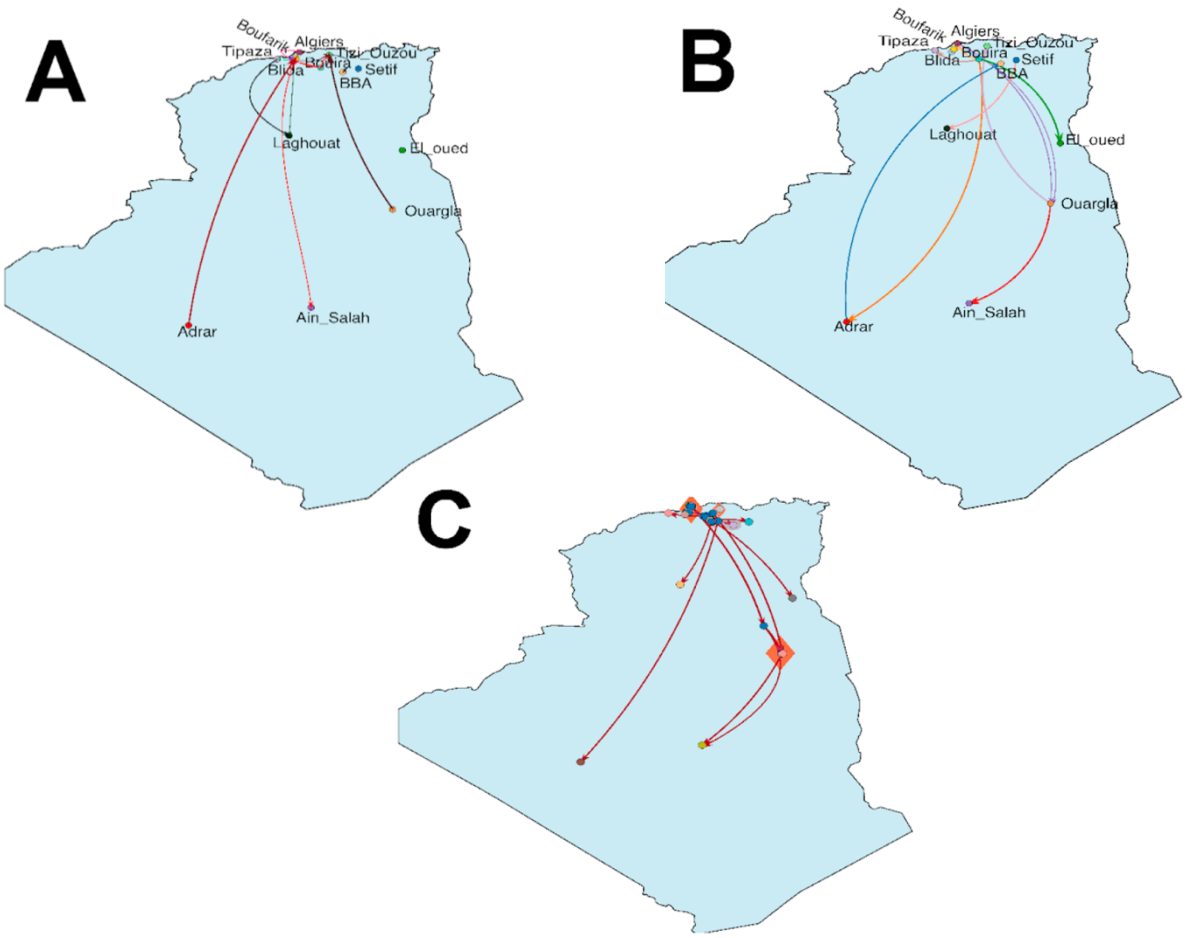

Figure 17. (A) Bayes factors represent significant discrete transitions. (B) SARS-CoV-2 diffusion in discrete areas in Algeria. The arrows indicate the spread direction, and they are colored differently to distinguish different transmission routes. (C) SARS-CoV-2 spread in continuous areas in Algeria. The arrows indicate the diffusion direction; they are colored according to posterior probabilities (gradient from blue = 0.3 to red = 0.8–1), polygons display the uncertainty, and are colored according to the posterior probabilities (gradient from blue = 0.3, to orange = 0.8–1). Blue circles indicate internal nodes, (B & C) different colored circles indicate the sampling locations.

Similarly, when considering the Wuhan reference sequence and the 18 Algerian complete genomes, the evolutionary selection pressure was assessed for each of the following genes: *ORF1a, ORF1b, S, N, M, ORF3a, and ORF8*, based on both the codon-by-codon cumulative behavior plots for synonymous and non-synonymous substitutions displayed in Fig 18 and the calculated values of the non-synonymous (dn) to synonymous (ds) mutations ratio (ω). In the *ORF1a* gene, for the first 200 codons, only a moderate rate of synonymous mutations was observed, then it was stationary. At the same time, the non-synonymous rates increased until the codon 1100. Subsequently, both synonymous and non-synonymous rates increased with higher synonymous mutations until the end of the coding region. The average regarding the pairwise (ω) ratio was 0.2. In parallel, at the beginning of the coding region of the *ORF1b* gene, only non-synonymous mutations were perceived until the codon 680, after which, both synonymous and non-synonymous mutation rates showed an alternating pattern between increase and stationary phases until the stop codon. Yet the non-synonymous rates were superior. The dn/ds ratio was equal to 0.22. Across the *S* gene, an increase in the synonymous rates was apparent from codon 208 with the alternance of sharp increase and stationary phases until codon 600, in which the non-synonymous rate leveled up with the same alternance pattern and a higher ds rate till codon 92. At this point, a neutral stationary phase was observed (ds = dn) until codon 1160 in which a higher synonymous rate was detected. The average ω ratio was 0.3. Similarly, in reference to the *M* gene, the codon-by-codon cumulative behavior demonstrated a sharp increase of the synonymous rate in the codon position 35, followed by a stagnant rate until codon 69, after which, a sharp rate increase in codon position 70, followed by a stationary phase until the end of the coding sequence. Interestingly, non-synonymous mutation cumulations were not observed, thus the calculated dn/ds ratio was <1 (0.3). As for the *N* gene, a higher non-synonymous rate was observed compared to the synonymous mutation rate. The ω ratio was 0.38. Likewise, the *E* gene displayed only a high non-synonymous mutation rate in the codon 72 with a dn/ds ratio equal to 0.08. Regarding the *ORF8* gene, codon positions 24 and 116 cumulated synonymous mutation rates with a constant rate between the two positions, whereas the codon position 120 cumulated non-synonymous mutations, the dn/ds was 0.25. Finally, the *ORF3a* displayed a higher cumulation rate of non-synonymous than synonymous mutations with a ω value of 0.33. All observed dn/ds values were less than one for all genes indicating negative selection pressure.

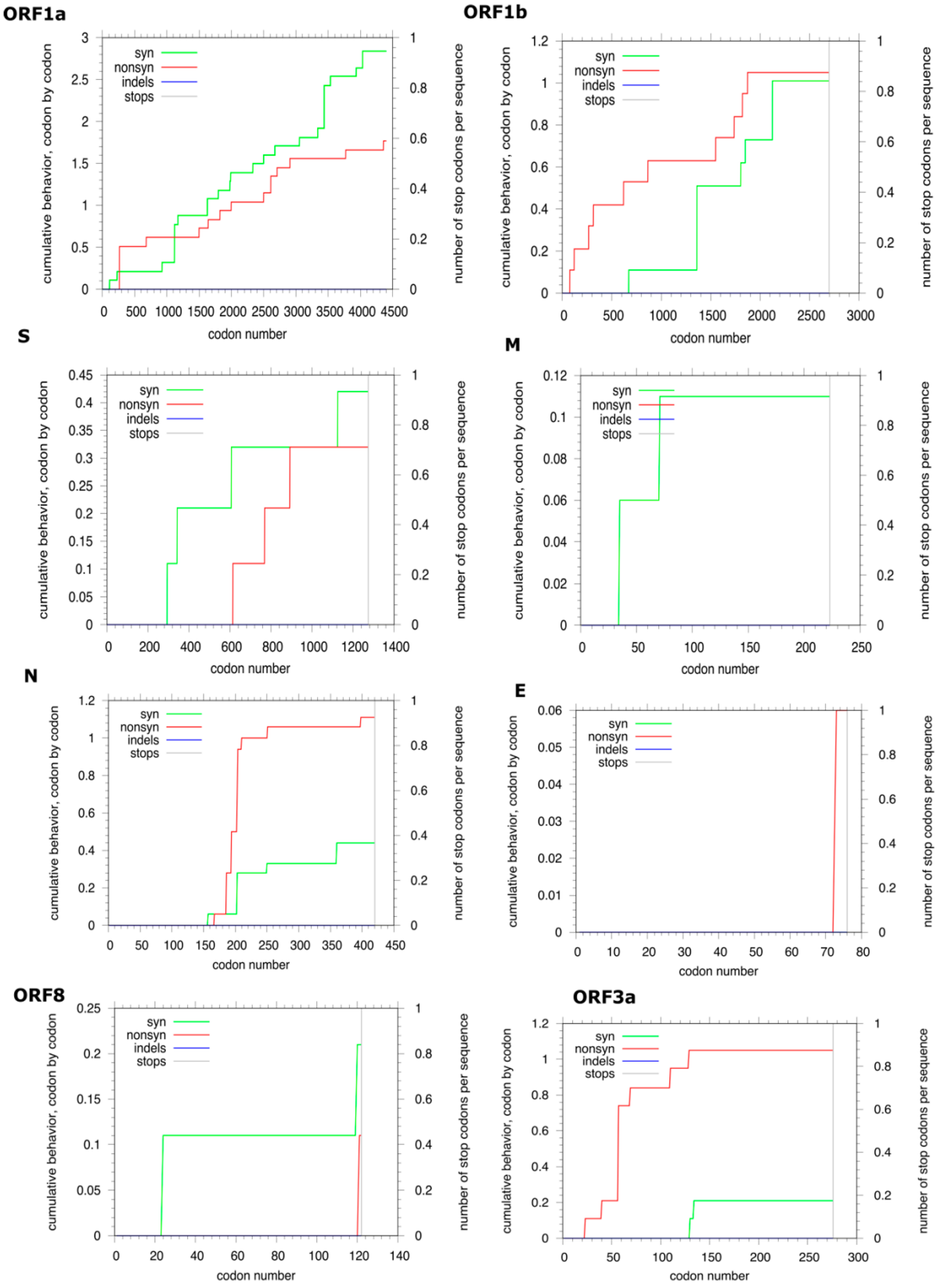

Figure 18. Cumulative behavior regarding synonymous and non-synonymous substitutions along each of the eight analyzed genes. Accumulation of amino acid substitutions for nineteen SARS-CoV-2 sequences is plotted. The x-axis represents codons for the entire coding region of each gene. The y-axis refers to the number of substitutions. The plot for synonymous substitutions is in red, while green depicts the non-synonymous substitutions. The grey vertical lines indicate stop codons.

Henceforth, based on genome lineage attribution established by Rambaut et al., and the GISAID clade classification, the Algerian sequences appertained to different lineages and clades (Elbe & Buckland-Merrett, 2017; Rambaut et al., 2020). Along with this, several SNPs were detected in the Algerian sequences in comparison with the reference sequence (NCBI RefSeq NC_045512). All results are included in Table 6

Table 6. Clades and lineages assigned to the Algerian sequences according to Gisaid and Pangolin classification respectively, in addition to all observed SNPs.

Query	Gisaid Pangolin	**SNPs**	**Query**	Gisaid Pangolin	**SNPs**
EPI_ISL_766874	GH B.1	C601T, C1059T, C3037T, C6255T, C8290T, C10582T, A13693G, C13829T, C14408T, A23403G, C25511T, G25563T, C29025T	**EPI_ISL_766861**	G B.1.597	C3037T, C3619T, C5144T, C10582T, C12367T, C14408T, C17550T, A23403G, C27804T, C28830A
EPI_ISL_766862	GH B.1.597	C1059T, C3037T, A4762C, C7765T, C10582T, C14408T, G15327T, A23403G, G25459A, G25563T, C27804T, C28830A	**EPI_ISL_420037**	GH B.1	C1059T, C3037T, C5730T, C10582T, C14408T, A23403G, G25563T
EPI_ISL_766866	GH B.1.597	C1059T, C3037T, T6199C, C10582T, C14408T, A23403G, G25563T, C25782T, C27804T, C28830A	**EPI_ISL_418242**	GH B.1	C1059T, C3037T, C10582T, C14408T, A23403G, G25563T, C29353T
EPI_ISL_766873	GH B.1	C1059T, C3037T, C10582T, C13335T, C14408T, A23403G, C24937T, G25563T, G25599T, A27965G	**EPI_ISL_418241**	GH B.1	C1059T, C3037T, C10582T, C14408T, C18115T, A23403G, G25563T, C25777T, C26461T, C29353T
EPI_ISL_766867	GH B.1.597	C1059T, C3037T, C5144T, T7264C, C7764T, C10279T, C10582T, G10870T, C12367T, C14408T, A23403G, G24236T, G25563T, C27804T, C28830A, C29466T	**EPI_ISL_1240721**	G A	G23012A, A23403G
EPI_ISL_766871	GR B.1.1	A949G, C3037T, C14408T, G18677T,	**EPI_ISL_1240723**	G A	G23012A, A23403G

		T19839C, A23403G, G28881A, G28882A, G28883C, G28903T			
EPI_ISL_766864	GR B.1.1	C3037T, C14408T, T19839C, A23403G, G28881A, G28882A, G28883C	**EPI_ISL_1240725**	G A	A23063T, C23271A, A23403G
EPI_ISL_766869	GR B.1.1	G2305T, C3037T, C14408T, C18928T, A23403G, G28881A, G28882A, G28883C	**EPI_ISL_1093430**	G A	A23063T, C23277T, A23403G
EPI_ISL_766865	GR B.1.1	C3037T, C5654T, G12070T, C14267T, C14408T, T19839C, A23403G, G26501C, G28881A, G28882A, G28883C, T29023G	**EPI_ISL_1093428**	G A	C23271A, A23403G
EPI_ISL_766872	G B.1	C3037T, C3619T, T6232C, C10582T, C14408T, C17550T, A23403G, T25794C, A26627G, G28774T, C28854T	**EPI_ISL_1093427**	Other A	Del
EPI_ISL_766875	G B.1	C3037T, C3619T, C8097T, C14408T, C15480T, A16060C, C17550T, C19017T, A23403G, C28854T	**EPI_ISL_1240719**	Other A	Del
EPI_ISL_766870	G B.1	-	**EPI_ISL_1240720**	Other A	A21717G, C21762T
EPI_ISL_766863	GH B.1.36	C3037T, C3619T, C11580T, C14408T, C18877T, C22444T, C22591T, A23403G, G25563T, C26735T, C28854T	**EPI_ISL_1240722**	Other A	A21717G, C21762T
EPI_ISL_766868	G B.1	C3037T, C3619T, C5183T, C9430T, C10582T, C14408T, C17550T, G23383A, A23403G, G23868T, C28253T, A28254C, C28744T	**EPI_ISL_1240724**	Other A	Del

Similarly, amino acid replacements were perceived in the Algerian sequences across different genes when compared to the reference sequence. Strikingly, several replacements with or without an impact upon the matching protein were proper to our genomes (Table 7).

Table 7. Amino acid replacements detected across different genes in the Algerian sequences.
*Replacements in bold indicate unique Algerian mutations.

Query	Gene/Amino Acid Replacement *
EPI_ISL_766874	NSP2_T85I, NSP3_A1179V, NSP12_P323L, **NSP12_A130V**, NSP12_T85A, Spike_D614G, NS3_Q57H, NS3_S40L, N_A251V
EPI_ISL_766862	NSP2_T85I, **NSP3_E681D**, NSP12_P323L, NSP12_M629I, Spike_D614G, NS3_Q57H, **NS3_A23T**, N_S186Y
EPI_ISL_766866	NSP2_T85I, NSP12_P323L, Spike_D614G, NS3_Q57H, N_S186Y
EPI_ISL_766873	NSP2_T85I, NSP10_A104V, NSP12_P323L, Spike_D614G, NS3_W69C, NS3_Q57H
EPI_ISL_766867	NSP2_T85I, NSP3_S1682F, NSP12_P323L, Spike_D614G, Spike_A892S, NS3_Q57H, N_S186Y, N_A398V
EPI_ISL_766871	NSP12_P323L, NSP14_R213L, Spike_D614G, N_M210I, N_G204R, N_R203K
EPI_ISL_766864	NSP12_P323L, Spike_D614G, N_G204R, N_R203K
EPI_ISL_766869	NSP2_K500N, NSP12_P323L, NSP14_P297S, Spike_D614G, N_G204R, N_R203K
EPI_ISL_766865	NSP12_P323L, NSP12_T276M, Spike_D614G, N_G204R, N_R203K
EPI_ISL_766872	NSP12_P323L, Spike_D614G, N_L167F, N_S194L
EPI_ISL_766875	NSP3_T1793I, **NSP12_N874H**, NSP12_P323L, Spike_D614G, N_S194L
EPI_ISL_766870	NSP3_T1793I, NSP12_P323L, NSP14_K349N, Spike_D614G, NS3_A110V, N_S194L
EPI_ISL_766863	NSP6_T203I, NSP12_P323L, Spike_D614G, NS3_Q57H, N_S194L
EPI_ISL_766868	NSP3_P822S, NSP12_P323L, Spike_G769V, Spike_D614G, NS8_I121L
EPI_ISL_766861	NSP12_P323L, Spike_D614G, N_S186Y
EPI_ISL_420037	NSP2_T85I, NSP3_T1004I, NSP12_P323L, Spike_D614G, NS3_Q57H
EPI_ISL_418242	NSP2_T85I, NSP12_P323L, Spike_D614G, NS3_Q57H
EPI_ISL_418241	NSP2_T85I, NSP12_P323L, **NSP14_H26Y**, Spike_D614G, NS3_Q57H, **NS3_L129F**, **E_L73F**
EPI_ISL_1240721	Spike_D614G, Spike_E484K
EPI_ISL_1240723	Spike_D614G, Spike_E484K
EPI_ISL_1240725	Spike_A570D, Spike_D614G, Spike_N501Y
EPI_ISL_1093430	Spike_T572I, Spike_D614G, Spike_N501Y
EPI_ISL_1093428	Spike_A570D, Spike_D614G
EPI_ISL_1093427	Spike_V70del, Spike_H69del
EPI_ISL_1240719	Spike_Y144del, Spike_V70del, Spike_H69del
EPI_ISL_1240720	Spike_Y144del, Spike_A67V, Spike_V70del, Spike_H69del, Spike_Q52R
EPI_ISL_1240722	Spike_Y144del, Spike_A67V, Spike_V70del, Spike_H69del, Spike_Q52R
EPI_ISL_1240724	Spike_Y144del, Spike_V70del, Spike_H69del

Therefore, the effect of the unique amino acid replacements regarding the Algerian sequences was first assessed in CoV-GLUE (data not included). Also, accuracy scores for the PredictSNP webserver are indicated in Table 8 and color-coded according to the mutation type, in which Green represents a neutral mutation and Red reflects a deleterious mutation

Table 8. Analysis of the unique Amino acid replacements in the Algerian sequences. The percentage of accuracy is indicated between brackets. The Red color stands for deleterious mutation, whereas Green represents neutral mutation.

Mutation	PredictSNP	PhD-SNP	PolyPhen-1	PolyPhen-2	SIFT	SNAP
NSP12_A130V	64%	59%	67%	45%	79%	62%
NSP12_N874H	72%	58%	74%	60%	79%	62%
NSP3_E681D	74%	78%	67%	75%	65%	55%
NS3_A23T	55%	72%	59%	54%	53%	50%
NSP14_H26Y	75%	83%	74%	87%	87%	71%
E_L73F	65%	89%	68%	87%	65%	56%
NS3_L129F	72%	68%	59%	68%	45%	72%

Nevertheless, no recombination events were detected among the sequences based on the RDP4 program, however, a total of 61 Haplotypes were identified. The Algerian sequences are dispersed across the network as demonstrated in Fig 19. For example, Algeria/G35155-8850/2020|EPI_ISL_766864 clustered with sequences from Mexico, Sri Lanka, Austria, Netherlands, Turkey, Italy, Greece, Guadeloupe, Thailand, Belgium and formed one Haplogroup. In contrast, each of the 17 remaining sequences was considered as an individual haplotype. Algeria/G38599-8859/2020|EPI_ISL_766871, Algeria/G38218-8852/2020|EPI_ISL_766865, and Algeria/G35014-8856/2020|EPI_ISL_766869 were directly linked to the previously mentioned Haplogroup. Similarly, Algeria/G0638_2264/2020|EPI_ISL_418241 and Algeria/G0640_2265/2020|EPI_ISL_418242 were directly interconnected. In parallel, Algeria/G37138-8854/2020|EPI_ISL_766867 and Algeria/G41498-8846/2020|EPI_ISL_766861 were joined with the presence of a median vector indication missing unsampled data.

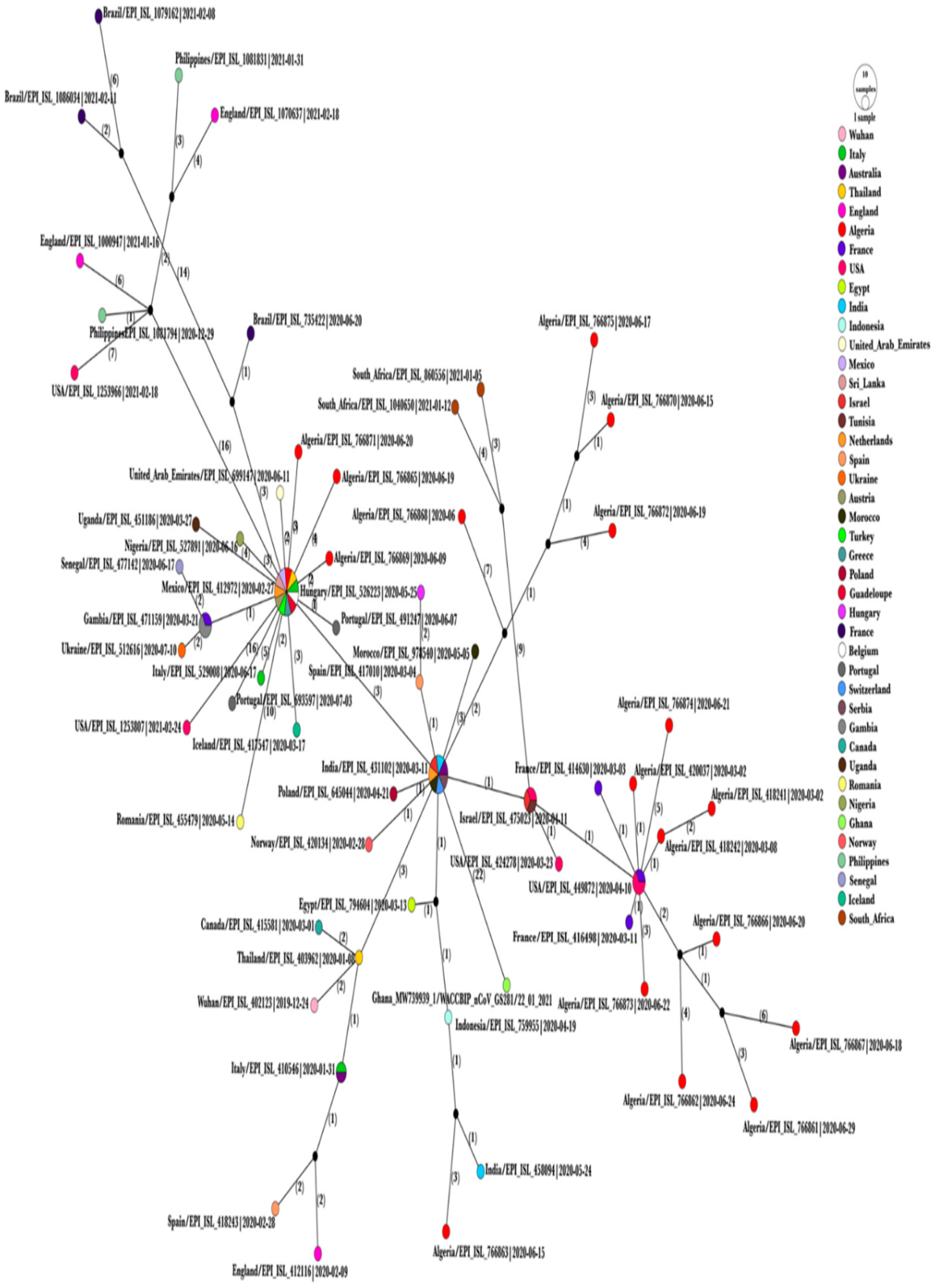

Figure 19. A Haplotype network analysis representing eighty-one SARS-CoV-2 genomes. The median-joining algorithm with epsilon = 1 parameter was used in the network construction. Ellipses and diameters are proportional to the number of sequences. Mutation steps between Haplotypes are represented by the bracketed numbers. All mutations were enclosed. Colors symbolize the different geographic sampling locations.

Lastly, when exploring the epidemiological aspect regarding the Algerian pandemic as demonstrated in Fig 20A and B, the R^2 values in reference to the time series plot of the cumulative confirmed cases were 0.62, 0.97, and 0.97 for the exponential, linear, and logarithmic trend lines, respectively. Still, further, the same results were obtained regarding recovery cases. Simultaneously, the cumulative fatality cases exhibited the following R^2 values: 0.77 for the exponential trend line and 0.99 for the linear and the logarithmic model. In parallel, the R^2 calculated between the confirmed cases and the population density for each of the 48 Algerian cities was 0.78.

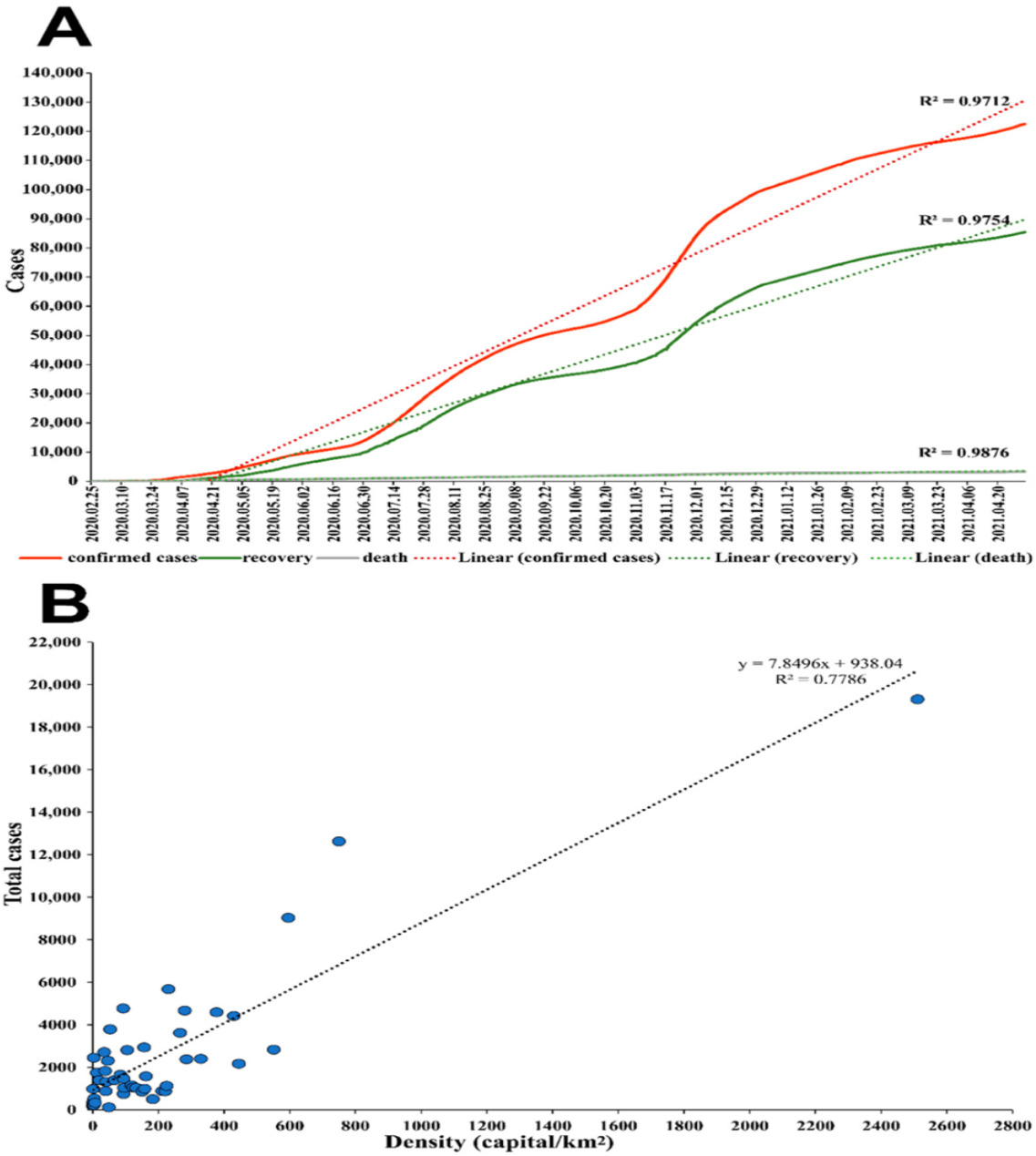

Figure 20. (A) Time series plot representing the COVID-19 confirmed cases (Red), recovery (Green), and death (Grey) depicting corresponding R2 values. (B) Correlation plot between the population density and the total confirmed cases.

5. Discussion

5.1. Discussion of bat-related *Picornaviradae* results

Several factors (such as geographical, demographical, or ecological) likely influence the occurrence of spillover events and act as driver factors in viral evolution (Cortes et al., 2018; Wang & Crameri, 2014). Global destruction of the natural habitat of bats triggered the urbanization of several dedicated species or simply established more opportunities for human-bat interactions (Russo & Ancillotto, 2015). Subsequently, this may constitute potential novel factors regarding viral emergence as already seen with coronaviruses and rabies (Hu et al., 2015; Pape et al., 1999). In consideration of the above, understanding and filling the lack of the evolutionary mechanisms regarding BtPVs is today, a prominent direction of research. Furthermore, despite how animal originated PVs were previously exemplified as potential zoonotic agents, as in the case of the encephalomyocarditis virus, which was clearly revealed through experimental infections on human tissues and primary cell cultures (Carocci & Bakkali-Kassimi, 2012), the zoonotic potential of all documented BtPVs remains blurred and fairly misunderstood (Geldenhuys et al., 2018). As previously demonstrated, picornaviruses exhibit a high genetic diversity (quasi-species) similar to other RNA viruses (Kurosu, 2011; Lewis-Rogers & Crandall, 2010), and a broad geographical spectrum in Chiroptera order. For instance, BtPVs originating from the same host genus were very distinct and not closely related, hence, both bat mischiviruses and BtPVs did not exhibit any specificity, whether upon the species level or on the genus level. This was the same regarding the tortoise picornavirus (Farkas et al., 2015), and inversely for coronaviruses (Anthony et al., 2013). Additionally, a positive relationship was previously described between the viral richness and geographical distribution of bats (Turmelle & Olival, 2009; Webber et al., 2017). This was the case in the present study, in which a positive correlation between PV diversity, species richness, and geographical distribution was revealed. Also, larger viral clusters and more than one cluster were obtained for genera in which more species have been sampled in a large geographical range. Furthermore, some drawbacks were encountered during the analysis. Several BtPVs clusters hold a single viral sequence whereas numerous sequences were considerably short. For instance, mischiviruses displayed three host genus-related clusters. The Miniopterus genus cluster comprised the Asian mischivirus sequence (8468 bp), the new Algerian sequence (6,961 pb), the six Hungarian sequences (6,855 bp), and four partial 3Dpol Bulgarian sequences (three sequences 343 bp, one 983 bp). The *Myotis* genus group is composed of three Romanian

partial 3D pol sequences (993 bp), while the *Hipposideros* genus cluster consisted of a single Mischivirus C sequence from the Congo (8096 bp). Both the number of the sequences within the dataset and the sequence's length often limit the analyses. By way of illustration through the use of BaTS software, if and when the number of sequences regarding a character trait is lower than three, the result is declared insignificant (in the case of America) and distinctively, short sequences may likely be misclassified.

Lewis-Rogers and Crandall demonstrated the evolution of Picornaviruses and their hosts occur through host-jumping events and not via co-speciation (Lewis-Rogers & Crandall, 2010). However, the chiropteran order was not included in the previous study. The main finding of the present study was the frequency regarding host-jumping events occurring in the evolutionary history regarding BtPVs, which is reflected as incongruence between the virus and the host phylogeny. This completed what was formerly mentioned. Furthermore, nearly all bat genera host phylogenetically divergent viruses, and an absence of species specificity was observed. According to studies performed on coronaviruses (Leopardi et al., 2018), it may likely be due to multiple introductions of PVs. This hypothesis is consistent with the detection of highly related PVs in humans and different animal species, by way of illustration, the virus species Aichivirus A in the genus Kobuvirus comprising: aichivirus 1 in humans (Yamashita et al., 1998), canine kobuvirus 1 (Carmona-Vicente et al., 2013; L. Li et al., 2011), murine kobuvirus 1 (Phan et al., 2011) and the feline kobuvirus (Cho et al., 2014, 2015). Notably, the Mischivirus genus which was supposedly restricted to the *M. schreibersii* species was later associated with the *H. gigas, M. oxygnathus, M. myotis* and surprisingly, to the foxhound (Norby et al., 2017). It is well established in which cross-species transmission event occurrence is multifactorial, nevertheless, we deduced the role of sympatry in increasing host-jumping events. For example, co-roosting of Myotis and Miniopterus bats may likely explain the detection of closely related kobuvirus associated among these bats (Leopardi et al., 2018). Additionally, the migratory ability of Miniopterus bats associated with the longest distance of 883 km recorded in Europe, possibly eases the spread of viruses among bat populations located in geographically distant areas. For example, *M. schreibersii*, originating from Europe and Algeria, which possess different geographical distributions yet share the same virus species Mischivirus B. Despite the fact in which no interaction is known regarding *M. oxygnathus* and *H. gigas*, in accordance with their ecologies, some hypothetical cross-species transmission events were detected among them. However, the length of the sequence obtained from *M. oxygnathus* (993 bp) is a

limitation regarding accurate classification. Namely, when relying on the phylogenetic analyses (Fig. 2), the putative mischivirus sequence obtained from *M. oxygnathus* and *M. myotis* were closely related to *Mischivirus C*, identified from *H. gigas*. Clearly, they displayed an identical branching pattern as Mischivirus A from *M. schreibersii* sampled in China and *Mischivirus B* from Algeria and both Bulgaria and Hungary, directing BtPVs from Romania may not belong to Mischivirus C. Likewise, host misidentification may lead to distorting the obtained results. Specifically, it has been demonstrated M. schreibersii bats from Hainan were actually M. fuliginosus (S. Li et al., 2015; Wu et al., 2012). This is caused by the cryptic nature of several Miniopterus bat species. The morphology-based identification is not sufficient, and usually requires the use of DNA barcoding or echolocation studies (Puechmaille et al., 2014).

Recombination incidence was emphasized in this research and thought to play a role in both the diversity and the evolution regarding BtPVs, as adequately demonstrated in former studies (Lukashev, 2010; Simmonds, 2006). In parallel, we observed some polytomies across the phylogenetic tree reflecting missing data. This is due to the small BtPVs data panel (n = 69) and sampling imbalance. In other words, since most studies were undertaken primarily throughout Europe and Asia, other continents are characteristically under-represented (America n = 1, Australia = 0). Additionally, the sampled bats included in this study represent just 4.8% of the total currently recognized bat genera, and 2.2% of the total bat species known thus far, leaving the greater majority yet unexplored.

In summary, our results described the first picornavirus genome from Algeria. Additionally, it emphasized the horizontal evolution among PVs within bats without any host specificity and the major evolutionary role of host switch mechanisms which may increase with sympatry. Nevertheless, despite the exploitation of all available information in reference to BtPVs, this study bears limitations, mainly related either to the quality of the available data, or their lack thereof. Frankly speaking, our study is a starting point regarding further investigations in pursuit of the evolution of the PV family within these important flying mammals. Specifically, for this very reason, we support additional sampling, detection, and the acquisition of more BtPVs with longer sequences including accurate host species identification.

5.2. Discussion of bat-related *Coronaviridae* results

To date, it is well-known bats are important reservoirs hosting several viruses with zoonotic potential (Calisher et al., 2006). However, in Algeria, bat-related viruses are poorly investigated. When researching references regarding zoonoses in Algeria, the main studies were either conducted on canines in reference to rabies (Kardjadj & Ben-Mahdi, 2019) or bacterial agents (Kardjadj M, 2016). In consideration of the chiropteran order, only the ecology (Ahmim, 2018) and dietary research (Ahmima et al., 2013) are conducted, leaving an immense gap of knowledge apropos of bat born viruses in Algeria. For instance, the fruit bat, *Pteropus medius,* was linked with the Nipah outbreak in Bangladesh and India with a >75% mortality rate (Epstein et al., 2020). Similarly, several bat families were most likely the origin of coronaviruses outbreaks. In 2003, the severe acute respiratory syndrome coronavirus (SARS-CoV), which originated from the Hipposideridae bat family, was responsible for the SARS pandemic in China with an 11% mortality rate (Y. Yang et al., 2020). Furthermore, despite the elusive origin regarding the current COVID pandemic (Wacharapluesadee et al., 2021), the most likely reservoir hosts are indeed bats (Lytras et al., 2021; H. Zhou et al., 2021). Accordingly, we searched for coronaviruses in bats sampled from caves located in urban areas, which, are certainly nearby and have direct contact with humans. Both alphacoronaviruses and betacoronaviruses were detected among four different species. The alphacoronavirus isolated from *Myotis punicus* was related to *Miniopterus bat coronavirus HKU8* and formed a sister taxon with MN823620 Algerian alphacoronavirus detected in a *Miniopterus schreibersii* bat located in another city. Both sequences shared 97.96% nucleotide identity with an alphacoronavirus described previously from *Miniopterus schreibersii* in France. the relationship regarding these viruses originating from different species may be explained by their co-roosting habits, formerly demonstrated (Ar Gouilh et al., 2018). Furthermore, it has been shown coronaviruses didn't have any association with sampling locations (Leopardi et al., 2018). This can be clearly confirmed, even on a smaller scale, as the clustered sequences mentioned above were sampled from different cities (Constantine and Bejaia). Strikingly, the alphacoronavirus MN701039 was discovered in a *Plecotus gaisleri*, and it is the first described coronavirus originating from this species. It formed a monophyletic clade together with Rhinolophus related alphacoronaviruses found in Kenyan (Waruhiu et al., 2017) and Guinean bats (Lacroix et al., 2020) and didn't cluster with the Algerian sequences. Unfortunately, as of today, there is no literature regarding Coronaviruses in *Plecotus gaisleri*. Hence, more research efforts are needed to complete our

primary results. The last alphacoronavirus revealed from a *Rhinolophus ferrumequinum* bat bunched with a Chinese *Rhinolophus bat coronavirus HKU2*, which, is related to HCoV/NL63 (Vijaykrishna et al., 2007). Interestingly, it was co-circulating with the Algerian betacoronavirus MN823618. This co-infection was previously reported in a Rhinolophus bat from West Africa (Lacroix et al., 2020). Importantly, this may trigger recombination events, thus, the emergence of new CoVs including the ability to acclimate to new hosts (Ar Gouilh et al., 2018; Wu et al., 2016). Moreover, the formerly mentioned betacoronavirus was closely related to its Algerian homologous from a *Myotis punicus* bat (MN823619). They formed a monophyletic clade with MZ558550 and KP876546 betacoronaviruses. The latter one was 100% identical to RATG13 and shared 98.92% nucleotide identity with human SARS-CoV-2. Distinctively, before the discovery of SARS-CoV-2 and RATG13, the sequence KP876546 had long since displayed more divergence from human SARS-CoV and was classified as a potential new strain of SARS-LIKE- CoV (SL-COV)(Ge et al., 2016). Additionally, The RATG13 is considered as the closest relative of the SARS-COV-2 in bats (H. Zhou et al., 2021). Supposedly, this may indicate the relatedness of our bat coronaviruses to the novel SARS-CoV-2. However, sequences length is an obstacle for proper analysis, and therefore, it is impossible to draw an overall conclusion based solely on this premise. Generally, with respect to the following analysis, we were able to highlight the diversity and co-infectivity among coronaviruses within different bat species in Algeria, which, signal the potential emergence of a new virus. Furthermore, the description of a new alphacoronavirus originating from the African species *Plecotus gaisleri* is key in finding and highlights the importance of bat investigations. However, an increase in both explorations and sampling efforts are needed to both generate complete genomes for accurate classification and evolutionary analysis.

5.3. Discussion of Human coronaviruses (*SARS-CoV-2*) results

Molecular epidemiology based on whole-genome sequencing of viral samples after a molecular diagnosis is a strong investigation tool that can efficiently aid in establishing transmission chains, detecting new variants, and serve towards establishing new mitigation measures during a pandemic. In an attempt to draw an overview regarding the SARS-CoV-2 pandemic in Algeria, a dataset comprising 95 SARS-CoV-2 genomes sampled worldwide including our sequences and a sub-dataset comprising only the 29 Algerian sequences were analyzed, respectively. First, our estimations of the MRCA regarding the SARS-CoV-2

Algerian pandemic under a relaxed molecular clock using the Skyline model was set for 28 January 2020 [29 October 2019, 29 February 2020]. These results are aligned with the beginning of the restrictive measures throughout Algeria implemented in mid-March, 2020 (Hamidouche, 2020). As of March 2021, the evolutionary rate of the SARS-CoV-2 pandemic in the present study was 5.4043×10^{-4} substitution/site/year. Note how the substitution rates earlier reported in the pandemic were 1.66×10^{-3} in February 2020 and 8.99×10^{-4} in early August 2020. This represents the time-dependent pattern regarding substitution rates observed in viruses (Coronaviridae Study Group of the International Committee on Taxonomy of Viruses, 2020; Ghafari et al., 2021; X. Li et al., 2020; *Time Dependence of SARS-CoV-2 Substitution Rates - SARS-CoV-2 Coronavirus / NCoV-2019 Evolutionary History*, 2020). Thereafter, the phylogenetic analysis revealed both multiple disease introductions into Algeria including local transmissions, drawing attention to the impact regarding international and domestic travel in the spread of the disease. The first three sequenced samples from March 2020 were imported from France to Algeria as previously demonstrated, through contact tracing and phylogenetic analysis, however, they didn't cluster together within the current study indicating indirect contamination (Gámbaro et al., 2020; Hamidouche, 2020). In parallel, the discrete phylogeographic analysis of the virus expansion in Algeria underlined city transmissions, both vertically (from the north to the south and vice versa) and horizontally (within only northern cities or just southern cities). By way of illustration, within the northern part of Algeria from Bouira to Blida (BF 37.19) and Bouira to Tizi Ouzou (BF = 6.01), from the north to the south of the country, Blida to Ain Salah (BF = 5.69,) and from Adrar, a southern city to Boufarik, a municipality in the town of Blida in the North of Algeria (BF = 91.69). On the other hand, the continuous phylogeographic analysis provided more details regarding the diffusion route by reconstructing the ancestral locations of the virus indicated as internal nods. Predictably, internal nods were placed in municipalities representing crossing points between several cities, such as Djebahia, located in the city of Bouira, which has a rest and service area. Another illustration is Hassi Messaoud, situated in Ouargla, in which a large oil station employing several international employees is located. Actually, the first formally reported coronavirus case in Algeria was an Italian employee from this oil station (Hamidouche, 2020). Accordingly, the phylogeographic results are in line with the phylogenetic analysis, emphasizing the importance of local travel and social contact in the spread of the disease.

Globally, when comparing the Algerian sequences to the reference sequence, the ω ratios across all the analyzed coding genes (*ORF1a, ORF1b, S, M, N, E,* and *ORF3a*) were

inferior to one signifying purifying selection. These results were the same in a comparable study conducted by Zhang et al on SARS-CoV-2 among a Canadian population (Zhang et al., 2021). Likewise, the rarity regarding positive selection in SARS-CoV-2 protein-coding genes was emphasized in a recent analysis performed on 260,673 whole-genome sequences to study the selection pressure (Miao et al., 2021). Complementary to this, numerous frequent non-synonymous mutations previously described (Pohl et al., 2020) were found amid the Algerian sequences, namely, T85I in the *nsp2* gene, P323L in the *nsp12* gene, D614G in the *S* gene, and Q57H in the *ORF3a* gene. These amino acid replacements are considered positively selected since they were identified across 84 countries (Jacob et al., 2021). Furthermore, the identification of the spike protein mutations characteristic of the recently discovered SARS-Cov-2 variants (H69del, V70del, E484K, Y144del, and Q52R) following the repatriation of Algerians from abroad enforced a second full lockdown. Remarkably, characteristic non-synonymous amino acid replacements were also distinguished. For instance, in the sequence Algeria_EPI_ISL_420037, the T1004I replacement in the *nsp3* gene was spotted. Early in the pandemic, this was described as a unique mutation in the USA in sequences sampled from 19 January 2020 through 15 April 2020 and was not reported elsewhere. Hence, the individual who contaminated Algeria_EPI_ISL_420037 had either a travel history to the USA or was in contact with an individual who introduced the disease to France from the USA (Kaushal et al., 2020). Strikingly, Algerian unique non-synonymous amino-acid changes were perceived. To cite an example, the amino acid substitution A130V in the *RdRp* gene resulted in a harmful functional effect upon the protein responsible for viral replication was encountered in the sequence Algeria/EPI_ISL_766874. The former mutation was first reported in the United Arab Emirates on 12 June 2020. Amid the entire group of declared samples thus far, it occurred only in 75 samples worldwide among 13 countries. In Algeria, it was revealed on 21 June 2020, supposedly, all locations in which this mutation was described were excluded from the originating country of the disease, if the sample collection dates occurred after the Algerian sampling date. Thus, only EPI_ISL_698151 from Abu Dhabi (collection date: 12 June 2020) was directly connected to the sample Algeria/EPI_ISL_766874. In the same manner, the deleterious non-synonymous amino acid replacement N874H in the *NSP12* was reported for the first time in the sequence Algeria/EPI_ISL_766875 and happened only in seven samples worldwide. According to collection dates, this sequence can be linked directly to the EPI_ISL_557768 genome from England sampled immediately following the original sequence on 6 July 2020. Similarly, an association between the sequence Algeria/

EPI_ISL_766862 and sequences from Texas (USA) were established through the deleterious mutation A23T in the accessory gene *ORF3a*, which, plays a pivotal in virulence, infectivity, and virus release. This replacement was first declared in the USA and subsequently sampled 62 times in 15 countries (Issa et al., 2020). Lastly, the deleterious mutation L129F was spotted for the first time in Algeria, then in 997 samples worldwide. It affected the third functional domain of the ORF3a protein (K+ ion channel) and may seriously impact the protein function and consequently, the virus phenotype (Issa et al., 2020). Results regarding the presence of deleterious mutations are in accordance with previous studies reporting deleterious mutations in RNA viruses with zoonotic potential. For instance, the occurrence of different deleterious mutations simultaneously with the presence of stabilizing mutations may increase virus fitness. This is the case regarding influenza A/H5N1, the acquisition of airborne transmissibility required a combination of mutations, of which, two were deleterious (Fonville, 2015). Nevertheless, deleterious mutations can't be directly eliminated after their occurrence, due to the insufficient strength of the purifying selection; henceforth they may circulate for a sufficient period and impact the viral infection path (Koelle & Rasmussen, 2015). Secondly, deleterious mutations may be used to develop various forms of treatment, such as the Favipiravir, to induce a mutational meltdown phenomenon (population extinction) by increasing the accumulation rate of harmful mutations, consequently provoking population collapse (Jensen & Lynch, 2020). Jointly, three neutral amino acid replacements were identified among the Algerian sequences, meanwhile, no changes were reported regarding the protein function (Das et al., 2021). In the protease gene (*NSP3*), the E681D amino acid replacement was first acknowledged in the Algerian genome EPI_ISL_766862 and it occurred only in three samples worldwide. Based on sampling dates, disease exportation from Algeria to Austria (EPI_ISL_853900) could be established through the former mutation detection. Furthermore, two neutral amino acid replacements were identified in Algeria/EPI_ISL_418241. First, H26Y amino acid substitution in the exonuclease gene (*NSP14*), originally discovered for the first time in the aforementioned Algerian sequence and immediately following in the Greek sequence EPI_ISL_437907, subsequently supporting relatedness of the two genomes. Secondly, in the envelope gene, the Leucine substitution with Phenylalanine in position 73 was originally reported from Algeria, then in 2,795 samples worldwide. Earlier, it was proven this mutation alters the DLLV motif (change to DFLV). Distinctly, it may delay Tight Junction formation and therefore may hypothetically affect viral replication and/or infectivity (CDC, 2020). As previously demonstrated, all the above-mentioned viral mutation fingerprints may help

characterize and identify both transmission patterns and super-spreaders (Lau et al., 2021). In the meantime, the Algerian genomes were dispatched among five lineages. The first one is lineage A, considered as the root of the pandemic, encompassing primarily sequences originating in China. All Algerian sequences related to this lineage were partial genomes (*S, NSP16*) and were characterized with either the B.1.1.7 (UK), B.1.351 (South Africa), or B.1.525 (Nigeria) related mutations. Hence, the length of the sequence is one of the biggest drawbacks of an accurate classification. Furthermore, the lineage B.1, which is a large European clade corresponding approximately to the Italian outbreak, in addition to the clade B.1.1 matching the European lineage with three clear SNPs: G28881A, G28882A, and G28883C were clearly detected amid the Algeria genomes. Unsurprisingly, the clade B.1.597 corresponding to sequences primarily from France was also present. Interestingly, Algeria/EPI_ISL_766863 isolated from an 82-year-old female appertained to the B.1.36 lineage acknowledged for the first time in February 2020, in Saudi Arabia, and clustered with both an Indian (PP = 94%) and a Malaysian sequence (PP = 92%). This may be explained through the means of disease importation from Saudi Arabia, while performing a religious pilgrimage, since no repatriation flights were scheduled for either Malaysia or India, unlike Saudi Arabia. This is confirmed by reports regarding Algerian deportation from abroad (*Algerian Ministry of Health*, 2020). In parallel, the Haplotype network analysis exhibited seven median vectors among the Algerian sequences indicating either missing or unsampled data, of which, the multiple disease introduction hypothesis was clearly confirmed by both the heterogeneity of the Algerian haplotypes and the scattered pattern observed among them. Note that all the results mentioned above are hypothetical as they might change with the inclusion of more data.

Lastly, the strong correlation between the population density and the number of SARS-CoV-2 confirmed cases in each Algerian city suggests the spread of the virus is mainly linked to social contact, the consciousness of the community, and respectful compliance regarding social distancing. This is clearly manifested in lower infection cases in relatively high population density cities and vice-versa. To cite an illustration, Ouargla, a city located in the southern portion of Algeria, has a population density of 2.63 habitant/km^2, although the number of confirmed cases is 2,453. Whereas, in Bordj Bou Arreridj, situated in the northern region of Algeria, the number of confirmed cases was 506 cases for 182.76 habitant/km^2. Accordingly, when assessing the Algerian governmental containment measures, we undoubtedly observe their effectiveness in preventing catastrophic scenarios such as the

Italian one (Megna, 2020). This was differently demonstrated in a prior epidemiological study conducted to evaluate the mitigation measures implemented in Algeria in the early SARS-CoV-2 pandemic (dated 26 April 2020). The analysis was founded on the basic reproduction number R0 before and after the implementation of the preventive strategies (Hamidouche, 2020).

Overall, our study is the first of its kind in Algeria. We investigated the evolutionary, genetic, and epidemiological aspects regarding the Algerian SARS-CoV-2 pandemic, pertinently demonstrating the multiple introductions of the disease and the heterogeneity of the genomes. Additionally, our research outcomes unveiled unique amino-acid swapping by characterizing the mutational patterns and the effect on the corresponding proteins. Furthermore, concise tracing could be performed based on both unique mutations and travel history. In parallel, we statistically assessed the effectiveness regarding the mitigation majors implemented against the SARS-CoV-2 pandemic.

Admittedly, the main drawback regarding our study was the length of several sequenced genomes and the size of the Algerian data panel. Consequently, we emphasized the importance of massive sampling and sequencing in disease comprehension and increased efforts regarding diagnostics, therapy, drug, and vaccine development. Acknowledging Algeria was under complete travel restrictions since 15 March 2020, the number of cases kept increasing, indicating local transmissions. Therefore, these local viral variants may potentially represent a distinct strain as previously occurred (Hossain et al., 2021).

6. Conclusion

More than 200 viruses were detected among bats, several of which were linked to deadly human diseases such as the Nipah virus disease, ebola virus disease, SARS, MERS, and possibly to the novel COVID-19 pandemic. Nevertheless, they play key roles in the ecosystem such as pest control, pollination, and dispersal of a variety of plant seeds. Additionally, human activities are the main driver for pathogens spread between humans and animals, therefore, preventive measures regarding potential disease emergence must be focused on human activities (Schneeberger & Voigt, 2015).

To develop improved strategies towards managing and preventing novel human disease emergence, the comprehension of the factors involved in zoonotic spillover events is primordial. These include but are not limited to host viral and environmental factors. For instance, host susceptibility is dependent upon adequate receptors permitting the virus entry, whereas the immune response and metabolic features of host cells can either increase or decrease the replication of the virus. In parallel, virus evolution through recombination, mutation accumulation leads either to new host adaptation and/or increased transmission or virulence within its already known host. On the other hand, the increase in ecological interference, such as wildlife trading, contributes to spillover events.

The emergence of the novel SARS-CoV-2 sums up all the previously indicated statements. However, it highlights the bared failures to strategically respond to the pandemic, which is neither the first nor the last to occur. Hence, in regards to the future X pandemic, effective strategies need to be established (Carroll et al., 2021; da Silva et al., 2021). Health authorities and researchers must collaborate first with society to counter and sensibilize against the main risk factors for zoonotic spillover in each country to initiate both preventive and response actions to rapidly contain the disease X. For instance, the involvement of initiatives such as The Research and Development (R&D) Blueprint from the World Health Organization and the commitment of both health authorities and society (the whole of society approach) may help in altering a pandemic's course (Carroll et al., 2021).

To comply with the previously mentioned solutions, our aim in the present thesis was to generate the maximal amount of knowledge regarding bat-related viral zoonoses throughout Algeria. We combined two strategies: large-scale virus discovery and evolutionary analysis. As a potential outcome, we were able to describe the vast viral diversity among the Algerian bats, subsequently establish connections with their homologous worldwide and study their evolution. First, we detected and obtained almost a

full picornavirus (*Mischivirus)* genome from a *Miniopterus schreibersii* bat. Subsequently, we performed an evolutionary analysis, and we highlighted the role of recombination and host switches in the evolution and diversity of bat-related picornaviruses. In parallel, we described both Alpha and Betacoronaviruses from different bat species. Strikingly, we are the first to report an alphacoronavirus originating from a novel bat host (*Plecotus gaisleri*). Additionally, we achieved a detailed molecular study regarding the SARS-CoV-2 pandemic in Algeria, establishing the transmission route using phylogeography while highlighting multiple disease origins and missing unsampled data based on both phylogeny and Haplotype analysis. Notably, we emphasized the occurrence of Algerian characteristic mutations which may lead to a new variant, thus proving influential in both vaccine and drug development.

To the best of our knowledge, our work is of great importance since it is the only molecular-based research performed in Algeria that covers all the mentioned aspects. Furthermore, this pilot project is a good foundation for future research capacity building and promoting bat-related studies. It can also help in outbreak response and disease containment. Lastly, on the basis of our work, we established further research plans to follow in the future.

7. Összefoglalás

Több mint 200 vírust mutattak ki a denevérekben, amelyek közül több halálos emberi betegség ismert, mint például a Nipah vírus, az ebola vírus, a SARS, a MERS, és feltehetően az új COVID-19 világjárvány is. Ennek ellenére a denevérek kulcsszerepet játszanak az ökoszisztémában, például a kártevő rovarok elleni védekezésben, a beporzásban és a különféle növényi magvak elterjedésében is fontos szerepet töltenek be. Továbbá, az emberi tevékenységek a fő mozgatói a kórokozók emberek és állatok között történő átadásának, ezért a lehetséges betegségek kialakulásával kapcsolatos megelőző intézkedéseket az emberi tevékenységekre kell összpontosítani (Schneeberger & Voigt, 2015).

Az új emberi betegségek kialakulásának kezelésére és megelőzésére irányuló hatékonyabb stratégiák kidolgozásában elsődleges fontosságú a zoonózisok átvitelében szerepet játszó tényezők megértése. Ezek közé tartoznak, de nem kizárólagosan, a vírusgazda és a környezeti tényezők. A gazdaszervezet érzékenysége például függ a vírus bejutását segítő receptoroktól, míg a gazdasejtek immunválasza és metabolikus jellemzői növelhetik vagy csökkenthetik a vírus replikációját. Ezzel párhuzamosan a vírus evolúciója rekombináció során, a mutációk felhalmozódásán keresztül vagy új gazdaszervezet adaptációjához és/vagy fokozott átvitelhez vagy virulenciához vezet a már ismert gazdaszervezetben. Másrészt a természetbe való beavatkozások fokozódása, például a vadon élő állatokkal való kereskedés növekedése hozzájárul az átviteli eseményekhez.

A SARS-CoV-2 mostani megjelenése magában foglalja az összes korábban említett állítást. Mindazonáltal rávilágít a világjárványra való felkészültség hiányosságaira, amely nem az első és nem is az utolsó ilyen eset. Ezért hatékony stratégiákat szükséges kidolgozni a jövőbeli X-járványra való felkészülésre (Carroll et al., 2021; da Silva et al., 2021). Az egészségügyi hatóságoknak és a kutatóknak először a társadalommal kell együttműködnie a zoonózisok átviteli fő kockázati tényezőinek ellensúlyozása és megismertetése érdekében az egyes országokban, hogy megelőző és válaszlépéseket kezdeményezhessenek az X betegség gyors megfékezésére. Hatékony lehet például olyan programok bevonása, mint az Egészségügyi Világszervezet (WHO) “The Research and Development (R&D)” kezdeményezése, emellett az egészségügyi hatóságok és a társadalom elkötelezettsége (a társadalom egészét átfogó megközelítés) segíthet a világjárvány lefolyásának megváltoztatásán (Carroll et al., 2021).

A fent említett megoldási lehetőségek megvalósítása érdekében jelen disszertáció célja, hogy az Algériában jelen levő, denevérektől származó vírusos zoonózisokról a lehető

legtöbbet tudjuk meg. Célunk eléréséhez két stratégiát kombináltunk: széles skálájú vírusfelderítést és evolúciós elemzést. Eredményeink között sikerült leírnunk az algériai denevérek hatalmas vírusdiverzitását. Ezt követően e vírusok világszerte jelen levő homológjait is felkutattuk és tanulmányoztuk evolúciójukat. Elsőként, egy Miniopterus schreibersii denevérben detektált picornavirus (Mischivirus), szinte teljes genomját sikerült meghatároznunk. Ezt követően evolúciós elemzést végeztünk, és rávilágítottunk a rekombináció, illetve a gazdaváltások szerepére a denevérekkel kapcsolatos picornavírusok evolúciójában és sokféleségében. Ezzel párhuzamosan leírtunk különböző denevérfajokból származó alfa- és betakoronavírusokat is. Ennek köszönhetően elsőként sikerült egy új denevérfajból (Plecotus gaisleri) származó alfakoronavírust kimutatnunk. Ezen kívül részletes molekuláris vizsgálatokat végeztünk az algériai SARS-CoV-2 világjárványról, filogeográfia segítségével meghatároztuk a transzmissziós útvonalakat, miközben filogenetikai-, és haplotípus-analízissel rávilágítottunk több megbetegedés eredetére, illetve hiányzó adatokra. Emellett kiemelt figyelmet szenteltünk az Algériában előforduló jellegzetes mutációkra és azok előfordulására, melyek egy új variáns kialakulásához vezethetnek, így mind a vakcina, mind a gyógyszerfejlesztésre befolyást gyakorolhatnak.

Munkánk nagy jelentőséggel bír, hiszen tudomásunk szerint ez az egyetlen Algériában végzett molekuláris alapú kutatás, amely az összes fent említett szempontot figyelembe veszi. Emellett jelen kísérleti projekt jó alapot biztosít a jövőbeni kutatási kapacitásépítéshez és a denevérekkel kapcsolatos tanulmányok előremozdításához. Segíthet a járványra való válaszadásban, illetve a betegségek megfékezésében is. Eddigi munkánk alapján további, a jövőben követendő kutatási terveket is kidolgoztunk.

8. References

Aarestrup, F. M., Bonten, M., & Koopmans, M. (2021). Pandemics– One Health preparedness for the next. *The Lancet Regional Health - Europe*, *9*, 100210. https://doi.org/10.1016/j.lanepe.2021.100210

Adzhubei, I., Jordan, D. M., & Sunyaev, S. R. (2013). Predicting Functional Effect of Human Missense Mutations Using PolyPhen-2. *Current Protocols in Human Genetics / Editorial Board, Jonathan L. Haines ... [et Al.]*, *0 7*, Unit7.20. https://doi.org/10.1002/0471142905.hg0720s76

Agnarsson, I., Zambrana-Torrelio, C. M., Flores-Saldana, N. P., & May-Collado, L. J. (2011). A time-calibrated species-level phylogeny of bats (Chiroptera, Mammalia). *PLoS Currents*, *3*, RRN1212. https://doi.org/10.1371/currents.RRN1212

Ahmim, M. (2018). The Bat: A Benefactor Animal Poorly Understood in Algeria. In *Bats*. IntechOpen. https://doi.org/10.5772/intechopen.75547

Ahmima, M., Moalia, A., Algeria, N., Gaisler, J., Racey, P., & Russo, D. (2013). *Acknowledgements*.

Algerian Ministry of Health. (2020). Retrieved from http://covid19.sante.gov.dz/carte/

Alkan, F., Karayel, İ., Catella, C., Bodnar, L., Lanave, G., Bányai, K., Di Martino, B., Decaro, N., Buonavoglia, C., & Martella, V. (2015). Identification of a Bovine Enteric Calicivirus, Kırklareli Virus, Distantly Related to Neboviruses, in Calves with Enteritis in Turkey. *Journal of Clinical Microbiology*, *53*(11), 3614–3617. https://doi.org/10.1128/JCM.01736-15

Anthony, S. J., Ojeda-Flores, R., Rico-Chávez, O., Navarrete-Macias, I., Zambrana-Torrelio, C. M., Rostal, M. K., Epstein, J. H., Tipps, T., Liang, E., Sanchez-Leon, M., Sotomayor-Bonilla, J., Aguirre, A. A., Ávila-Flores, R., Medellín, R. A., Goldstein, T., Suzán, G., Daszak, P., & Lipkin, W. I. (2013). Coronaviruses in bats from Mexico. *The Journal of General Virology*, *94*(Pt 5), 1028–1038. https://doi.org/10.1099/vir.0.049759-0

Ar Gouilh, M., Puechmaille, S. J., Diancourt, L., Vandenbogaert, M., Serra-Cobo, J., Lopez Roïg, M., Brown, P., Moutou, F., Caro, V., Vabret, A., & Manuguerra, J.-C. (2018). SARS-CoV related Betacoronavirus and diverse Alphacoronavirus members found in western old-world. *Virology*, *517*, 88–97. https://doi.org/10.1016/j.virol.2018.01.014

Bandelt, H. J., Forster, P., & Rohl, A. (1999). Median-joining networks for inferring intraspecific phylogenies. *Molecular Biology and Evolution*, *16*(1), 37–48. https://doi.org/10.1093/oxfordjournals.molbev.a026036

Banerjee, R., & Dasgupta, A. (2001). Interaction of picornavirus 2C polypeptide with the viral negative-strand RNA. *Journal of General Virology*, *82*(11), 2621–2627. https://doi.org/10.1099/0022-1317-82-11-2621

Batra, N., De Souza, C., Batra, J., Raetz, A. G., & Yu, A.-M. (2020). The HMOX1 Pathway as a Promising Target for the Treatment and Prevention of SARS-CoV-2 of 2019 (COVID-19). *International Journal of Molecular Sciences*, *21*(17), 6412. https://doi.org/10.3390/ijms21176412

Bendl, J., Stourac, J., Salanda, O., Pavelka, A., Wieben, E. D., Zendulka, J., Brezovsky, J., & Damborsky, J. (2014). PredictSNP: Robust and Accurate Consensus Classifier for Prediction of Disease-Related Mutations. *PLoS Computational Biology*, *10*(1), e1003440. https://doi.org/10.1371/journal.pcbi.1003440

Bidaisee, S., & Macpherson, C. N. L. (2014). Zoonoses and One Health: A Review of the Literature. *Journal of Parasitology Research*, *2014*, 1–8. https://doi.org/10.1155/2014/874345

Bielejec, F., Rambaut, A., Suchard, M. A., & Lemey, P. (2011). SPREAD: Spatial phylogenetic reconstruction of evolutionary dynamics. *Bioinformatics*, *27*(20), 2910–2912. https://doi.org/10.1093/bioinformatics/btr481

Bromberg, Y., & Rost, B. (2007). SNAP: Predict effect of non-synonymous polymorphisms on function. *Nucleic Acids Research*, *35*(11), 3823–3835. https://doi.org/10.1093/nar/gkm238

Buchfink, B., Xie, C., & Huson, D. H. (2015). Fast and sensitive protein alignment using DIAMOND. *Nature Methods*, *12*(1), 59–60. https://doi.org/10.1038/nmeth.3176

Calisher, C. H., Childs, J. E., Field, H. E., Holmes, K. V., & Schountz, T. (2006). Bats: Important Reservoir Hosts of Emerging Viruses. *Clinical Microbiology Reviews*, *19*(3), 531–545. https://doi.org/10.1128/CMR.00017-06

Capriotti, E., & Fariselli, P. (2017). PhD-SNPg: A webserver and lightweight tool for scoring single nucleotide variants. *Nucleic Acids Research*, *45*(Web Server issue), W247–W252. https://doi.org/10.1093/nar/gkx369

Carmona-Vicente, N., Buesa, J., Brown, P. A., Merga, J. Y., Darby, A. C., Stavisky, J., Sadler, L., Gaskell, R. M., Dawson, S., & Radford, A. D. (2013). Phylogeny and prevalence of kobuviruses in dogs and cats in the UK. *Veterinary Microbiology*, *164*(3–4), 246–252. https://doi.org/10.1016/j.vetmic.2013.02.014

Carocci, M., & Bakkali-Kassimi, L. (2012). The encephalomyocarditis virus. *Virulence*, *3*(4), 351–367. https://doi.org/10.4161/viru.20573

Carroll, D., Morzaria, S., Briand, S., Johnson, C. K., Morens, D., Sumption, K., Tomori, O., & Wacharphaueasadee, S. (2021). Preventing the next pandemic: The power of a global viral surveillance network. *The BMJ*, *372*, n485. https://doi.org/10.1136/bmj.n485

CDC. (2020, February 11). *Coronavirus Disease 2019 (COVID-19)*. Centers for Disease Control and Prevention. https://www.cdc.gov/coronavirus/2019-ncov/variants/variant-info.html

Chazal, N. (2021). Coronavirus, the King Who Wanted More Than a Crown: From Common to the Highly Pathogenic SARS-CoV-2, Is the Key in the Accessory Genes? *Frontiers in Microbiology*, *12*, 1970. https://doi.org/10.3389/fmicb.2021.682603

Chen, L., Liu, B., Yang, J., & Jin, Q. (2014). DBatVir: The database of bat-associated viruses. *Database: The Journal of Biological Databases and Curation*, *2014*, bau021. https://doi.org/10.1093/database/bau021

Cho, Y.-Y., Lim, S.-I., Kim, Y. K., Song, J.-Y., Lee, J.-B., & An, D.-J. (2014). Molecular Characterization of the Full Kobuvirus Genome in a Cat. *Genome Announcements*, *2*(2), e00420-14. https://doi.org/10.1128/genomeA.00420-14

Cho, Y.-Y., Lim, S.-I., Kim, Y. K., Song, J.-Y., Lee, J.-B., & An, D.-J. (2015). Molecular evolution of kobuviruses in cats. *Archives of Virology*, *160*(2), 537–541. https://doi.org/10.1007/s00705-014-2259-0

Cleemput, S., Dumon, W., Fonseca, V., Abdool Karim, W., Giovanetti, M., Alcantara, L. C., Deforche, K., & de Oliveira, T. (2020). Genome Detective Coronavirus Typing Tool for rapid identification and characterization of novel coronavirus genomes. *Bioinformatics*, *36*(11), 3552–3555. https://doi.org/10.1093/bioinformatics/btaa145

Conow, C., Fielder, D., Ovadia, Y., & Libeskind-Hadas, R. (2010). Jane: A new tool for the cophylogeny reconstruction problem. *Algorithms for Molecular Biology : AMB*, *5*, 16. https://doi.org/10.1186/1748-7188-5-16

Coronaviridae Study Group of the International Committee on Taxonomy of Viruses. (2020). The species Severe acute respiratory syndrome-related coronavirus: Classifying 2019-nCoV and naming it SARS-CoV-2. *Nature Microbiology*, *5*(4), 536–544. https://doi.org/10.1038/s41564-020-0695-z

Cortes, M. C., Cauchemez, S., Lefrancq, N., Luby, S. P., Jahangir Hossain, M., Sazzad, H. M. S., Rahman, M., Daszak, P., Salje, H., & Gurley, E. S. (2018). Characterization of the Spatial and Temporal Distribution of Nipah Virus Spillover Events in Bangladesh, 2007–2013. *The Journal of Infectious Diseases*, *217*(9), 1390–1394. https://doi.org/10.1093/infdis/jiy015

da Silva, P. G., Mesquita, J. R., de São José Nascimento, M., & Ferreira, V. A. M. (2021). Viral, host and environmental factors that favor anthropozoonotic spillover of coronaviruses: An opinionated review, focusing on SARS-CoV, MERS-CoV and SARS-CoV-2. *Science of The Total Environment*, *750*, 141483. https://doi.org/10.1016/j.scitotenv.2020.141483

Das, J. K., Sengupta, A., Choudhury, P. P., & Roy, S. (2021). Characterizing genomic variants and mutations in SARS-CoV-2 proteins from Indian isolates. *Gene Reports*, 101044. https://doi.org/10.1016/j.genrep.2021.101044

de Souza Luna, L. K., Heiser, V., Regamey, N., Panning, M., Drexler, J. F., Mulangu, S., Poon, L., Baumgarte, S., Haijema, B. J., Kaiser, L., & Drosten, C. (2007). Generic Detection of Coronaviruses and Differentiation at the Prototype Strain Level by Reverse Transcription-PCR and Nonfluorescent Low-Density Microarray. *Journal of Clinical Microbiology*, *45*(3), 1049–1052. https://doi.org/10.1128/JCM.02426-06

Dellicour, S., Gill, M. S., Faria, N. R., Rambaut, A., Pybus, O. G., Suchard, M. A., & Lemey, P. (2021). Relax, Keep Walking—A Practical Guide to Continuous Phylogeographic Inference with BEAST. *Molecular Biology and Evolution*, *38*(8), 3486–3493. https://doi.org/10.1093/molbev/msab031

Djikeng, A., Halpin, R., Kuzmickas, R., DePasse, J., Feldblyum, J., Sengamalay, N., Afonso, C., Zhang, X., Anderson, N. G., Ghedin, E., & Spiro, D. J. (2008). Viral genome sequencing by random priming methods. *BMC Genomics*, *9*, 5. https://doi.org/10.1186/1471-2164-9-5

Dong, E., Du, H., & Gardner, L. (2020). An interactive web-based dashboard to track COVID-19 in real time. *The Lancet. Infectious Diseases*, *20*(5), 533–534. https://doi.org/10.1016/S1473-3099(20)30120-1

Drummond, A. J. (2005). Bayesian Coalescent Inference of Past Population Dynamics from Molecular Sequences. *Molecular Biology and Evolution*, *22*(5), 1185–1192. https://doi.org/10.1093/molbev/msi103

Drummond, A. J., Ho, S. Y. W., Phillips, M. J., & Rambaut, A. (2006). Relaxed Phylogenetics and Dating with Confidence. *PLoS Biology*, *4*(5), e88. https://doi.org/10.1371/journal.pbio.0040088

Drummond, A. J., & Rambaut, A. (2007). BEAST: Bayesian evolutionary analysis by sampling trees. *BMC Evolutionary Biology*, *7*(1), 214. https://doi.org/10.1186/1471-2148-7-214

Ebranati, E., Veo, C., Carta, V., Percivalle, E., Rovida, F., Frati, E. R., Amendola, A., Ciccozzi, M., Tanzi, E., Galli, M., Baldanti, F., & Zehender, G. (2019). Time-scaled phylogeography of complete Zika virus genomes using discrete and continuous space diffusion models. *Infection, Genetics and Evolution*, *73*, 33–43. https://doi.org/10.1016/j.meegid.2019.04.006

Elbe, S., & Buckland-Merrett, G. (2017). Data, disease and diplomacy: GISAID's innovative contribution to global health. *Global Challenges*, *1*(1), 33–46. https://doi.org/10.1002/gch2.1018

Epstein, J. H., Anthony, S. J., Islam, A., Kilpatrick, A. M., Ali Khan, S., Balkey, M. D., Ross, N., Smith, I., Zambrana-Torrelio, C., Tao, Y., Islam, A., Quan, P. L., Olival, K. J., Khan, M. S. U., Gurley, E. S., Hossein, M. J., Field, H. E., Fielder, M. D., Briese, T., … Daszak, P. (2020). Nipah virus dynamics in bats and implications for spillover to humans. *Proceedings of the National Academy of Sciences*, *117*(46), 29190–29201. https://doi.org/10.1073/pnas.2000429117

Farkas, S. L., Ihász, K., Fehér, E., Bartha, D., Jakab, F., Gál, J., Bányai, K., & Marschang, R. E. (2015). Sequencing and phylogenetic analysis identifies candidate members of a new picornavirus genus in terrestrial tortoise species. *Archives of Virology*, *160*(3), 811–816. https://doi.org/10.1007/s00705-014-2292-z

Fehr, A. R., & Perlman, S. (2015). Coronaviruses: An Overview of Their Replication and Pathogenesis. *Coronaviruses*, *1282*, 1–23. https://doi.org/10.1007/978-1-4939-2438-7_1

Fonville, J. M. (2015). Expected Effect of Deleterious Mutations on Within-Host Adaptation of Pathogens. *Journal of Virology*, *89*(18), 9242–9251. https://doi.org/10.1128/JVI.00832-15

Gámbaro, F., Behillil, S., Baidaliuk, A., Donati, F., Albert, M., Alexandru, A., Vanpeene, M., Bizard, M., Brisebarre, A., Barbet, M., Derrar, F., van der Werf, S., Enouf, V., & Simon-Loriere, E. (2020). *Introductions and early spread of SARS-CoV-2 in France* [Preprint]. Genomics. https://doi.org/10.1101/2020.04.24.059576

Ge, X.-Y., Wang, N., Zhang, W., Hu, B., Li, B., Zhang, Y.-Z., Zhou, J.-H., Luo, C.-M., Yang, X.-L., Wu, L.-J., Wang, B., Zhang, Y., Li, Z.-X., & Shi, Z.-L. (2016). Coexistence of multiple coronaviruses in several bat colonies in an abandoned mineshaft. *Virologica Sinica*, *31*(1), 31–40. https://doi.org/10.1007/s12250-016-3713-9

Geldenhuys, M., Mortlock, M., Weyer, J., Bezuidt, O., Seamark, E. C. J., Kearney, T., Gleasner, C., Erkkila, T. H., Cui, H., & Markotter, W. (2018). A metagenomic viral discovery approach identifies potential zoonotic and novel mammalian viruses in

Neoromicia bats within South Africa. *PLoS ONE*, *13*(3), e0194527. https://doi.org/10.1371/journal.pone.0194527

Ghafari, M., Simmonds, P., Pybus, O. G., & Katzourakis, A. (2021). *Prisoner of War dynamics explains the time-dependent pattern of substitution rates in viruses* [Preprint]. Evolutionary Biology. https://doi.org/10.1101/2021.02.09.430479

Grantham, R. (1974). Amino Acid Difference Formula to Help Explain Protein Evolution. *Science*, *185*(4154), 862–864. https://doi.org/10.1126/science.185.4154.862

Haider, N., Rothman-Ostrow, P., Osman, A. Y., Arruda, L. B., Macfarlane-Berry, L., Elton, L., Thomason, M. J., Yeboah-Manu, D., Ansumana, R., Kapata, N., Mboera, L., Rushton, J., McHugh, T. D., Heymann, D. L., Zumla, A., & Kock, R. A. (2020). COVID-19—Zoonosis or Emerging Infectious Disease? *Frontiers in Public Health*, *8*, 596944. https://doi.org/10.3389/fpubh.2020.596944

Hall, R. J., Wang, J., Todd, A. K., Bissielo, A. B., Yen, S., Strydom, H., Moore, N. E., Ren, X., Huang, Q. S., Carter, P. E., & Peacey, M. (2014). Evaluation of rapid and simple techniques for the enrichment of viruses prior to metagenomic virus discovery. *Journal of Virological Methods*, *195*, 194–204. https://doi.org/10.1016/j.jviromet.2013.08.035

Hamidouche, M. (2020). *COVID-19 Epidemic in Algeria: Assessment of the implemented preventive strategy* [Preprint]. Epidemiology. https://doi.org/10.1101/2020.04.21.20074443

Han, H.-J., Wen, H., Zhou, C.-M., Chen, F.-F., Luo, L.-M., Liu, J., & Yu, X.-J. (2015). Bats as reservoirs of severe emerging infectious diseases. *Virus Research*, *205*, 1–6. https://doi.org/10.1016/j.virusres.2015.05.006

Han, H.-J., Yu, H., & Yu, X.-J. (2016). Evidence for zoonotic origins of Middle East respiratory syndrome coronavirus. *The Journal of General Virology*, *97*(Pt 2), 274–280. https://doi.org/10.1099/jgv.0.000342

Hanada, K., Gojobori, T., & Li, W.-H. (2006). Radical amino acid change versus positive selection in the evolution of viral envelope proteins. *Gene*, *385*, 83–88. https://doi.org/10.1016/j.gene.2006.06.029

Hassell, J. M., Begon, M., Ward, M. J., & Fèvre, E. M. (2017). Urbanization and Disease Emergence: Dynamics at the Wildlife–Livestock–Human Interface. *Trends in Ecology & Evolution*, *32*(1), 55–67. https://doi.org/10.1016/j.tree.2016.09.012

Hoang, D. T., Chernomor, O., von Haeseler, A., Minh, B. Q., & Vinh, L. S. (2018). UFBoot2: Improving the Ultrafast Bootstrap Approximation. *Molecular Biology and Evolution*, *35*(2), 518–522. https://doi.org/10.1093/molbev/msx281

Hossain, M. K., Hassanzadeganroudsari, M., & Apostolopoulos, V. (2021). The emergence of new strains of SARS-CoV-2. What does it mean for COVID-19 vaccines? *Expert Review of Vaccines*, 1–4. https://doi.org/10.1080/14760584.2021.1915140

Hu, B., Ge, X., Wang, L.-F., & Shi, Z. (2015). Bat origin of human coronaviruses. *Virology Journal*, *12*(1), 221. https://doi.org/10.1186/s12985-015-0422-1

Huson, D. H., Beier, S., Flade, I., Górska, A., El-Hadidi, M., Mitra, S., Ruscheweyh, H.-J., & Tappu, R. (2016). MEGAN Community Edition—Interactive Exploration and Analysis of Large-Scale Microbiome Sequencing Data. *PLOS Computational Biology*, *12*(6), e1004957. https://doi.org/10.1371/journal.pcbi.1004957

Huson, D. H., & Scornavacca, C. (2012). Dendroscope 3: An Interactive Tool for Rooted Phylogenetic Trees and Networks. *Systematic Biology*, *61*(6), 1061–1067. https://doi.org/10.1093/sysbio/sys062

Huynh, J., Li, S., Yount, B., Smith, A., Sturges, L., Olsen, J. C., Nagel, J., Johnson, J. B., Agnihothram, S., Gates, J. E., Frieman, M. B., Baric, R. S., & Donaldson, E. F. (2012). Evidence supporting a zoonotic origin of human coronavirus strain NL63. *Journal of Virology*, *86*(23), 12816–12825. https://doi.org/10.1128/JVI.00906-12

Irving, A. T., Ahn, M., Goh, G., Anderson, D. E., & Wang, L.-F. (2021). Lessons from the host defences of bats, a unique viral reservoir. *Nature*, *589*(7842), 363–370. https://doi.org/10.1038/s41586-020-03128-0

Issa, E., Merhi, G., Panossian, B., Salloum, T., & Tokajian, S. (2020). SARS-CoV-2 and ORF3a: Nonsynonymous Mutations, Functional Domains, and Viral Pathogenesis. *MSystems*, *5*(3), e00266-20. https://doi.org/10.1128/mSystems.00266-20

Jackson, T., & Belsham, G. J. (2021). Picornaviruses: A View from 3A. *Viruses*, *13*(3), 456. https://doi.org/10.3390/v13030456

Jacob, J. J., Vasudevan, K., Pragasam, A. K., Gunasekaran, K., Veeraraghavan, B., & Mutreja, A. (2021). *Evolutionary Tracking of SARS-CoV-2 Genetic Variants Highlights an Intricate Balance of Stabilizing and Destabilizing Mutations*. *12*(4), 11.

Jensen, J. D., & Lynch, M. (2020). Considering mutational meltdown as a potential SARS-CoV-2 treatment strategy. *Heredity*, *124*(5), 619–620. https://doi.org/10.1038/s41437-020-0314-z

Jones, K. E., Patel, N. G., Levy, M. A., Storeygard, A., Balk, D., Gittleman, J. L., & Daszak, P. (2008). *Global trends in emerging infectious diseases*. *451*, 5.

Kardjadj M. (2016). *The Epidemiology of Human and Animal Brucellosis in Algeria*. *3*(2), 6.

Kardjadj, M., & Ben-Mahdi, M. H. (2019). Epidemiology of dog-mediated zoonotic diseases in Algeria: A One Health control approach. *New Microbes and New Infections*, *28*, 17–20. https://doi.org/10.1016/j.nmni.2019.01.001

Katoh, K., Misawa, K., Kuma, K., & Miyata, T. (2002). MAFFT: A novel method for rapid multiple sequence alignment based on fast Fourier transform. *Nucleic Acids Research*, *30*(14), 3059–3066.

Kaushal, N., Gupta, Y., Goyal, M., Khaiboullina, S. F., Baranwal, M., & Verma, S. C. (2020). Mutational Frequencies of SARS-CoV-2 Genome during the Beginning Months of the Outbreak in USA. *Pathogens*, *9*(7), 565. https://doi.org/10.3390/pathogens9070565

Kemenesi, G., Zhang, D., Marton, S., Dallos, B., Görföl, T., Estók, P., Boldogh, S., Kurucz, K., Oldal, M., Kutas, A., Bányai, K., & Jakab, F. (2015). Genetic characterization of a novel picornavirus detected in Miniopterus schreibersii bats. *Journal of General Virology*, *96*(4), 815–821. https://doi.org/10.1099/jgv.0.000028

King, A. M. Q., Lefkowitz, E. J., Mushegian, A. R., Adams, M. J., Dutilh, B. E., Gorbalenya, A. E., Harrach, B., Harrison, R. L., Junglen, S., Knowles, N. J., Kropinski, A. M., Krupovic, M., Kuhn, J. H., Nibert, M. L., Rubino, L., Sabanadzovic, S., Sanfaçon, H., Siddell, S. G., Simmonds, P., … Davison, A. J. (2018). Changes to taxonomy and the International Code of Virus Classification and Nomenclature ratified by the

International Committee on Taxonomy of Viruses (2018). *Archives of Virology*, *163*(9), 2601–2631. https://doi.org/10.1007/s00705-018-3847-1

Koelle, K., & Rasmussen, D. A. (2015). The effects of a deleterious mutation load on patterns of influenza A/H3N2's antigenic evolution in humans. *ELife*, *4*, e07361. https://doi.org/10.7554/eLife.07361

Kreuder Johnson, C., Hitchens, P. L., Smiley Evans, T., Goldstein, T., Thomas, K., Clements, A., Joly, D. O., Wolfe, N. D., Daszak, P., Karesh, W. B., & Mazet, J. K. (2015). Spillover and pandemic properties of zoonotic viruses with high host plasticity. *Scientific Reports*, *5*(1), 14830. https://doi.org/10.1038/srep14830

Kumar, S., Nyodu, R., Maurya, V. K., & Saxena, S. K. (2020). Morphology, Genome Organization, Replication, and Pathogenesis of Severe Acute Respiratory Syndrome Coronavirus 2 (SARS-CoV-2). *Coronavirus Disease 2019 (COVID-19)*, 23–31. https://doi.org/10.1007/978-981-15-4814-7_3

Kurosu, T. (2011). Quasispecies of dengue virus. *Tropical Medicine and Health*, *39*(4SUPPLEMENT), S29–S36. https://doi.org/10.2149/tmh.2011-S02

Lacroix, A., Vidal, N., Keita, A. K., Thaurignac, G., Esteban, A., De Nys, H., Diallo, R., Toure, A., Goumou, S., Soumah, A. K., Povogui, M., Koivogui, J., Monemou, J.-L., Raulino, R., Nkuba, A., Foulongne, V., Delaporte, E., Ayouba, A., & Peeters, M. (2020). Wide Diversity of Coronaviruses in Frugivorous and Insectivorous Bat Species: A Pilot Study in Guinea, West Africa. *Viruses*, *12*(8), 855. https://doi.org/10.3390/v12080855

Lai, A., Bergna, A., Acciarri, C., Galli, M., & Zehender, G. (2020). Early phylogenetic estimate of the effective reproduction number of SARS-CoV-2. *Journal of Medical Virology*, 10.1002/jmv.25723. https://doi.org/10.1002/jmv.25723

LARCHER Gérald. (2020, December 1). Bats and viruses or how to live together in harmony. *Encyclopedia of the Environment*. https://www.encyclopedie-environnement.org/en/life/bats-viruses-how-live-together-harmony/

Lau, B. T., Pavlichin, D., Hooker, A. C., Almeda, A., Shin, G., Chen, J., Sahoo, M. K., Huang, C. H., Pinsky, B. A., Lee, H. J., & Ji, H. P. (2021). Profiling SARS-CoV-2 mutation fingerprints that range from the viral pangenome to individual infection quasispecies. *Genome Medicine*, *13*(1), 62. https://doi.org/10.1186/s13073-021-00882-2

Leigh, J. W., & Bryant, D. (2015). popart: Full-feature software for haplotype network construction. *Methods in Ecology and Evolution*, *6*(9), 1110–1116. https://doi.org/10.1111/2041-210X.12410

Lemey, P., Rambaut, A., Welch, J. J., & Suchard, M. A. (2010). Phylogeography Takes a Relaxed Random Walk in Continuous Space and Time. *Molecular Biology and Evolution*, *27*(8), 1877–1885. https://doi.org/10.1093/molbev/msq067

Leopardi, S., Holmes, E. C., Gastaldelli, M., Tassoni, L., Priori, P., Scaravelli, D., Zamperin, G., & De Benedictis, P. (2018). Interplay between co-divergence and cross-species transmission in the evolutionary history of bat coronaviruses. *Infection, Genetics and Evolution: Journal of Molecular Epidemiology and Evolutionary Genetics in Infectious Diseases*, *58*, 279–289. https://doi.org/10.1016/j.meegid.2018.01.012

Letko, M., Seifert, S. N., Olival, K. J., Plowright, R. K., & Munster, V. J. (2020). Bat-borne virus diversity, spillover and emergence. *Nature Reviews Microbiology*, *18*(8), 461–471. https://doi.org/10.1038/s41579-020-0394-z

Letunic, I., & Bork, P. (2016). Interactive tree of life (iTOL) v3: An online tool for the display and annotation of phylogenetic and other trees. *Nucleic Acids Research*, *44*(Web Server issue), W242–W245. https://doi.org/10.1093/nar/gkw290

Lewis-Rogers, N., & Crandall, K. A. (2010). Evolution of Picornaviridae: An examination of phylogenetic relationships and cophylogeny. *Molecular Phylogenetics and Evolution*, *54*(3), 995–1005. https://doi.org/10.1016/j.ympev.2009.10.015

Li, L., Pesavento, P. A., Shan, T., Leutenegger, C. M., Wang, C., & Delwart, E. (2011). Viruses in diarrhoeic dogs include novel kobuviruses and sapoviruses. *The Journal of General Virology*, *92*(Pt 11), 2534–2541. https://doi.org/10.1099/vir.0.034611-0

Li, S., Sun, K., Lu, G., Lin, A., Jiang, T., Jin, L., Hoyt, J. R., & Feng, J. (2015). Mitochondrial genetic differentiation and morphological difference of Miniopterus fuliginosus and Miniopterus magnater in China and Vietnam. *Ecology and Evolution*, *5*(6), 1214–1223. https://doi.org/10.1002/ece3.1428

Li, X., Wang, W., Zhao, X., Zai, J., Zhao, Q., Li, Y., & Chaillon, A. (2020). Transmission dynamics and evolutionary history of 2019-nCoV. *Journal of Medical Virology*, *92*(5), 501–511. https://doi.org/10.1002/jmv.25701

Lin, J.-Y., Chen, T.-C., Weng, K.-F., Chang, S.-C., Chen, L.-L., & Shih, S.-R. (2009). Viral and host proteins involved in picornavirus life cycle. *Journal of Biomedical Science*, *16*(1), 103. https://doi.org/10.1186/1423-0127-16-103

Lukashev, A. N. (2010). Recombination among picornaviruses. *Reviews in Medical Virology*, *20*(5), 327–337. https://doi.org/10.1002/rmv.660

Lukashev, A. N., Corman, V. M., Schacht, D., Gloza-Rausch, F., Seebens-Hoyer, A., Gmyl, A. P., Drosten, C., & Drexler, J. F. (2017). Close genetic relatedness of picornaviruses from European and Asian bats. *Journal of General Virology*, *98*(5), 955–961. https://doi.org/10.1099/jgv.0.000760

Lukashov, V. V., & Goudsmit, J. (2001). Evolutionary Relationships among Parvoviruses: Virus-Host Coevolution among Autonomous Primate Parvoviruses and Links between Adeno-Associated and Avian Parvoviruses. *Journal of Virology*, *75*(6), 2729–2740. https://doi.org/10.1128/JVI.75.6.2729-2740.2001

Lytras, S., Xia, W., Hughes, J., Jiang, X., & Robertson, D. L. (2021). The animal origin of SARS-CoV-2. *Science*, *373*(6558), 968–970. https://doi.org/10.1126/science.abh0117

Martin, D. P., Murrell, B., Golden, M., Khoosal, A., & Muhire, B. (2015). RDP4: Detection and analysis of recombination patterns in virus genomes. *Virus Evolution*, *1*(1). https://doi.org/10.1093/ve/vev003

Masatoshi Nei & Takashi Gojobori. (1986). Simple methods for estimating the numbers of synonymous and nonsynonymous nucleotide substitutions. *Molecular Biology and Evolution*. https://doi.org/10.1093/oxfordjournals.molbev.a040410

Megna, R. (2020). First month of the epidemic caused by COVID-19 in Italy: Current status and real-time outbreak development forecast. *Global Health Research and Policy*, *5*(1), 43. https://doi.org/10.1186/s41256-020-00170-3

Miao, M., Clercq, E. D., & Li, G. (2021). Genetic Diversity of SARS-CoV-2 over a One-Year Period of the COVID-19 Pandemic: A Global Perspective. *Biomedicines*, *9*(4), 412. https://doi.org/10.3390/biomedicines9040412

Miyata, T., Miyazawa, S., & Yasunaga, T. (1979). Two types of amino acid substitutions in protein evolution. *Journal of Molecular Evolution*, *12*(3), 219–236. https://doi.org/10.1007/BF01732340

Nahata, K. D., Bollen, N., Gill, M. S., Layan, M., Bourhy, H., Dellicour, S., & Baele, G. (2021). On the Use of Phylogeographic Inference to Infer the Dispersal History of Rabies Virus: A Review Study. *Viruses*, *13*(8), 1628. https://doi.org/10.3390/v13081628

Ng, P. C., & Henikoff, S. (2003). SIFT: Predicting amino acid changes that affect protein function. *Nucleic Acids Research*, *31*(13), 3812–3814.

Nguyen, L.-T., Schmidt, H. A., von Haeseler, A., & Minh, B. Q. (2015). IQ-TREE: A Fast and Effective Stochastic Algorithm for Estimating Maximum-Likelihood Phylogenies. *Molecular Biology and Evolution*, *32*(1), 268–274. https://doi.org/10.1093/molbev/msu300

Nicholas, K., & Nicholas, H. (1997). GeneDoc: A tool for editing and annotating multiple sequence alignments. *Undefined*. /paper/GeneDoc%3A-a-tool-for-editing-and-annotating-multiple-Nicholas-Nicholas/bb5b2fa84ff9f38fc03e257671d984409d355640

Norby, E. E., Jarman, R. G., Keiser, P. B., Binn, L. N., & Hang, J. (2017). Genome Sequence of a Novel Canine Picornavirus Isolated from an American Foxhound. *Genome Announcements*, *5*(20), e00338-17. https://doi.org/10.1128/genomeA.00338-17

Olson, S. H., Benedum, C. M., Mekaru, S. R., Preston, N. D., Mazet, J. A. K., Joly, D. O., & Brownstein, J. S. (2015). Drivers of Emerging Infectious Disease Events as a Framework for Digital Detection. *Emerging Infectious Diseases*, *21*(8), 1285–1292. https://doi.org/10.3201/eid2108.141156

Pandémie de Covid-19 en Algérie. (2021). In *Wikipédia*. https://fr.wikipedia.org/w/index.php?title=Pand%C3%A9mie_de_Covid-19_en_Alg%C3%A9rie&oldid=183752230

Pape, W. J., Fitzsimmons, T. D., & Hoffman, R. E. (1999). Risk for Rabies Transmission from Encounters with Bats, Colorado, 1977–1996. *Emerging Infectious Diseases*, *5*(3), 433–437. https://doi.org/10.3201/eid0503.990315

Parker, J., Rambaut, A., & Pybus, O. G. (2008). Correlating viral phenotypes with phylogeny: Accounting for phylogenetic uncertainty. *Infection, Genetics and Evolution*, *8*(3), 239–246. https://doi.org/10.1016/j.meegid.2007.08.001

Pfefferle, S., Oppong, S., Drexler, J. F., Gloza-Rausch, F., Ipsen, A., Seebens, A., Müller, M. A., Annan, A., Vallo, P., Adu-Sarkodie, Y., Kruppa, T. F., & Drosten, C. (2009). Distant Relatives of Severe Acute Respiratory Syndrome Coronavirus and Close Relatives of Human Coronavirus 229E in Bats, Ghana. *Emerging Infectious Diseases*, *15*(9), 1377–1384. https://doi.org/10.3201/eid1509.090224

Phan, T. G., Kapusinszky, B., Wang, C., Rose, R. K., Lipton, H. L., & Delwart, E. L. (2011). The fecal viral flora of wild rodents. *PLoS Pathogens*, *7*(9), e1002218. https://doi.org/10.1371/journal.ppat.1002218

Pohl, M. O., Busnadiego, I., Kufner, V., Schmutz, S., Zaheri, M., Abela, I., Trkola, A., Huber, M., Stertz, S., & Hale, B. G. (2020). *Distinct Phenotypes of SARS-CoV-2 Isolates Reveal Viral Traits Critical for Replication in Primary Human Respiratory Cells* (p. 2020.10.22.350207). https://doi.org/10.1101/2020.10.22.350207

Prince, T., Smith, S. L., Radford, A. D., Solomon, T., Hughes, G. L., & Patterson, E. I. (2021). SARS-CoV-2 Infections in Animals: Reservoirs for Reverse Zoonosis and Models for Study. *Viruses*, *13*(3), 494. https://doi.org/10.3390/v13030494

Puechmaille, S. J., Allegrini, B., Benda, P., Gürün, K., Srámek, J., Ibañez, C., Juste, J., & Bilgin, R. (2014). A new species of the Miniopterus schreibersii species complex (Chiroptera: Miniopteridae) from the Maghreb Region, North Africa. *Zootaxa*, *3794*, 108–124. https://doi.org/10.11646/zootaxa.3794.1.4

R Core Team. (2020). *R: A Language and Environment for Statistical Computing*. R Foundation for Statistical Computing. https://www.R-project.org/

Rambaut, A., Drummond, A. J., Xie, D., Baele, G., & Suchard, M. A. (2018). Posterior Summarization in Bayesian Phylogenetics Using Tracer 1.7. *Systematic Biology*, *67*(5), 901–904. https://doi.org/10.1093/sysbio/syy032

Rambaut, A., Holmes, E. C., Hill, V., O'Toole, Á., McCrone, J., Ruis, C., du Plessis, L., & Pybus, O. G. (2020). *A dynamic nomenclature proposal for SARS-CoV-2 to assist genomic epidemiology* [Preprint]. Microbiology. https://doi.org/10.1101/2020.04.17.046086

Rambaut, A., Lam, T. T., Max Carvalho, L., & Pybus, O. G. (2016). Exploring the temporal structure of heterochronous sequences using TempEst (formerly Path-O-Gen). *Virus Evolution*, *2*(1). https://doi.org/10.1093/ve/vew007

Ronquist, F., Teslenko, M., van der Mark, P., Ayres, D. L., Darling, A., Höhna, S., Larget, B., Liu, L., Suchard, M. A., & Huelsenbeck, J. P. (2012). MrBayes 3.2: Efficient Bayesian Phylogenetic Inference and Model Choice Across a Large Model Space. *Systematic Biology*, *61*(3), 539–542. https://doi.org/10.1093/sysbio/sys029

Rozas, J., Ferrer-Mata, A., Sánchez-DelBarrio, J. C., Guirao-Rico, S., Librado, P., Ramos-Onsins, S. E., & Sánchez-Gracia, A. (2017). DnaSP 6: DNA Sequence Polymorphism Analysis of Large Data Sets. *Molecular Biology and Evolution*, *34*(12), 3299–3302. https://doi.org/10.1093/molbev/msx248

Russo, D., & Ancillotto, L. (2015). Sensitivity of bats to urbanization: A review. *Mammalian Biology*, *80*(3), 205–212. https://doi.org/10.1016/j.mambio.2014.10.003

Sabin, N. S., Calliope, A. S., Simpson, S. V., Arima, H., Ito, H., Nishimura, T., & Yamamoto, T. (2020). Implications of human activities for (re)emerging infectious diseases, including COVID-19. *Journal of Physiological Anthropology*, *39*(1), 29. https://doi.org/10.1186/s40101-020-00239-5

Sahabi Abed, S., & Matzarakis, A. (2017). Seasonal Regional Differentiation of Human Thermal Comfort Conditions in Algeria. *Advances in Meteorology*, *2017*, 1–14. https://doi.org/10.1155/2017/9193871

Schneeberger, K., & Voigt, C. C. (2015). Zoonotic Viruses and Conservation of Bats. *Bats in the Anthropocene: Conservation of Bats in a Changing World*, 263–292. https://doi.org/10.1007/978-3-319-25220-9_10

Semenza, J. C., Lindgren, E., Balkanyi, L., Espinosa, L., Almqvist, M. S., Penttinen, P., & Rocklöv, J. (2016). Determinants and Drivers of Infectious Disease Threat Events

in Europe. *Emerging Infectious Diseases*, *22*(4), 581–589. https://doi.org/10.3201/eid2204.151073

Sharp, P. M., & Simmonds, P. (2011). Evaluating the evidence for virus/host co-evolution. *Current Opinion in Virology*, *1*(5), 436–441. https://doi.org/10.1016/j.coviro.2011.10.018

Shi, Z., & Hu, Z. (2008). A review of studies on animal reservoirs of the SARS coronavirus. *Virus Research*, *133*(1), 74–87. https://doi.org/10.1016/j.virusres.2007.03.012

Shu, Y., & McCauley, J. (2017). GISAID: Global initiative on sharing all influenza data – from vision to reality. *Eurosurveillance*, *22*(13), 30494. https://doi.org/10.2807/1560-7917.ES.2017.22.13.30494

Sikkema, R. S., & Koopmans, M. P. G. (2021). Preparing for Emerging Zoonotic Viruses. *Encyclopedia of Virology*, 256–266. https://doi.org/10.1016/B978-0-12-814515-9.00150-8

Simmonds, P. (2006). Recombination and selection in the evolution of picornaviruses and other Mammalian positive-stranded RNA viruses. *Journal of Virology*, *80*(22), 11124–11140. https://doi.org/10.1128/JVI.01076-06

Simpson, S., Kaufmann, M. C., Glozman, V., & Chakrabarti, A. (2020). Disease X: Accelerating the development of medical countermeasures for the next pandemic. *The Lancet Infectious Diseases*, *20*(5), e108–e115. https://doi.org/10.1016/S1473-3099(20)30123-7

Singer, J., Gifford, R., Cotten, M., & Robertson, D. (2020). *CoV-GLUE: A Web Application for Tracking SARS-CoV-2 Genomic Variation*. https://doi.org/10.20944/preprints202006.0225.v1

Subudhi, S., Rapin, N., & Misra, V. (2019). Immune System Modulation and Viral Persistence in Bats: Understanding Viral Spillover. *Viruses*, *11*(2), 192. https://doi.org/10.3390/v11020192

Suchard, M. A., Lemey, P., Baele, G., Ayres, D. L., Drummond, A. J., & Rambaut, A. (2018). Bayesian phylogenetic and phylodynamic data integration using BEAST 1.10. *Virus Evolution*, *4*(1). https://doi.org/10.1093/ve/vey016

Sun, D., Chen, S., Cheng, A., & Wang, M. (2016). Roles of the Picornaviral 3C Proteinase in the Viral Life Cycle and Host Cells. *Viruses*, *8*(3), 82. https://doi.org/10.3390/v8030082

Tamura, K., Stecher, G., Peterson, D., Filipski, A., & Kumar, S. (2013). MEGA6: Molecular Evolutionary Genetics Analysis Version 6.0. *Molecular Biology and Evolution*, *30*(12), 2725–2729. https://doi.org/10.1093/molbev/mst197

Tao, Y., Shi, M., Chommanard, C., Queen, K., Zhang, J., Markotter, W., Kuzmin, I. V., Holmes, E. C., & Tong, S. (2017). Surveillance of Bat Coronaviruses in Kenya Identifies Relatives of Human Coronaviruses NL63 and 229E and Their Recombination History. *Journal of Virology*, *91*(5), e01953-16. https://doi.org/10.1128/JVI.01953-16

Taylor, L. H., Latham, S. M., & Woolhouse, M. E. (2001). Risk factors for human disease emergence. *Philosophical Transactions of the Royal Society B: Biological Sciences*, *356*(1411), 983–989. https://doi.org/10.1098/rstb.2001.0888

Temmam, S., Vongphayloth, K., Salazar, E. B., Munier, S., Bonomi, M., Régnault, B., Douangboubpha, B., Karami, Y., Chretien, D., Sanamxay, D., Xayaphet, V., Paphaphanh, P., Lacoste, V., Somlor, S., Lakeomany, K., Phommavanh, N., Pérot, P., Donati, F., Bigot, T., … Eloit, M. (2021). *Coronaviruses with a SARS-CoV-2-like receptor-binding domain allowing ACE2-mediated entry into human cells isolated from bats of Indochinese peninsula* [Preprint]. In Review. https://doi.org/10.21203/rs.3.rs-871965/v1

Themes, U. F. O. (2016, August 11). Picornaviridae: The Viruses and their Replication. *Basicmedical Key*. https://basicmedicalkey.com/picornaviridae-the-viruses-and-their-replication/

Time dependence of SARS-CoV-2 substitution rates—SARS-CoV-2 coronavirus / nCoV-2019 Evolutionary History. (2020, October 27). Virological. https://virological.org/t/time-dependence-of-sars-cov-2-substitution-rates/542

Turmelle, A. S., & Olival, K. J. (2009). Correlates of Viral Richness in Bats (Order Chiroptera). *Ecohealth*, *6*(4), 522–539. https://doi.org/10.1007/s10393-009-0263-8

Tuthill, T. J., Groppelli, E., Hogle, J. M., & Rowlands, D. J. (2010). Picornaviruses. *Current Topics in Microbiology and Immunology*, *343*, 43–89. https://doi.org/10.1007/82_2010_37

Vijaykrishna, D., Smith, G. J. D., Zhang, J. X., Peiris, J. S. M., Chen, H., & Guan, Y. (2007). Evolutionary Insights into the Ecology of Coronaviruses. *Journal of Virology*, *81*(8), 4012–4020. https://doi.org/10.1128/JVI.02605-06

V'kovski, P., Kratzel, A., Steiner, S., Stalder, H., & Thiel, V. (2021). Coronavirus biology and replication: Implications for SARS-CoV-2. *Nature Reviews Microbiology*, *19*(3), 155–170. https://doi.org/10.1038/s41579-020-00468-6

Wacharapluesadee, S., Tan, C. W., Maneeorn, P., Duengkae, P., Zhu, F., Joyjinda, Y., Kaewpom, T., Chia, W. N., Ampoot, W., Lim, B. L., Worachotsueptrakun, K., Chen, V. C.-W., Sirichan, N., Ruchisrisarod, C., Rodpan, A., Noradechanon, K., Phaichana, T., Jantarat, N., Thongnumchaima, B., … Wang, L.-F. (2021). Evidence for SARS-CoV-2 related coronaviruses circulating in bats and pangolins in Southeast Asia. *Nature Communications*, *12*(1), 972. https://doi.org/10.1038/s41467-021-21240-1

Walker, F. M., Williamson, C. H. D., Sanchez, D. E., Sobek, C. J., & Chambers, C. L. (2016). Species From Feces: Order-Wide Identification of Chiroptera From Guano and Other Non-Invasive Genetic Samples. *PLoS ONE*, *11*(9), e0162342. https://doi.org/10.1371/journal.pone.0162342

Walker, P. J., Siddell, S. G., Lefkowitz, E. J., Mushegian, A. R., Dempsey, D. M., Dutilh, B. E., Harrach, B., Harrison, R. L., Hendrickson, R. C., Junglen, S., Knowles, N. J., Kropinski, A. M., Krupovic, M., Kuhn, J. H., Nibert, M., Rubino, L., Sabanadzovic, S., Simmonds, P., Varsani, A., … Davison, A. J. (2019). Changes to virus taxonomy and the International Code of Virus Classification and Nomenclature ratified by the International Committee on Taxonomy of Viruses (2019). *Archives of Virology*, *164*(9), 2417–2429. https://doi.org/10.1007/s00705-019-04306-w

Wang, L.-F., & Crameri, G. (2014). Emerging zoonotic viral diseases: -EN- -FR- Les maladies zoonotiques virales émergentes -ES- Enfermedades zoonóticas

emergentes de origen vírico. *Revue Scientifique et Technique de l'OIE*, *33*(2), 569–581. https://doi.org/10.20506/rst.33.2.2311

Waruhiu, C., Ommeh, S., Obanda, V., Agwanda, B., Gakuya, F., Ge, X.-Y., Yang, X.-L., Wu, L.-J., Zohaib, A., Hu, B., & Shi, Z.-L. (2017). Molecular detection of viruses in Kenyan bats and discovery of novel astroviruses, caliciviruses and rotaviruses. *Virologica Sinica*, *32*(2), 101–114. https://doi.org/10.1007/s12250-016-3930-2

Webber, Q. M. R., Fletcher, Q. E., & Willis, C. K. R. (2017). Viral Richness is Positively Related to Group Size, but Not Mating System, in Bats. *EcoHealth*, *14*(4), 652–661. https://doi.org/10.1007/s10393-017-1276-3

Wu, Z., Ren, X., Yang, L., Hu, Y., Yang, J., He, G., Zhang, J., Dong, J., Sun, L., Du, J., Liu, L., Xue, Y., Wang, J., Yang, F., Zhang, S., & Jin, Q. (2012). Virome Analysis for Identification of Novel Mammalian Viruses in Bat Species from Chinese Provinces. *Journal of Virology*, *86*(20), 10999–11012. https://doi.org/10.1128/JVI.01394-12

Wu, Z., Yang, L., Ren, X., He, G., Zhang, J., Yang, J., Qian, Z., Dong, J., Sun, L., Zhu, Y., Du, J., Yang, F., Zhang, S., & Jin, Q. (2016). Deciphering the bat virome catalog to better understand the ecological diversity of bat viruses and the bat origin of emerging infectious diseases. *The ISME Journal*, *10*(3), 609–620. https://doi.org/10.1038/ismej.2015.138

Yamashita, T., Sakae, K., Tsuzuki, H., Suzuki, Y., Ishikawa, N., Takeda, N., Miyamura, T., & Yamazaki, S. (1998). Complete nucleotide sequence and genetic organization of Aichi virus, a distinct member of the Picornaviridae associated with acute gastroenteritis in humans. *Journal of Virology*, *72*(10), 8408–8412. https://doi.org/10.1128/JVI.72.10.8408-8412.1998

Yang, Y., Peng, F., Wang, R., Guan, K., Jiang, T., Xu, G., Sun, J., & Chang, C. (2020). The deadly coronaviruses: The 2003 SARS pandemic and the 2020 novel coronavirus epidemic in China. *Journal of Autoimmunity*, *109*, 102434. https://doi.org/10.1016/j.jaut.2020.102434

Yang, Z., & Bielawski, J. P. (2000). Statistical methods for detecting molecular adaptation. *Trends in Ecology & Evolution*, *15*(12), 496–503. https://doi.org/10.1016/S0169-5347(00)01994-7

Zeghbib, S., Herczeg, R., Kemenesi, G., Zana, B., Kurucz, K., Urbán, P., Madai, M., Földes, F., Papp, H., Somogyi, B., & Jakab, F. (2019). Genetic characterization of a novel picornavirus in Algerian bats: Co-evolution analysis of bat-related picornaviruses. *Scientific Reports*, *9*(1), 15706. https://doi.org/10.1038/s41598-019-52209-2

Zeghbib, S., Somogyi, B. A., Zana, B., Kemenesi, G., Herczeg, R., Derrar, F., & Jakab, F. (2021). The Algerian Chapter of SARS-CoV-2 Pandemic: An Evolutionary, Genetic, and Epidemiological Prospect. *Viruses*, *13*(8), 1525. https://doi.org/10.3390/v13081525

Zell, R., Delwart, E., Gorbalenya, A. E., Hovi, T., King, A. M. Q., Knowles, N. J., Lindberg, A. M., Pallansch, M. A., Palmenberg, A. C., Reuter, G., Simmonds, P., Skern, T., Stanway, G., & Yamashita, T. (2017). ICTV Virus Taxonomy Profile: Picornaviridae. *The Journal of General Virology*, *98*(10), 2421–2422. https://doi.org/10.1099/jgv.0.000911

Zhang, M., Li, L., Luo, M., & Liang, B. (2021). Genomic characterization and evolution of SARS-CoV-2 of a Canadian population. *PLOS ONE*, *16*(3), e0247799. https://doi.org/10.1371/journal.pone.0247799

Zhou, H., Ji, J., Chen, X., Bi, Y., Li, J., Wang, Q., Hu, T., Song, H., Zhao, R., Chen, Y., Cui, M., Zhang, Y., Hughes, A. C., Holmes, E. C., & Shi, W. (2021). Identification of novel bat coronaviruses sheds light on the evolutionary origins of SARS-CoV-2 and related viruses. *Cell*, *184*(17), 4380-4391.e14. https://doi.org/10.1016/j.cell.2021.06.008

Zhou, Z., Qiu, Y., & Ge, X. (2021). The taxonomy, host range and pathogenicity of coronaviruses and other viruses in the Nidovirales order. *Animal Diseases*, *1*(1), 5. https://doi.org/10.1186/s44149-021-00005-9

9. Acknowledgment

First, I would like to express my special thanks and appreciation to my supervisor Prof. Dr. Ferenc Jakab, for his patience, support, guidance, and continuous encouragement. He gave me endless opportunities to plan, work, study, and travel in order to improve myself as a scientist. Above this, I am really thankful to him for giving me the chance to work in a BSL-4 laboratory and to be open for new research plans establishment. I couldn't have imagined having a better advisor for my Ph.D.

I would like to express my deep and sincere gratitude to Dr. Gábor Kemenesi, who trained me and guided me through the whole process. I must say thanks also for his encouragement and comfort whenever I felt disappointed.

Additionally, I would like to thank my second family: all my colleagues in the National Virology Laboratory namely: Brigitta Zana, Földes Fanni Vivien, Mónika Madai, Henrietta Papp, Zsófia Lanszki, Balázs Somogyi, Gábor Endre Tóth, Nyari Viktoria, Varga Zsaklin, as well as: Dr. Kornélia Kemenesiné Kurucz and Dr. Anett Kuczmog. None of these accomplishments would have been possible without them.

Big gratitude goes to Dr. Miklós Oldal and Dr. Herczeg Róbert they helped a lot with their advice and shared knowledge.

Also, I would like to acknowledge Dr. Ahmim Mourad, Dr. Ettayib Bensaci, Dr. Boudrissa Karim, Mr. Filali Aissa, Mr. Boutamina Ali, and the Ph.D. student Ait Ouakli Thilelli for their help in the fieldwork, as well as Dr. Derrar Fawzi for his collaboration within the SARS-CoV-2 pandemic framework.

Above all, I express my deep gratitude for my parents: Zeghbib Nabil and Saighi Hanifa. For their unceasing support and presence and help in the fieldwork as well. I am Thankful for all what they have done for me to be an accomplished person.

Deep thanks to my sisters: Karimane Malek a biologist who was present during all the field works, and Rayane Zeghbib for her moral support, as well as Abir Abderrezag for her encouragement.

A particular recognition for my husband Abderrezag Samir for his continued and unfailing love, support, and understanding during my pursuit of a PhD degree that made the completion of thesis possible.

10. Supplementary material

10.1. Bat picornavirus analysis

10.1.1. Sequences used

BtPiV sequences: MG888045, HM228882, HQ595341, HQ595342,HQ595343, HQ595344, HQ595345, JQ814851, JQ814852, JQ916917, JQ916918, JQ916919, JQ916920, JQ916921, JQ916922, JQ916923, JQ916924, JQ916925, JQ916926, JQ916927, JQ916928, JQ916929, JQ916930, JQ916931, JQ916932, JQ916933, JQ916934, JQ916935, JQ916936, JQ916937, JQ916938, JQ916939, JQ916940, JQ916941, JQ916942, JQ916943,JQ916944, KJ641684, KJ641685, KJ641686, KJ641687, KJ641688, KJ641689, KJ641690, KJ641691, KJ641692, KJ641693, KJ641694, KJ641695, KJ641696, KJ641697, KJ641698, KJ641699, KP054273, KP054274, KP054275, KP054276, KP054277, KP054278, KP100644, KT452714, KT452729, KT452730, KT452742, KX644936, NC_015934, NC_015941, NC_027214, NC_033819, NC_033820.

Bat's cytochrome oxidase I sequences: AB085735, AB085738, AB355794, AF451338, AJ504448, AJ504452, DQ302094, DQ435073, EF517308, EF530348, EU360631, EU434934, EU434941, EU436673, EU934470, FJ215677, FJ383130, FJ457612, JQ956449, KJ735798, HNHM25833, HNHM24769.

9.1.2 BaTS analysis for all BtPiV and mischiviruses tables

Character trait	Statistics	Observed mean	Lower 95% CI	Upper 95% CU	Null mean	Lower 95% CI	Upper 95% CI	Significance
Host genus	AI	0.028	1.878E-5	0.031	0.746	0.344	1.122	0.0
	PS	2.00	2.0	2.0	4.562	3.995	5.0	0.0
	MC (Miniopterus)	11.999	12.0	12.0	3.300	1.966	5.836	9.999E-4
	MC (Hipposederos)	1.0	1.0	1.0	1.0	1.0	1.0	1.0
	MC (Myotis)	2.999	3.0	3.0	1.096	1.0	1.967	9.999E-4
Host species	AI	0.389	0.333	0.395	0.781	0.372	1.147	0.065
	PS	3.0	3.0	3.0	4.688	4.0	5.0	0.0
	MC (M. schreibersii)	11.999	12.0	12.0	3.211	1.964	5.836	9.999E-4
	MC (H. gigas)	1.0	1.0	1.0	1.0	1.0	1.0	1.0
	MC (M. oxygnathus)	1.0	1.0	1.0	1.0	1.0	1.0	1.0
	MC (M. myotis)	1.004	1.0	1.0	1.029	1.0	1.017	1.0
Sampling location	AI	0.029	$2.264E^{-4}$	0.031	0.622	0.211	1.022	0.003
	PS	3.0	3.0	3.0	3.735	3.0	4.0	0.235
	MC (Africa)	1.0	1.0	1.0	1.023	1.0	1.003	1.0
	MC (Europe)	9.996	10.0	10.0	3.822	2.036	5.875	0.009
	MC (Asia)	1.0	1.0	1.0	1.0	1.0	1.0	1.0

Table S1. Phylogeny trait association analysis using BaTS for all BtPiV.

Trait Statistics	Observed mean	Lower 95% CI	Upper 95% CI	Null mean	Lower 95% CI	Upper 95% CI	Significance
Host genus							
AI	2.254	1.979	2.562	5.419	4.603	6.192	0.0
PS	21.003	21.0	21.0	36.369	33.859	39.206	0.0
MC:							
Miniopterus	11.998	12.0	12.0	2.909	2.0	4.009	0.009
Myotis	3.840	3.0	4.0	1.415	1.0	2.238	0.009
Rhinolophus	8.966	9.0	9.0	1.822	1.0143	2.674	0.009
Nyctalus	1.0	1.0	1.0	1.006	1.0	1.0	1.0
Hipposederos	1.0	1.0	1.0	1.0	1.0	1.0	1.0
Eidolon	1.0	1.0	1.0	1.0	1.0	1.0	1.0
Vespertilio	1.0	1.0	1.0	1.0	1.0	1.0	1.0
Ia	1.009	1.0	1.0	1.083	1.0	1.644	1.0
Coleura	1.0	1.0	1.0	1.0	1.0	1.0	1.0
Host species							
AI	3.479	3.163	3.856	6.750	6.152	7.214	0.0
PS	32.988	33.0	33.0	47.595	45.728	49.726	0.0
MC:							
M. schreibersii	11.995	12.0	12.0	2.177	1.188	3.009	0.009
M. oxygnathus	1.0	1.0	1.0	1.0	1.0	1.0	1.0
M. myotis	2.998	3.0	3.0	1.124	1.0	1.894	0.009
M. bechsteinii	1.0	1.0	1.0	1.0	1.0	1.0	1.0
M. dasycneme	1.0	1.0	1.0	1.0	1.0	1.0	1.0
R. euryale	3.999	4.0	4.0	1.103	1.0	1.650	0.009
R. blasii	1.0	1.0	1.0	1.0	1.0	1.0	1.0
R. ferrumequinum	1.0	1.0	1.0	1.0	1.0	1.0	1.0
N. noctula	1.0	1.0	1.0	1.0	1.0	1.0	1.0
M. magnater	2.998	3.0	3.0	1.018	1.0	1.007	0.009
Ia io	1.0	1.0	1.0	1.0	1.0	1.0	1.0
R. sinicus	1.999	2.0	2.0	1.052	1.0	1.254	0.009
H. armiger	1.0	1.0	1.0	1.0	1.0	1.0	1.0
R. hipposideros	1.0	1.0	1.0	1.0	1.0	1.0	1.0
M. fuliginosus	2.999	3.0	3.0	1.079	1.0	1.978	0.009
R. lepidus	1.0	1.0	1.0	1.0	1.0	1.0	1.0
R. affinis	1.0	1.0	1.0	1.012	1.0	1.0	1.0
N. plancyi	1.0	1.0	1.0	1.0	1.0	1.0	1.0
V. superans	1.0	1.0	1.0	1.0	1.0	1.0	1.0
M. altarium	1.0	1.0	1.0	1.0	1.0	1.0	1.0
Eidolon helvum	1.009	1.0	1.0	1.070	1.0	1.990	1.0
M. ricketti	1.0	1.0	1.0	1.0	1.0	1.0	1.0
H. gigas	1.0	1.0	1.0	1.0	1.0	1.0	1.0
Coleura afra	1.0	1.0	1.0	1.0	1.0	1.0	1.0
R. landeri	1.0	1.0	1.0	1.0	1.0	1.0	1.0
M. manavi	1.0	1.0	1.0	1.0	1.0	1.0	1.0
Sampling location							
AI	0.603	0.476	0.944	4.551	3.711	5.361	0.0
PS	15.027	14.0	16.0	29.587	26.641	32.001	0.0
MC (Africa)	4.002	4.0	4.0	1.222	1.0	1.990	0.009
MC (Europe)	9.926	10.0	10.0	3.416	2.000	4.999	0.009
MC (Asia)	4.905	4.0	6.0	2.334	1.368	3.189	0.029
MC (America)	1.0	1.0	1.0	1.0	1.0	1.0	1.0

10.2.*Coronaviridae*

Bat related RdRp sequences: Z558552, MZ558551, MZ558550, MZ322309, MW652323, MW652322, MW652321, MW652320, MW652319, MW652318, MW652317, MW652316, MW652315, MW652314, MW652313, MW652312, MW652311, MW652310, MW652309, MT734810, MT586867, MT586866, MT586865, MT586864, MT586863, MT586862, MT586861, MT586860, MT586859, MT586858, MT586857,

MT586856, MT586855, MT586854, MT586853, MT586852, MT586851, MT586850, MT586849, MT586848, MT586847, MT586846, MT586845, MT586844, MT586843, MT586842, MT586841, MT586840, MT586839, MT586838, MT586837, MT586836, MT586835, MT586834, MT586833, MT586832, MT586831, MT586830, MT470445, MT470444, MT470443, MT470442, MT470441, MT470440, MT470439, MT470438, MT470437, MT350593, MT350592, MT350585, MT350584, MN872700, MN872699, MN872698, MN872697, MN872696, MN872695, MN872694, MN872693, MN872692, MN872691, MN872690, MN872689, MN872688, MN312866, MN312862, MN312825, MN312824, MN312823, MN312822, MN312748, MN312747, MN312746, MN312745, MN312744, MN312743, MN312737, MN312736, MN312735, MN312734, MN312733, MN312732, MN312731, MN312730, MN312729, MN312728, MN312727, MN312726, MN312725, MN312724, MN312723, MN312722, MN312721, MN312720, MN312719, MN312718, MN312717, MN312716, MN312715, MN312714, MN312713, MN312712, MN312690, MN312689, MN312687, MN312686, MN312685, MN312683, MN312682, MN312681, MN312679, MN312678, MN312674, MN312670, MN312669, MN312668, MN312667, MN312666, MN312665, MN312649, MN312648, MN312646, MN312631, MN312630, MN312629, MN312628, MN312627, MN312626, MN312624, MN312623, MN312622, MN312621, MN312620, MN312619, MN312618, MN312617, MN312616, MN312615, MN312614, MN312613, MN312612, MN312611, MN312610, MN312594, MN312593, MN312592, MN312591, MN312590, MN312589, MN312588, MN312587, MN312586, MN312585, MN312584, MN312583, MN312582, MN312581, MN312580, MN312579, MN312578, MN312577, MN312576, MN312568, MN312566, MN312563, MN312562, MN312561, MN312560, MN312559, MN312558, MN312557, MN312556, MN312555, MN312554, MN312553, MN312552, MN312551, MN312550, MN312549, MN312548, MN312547, MN312546, MN312545, MN312544, MN312543, MN312542, MN312541, MN312540, MN312539, MN312538, MN312537, MN312536, MN312535, MN312534, MN312533, MN312532, MN312531, MN312530, MN312529, MN312528, MN312527, MN312526, MN312525, MN312524, MN312523, MN312522, MN312521, MN312520, MN312519, MN312518, MN312517, MN312516, MN312515, MN312513, MN312512, MN312511, MN312510, MN312509, MN312508, MN312507, MN312506, MN312505, MN312504, MN312503, MN312502, MN312501, MN312500, MN312499, MN312498, MN312497, MN312496, MN312495, MN312494, MN312493, MN312492, MN312491, MN312490, MN312489, MN312488, MN312487, MN312486, MN312485, MN312484, MN312483, MN312480, MN312479, MN312478, MN312476, MN312471,

MN312470, MN312468, MN312466, MN312465, MN312464, MN312462, MN312461, MN312460, MN312458, MN312457, MN312456, MN312454, MN312453, MN312452, MN312451, MN312450, MN312449, MN312448, MN312447, MN312446, MN312445, MN312444, MN312443, MN312442, MN312441, MN312440, MN312439, MN312438, MN312437, MN312436, MN312435, MN312434, MN312433, MN312432, MN312431, MN312430, MN312429, MN312428, MN312427, MN312426, MN312425, MN312424, MN312423, MN312422, MN312421, MN312420, MN312419, MN312418, MN312416, MN312414, MN312413, MN312411, MN312410, MN312409, MN312408, MN312407, MN312406, MN312405, MN312404, MN312403, MN312402, MN312401, MN312400, MN312399, MN312398, MN312397, MN312396, MN312395, MN312394, MN312393, MN312392, MN312391, MN312390, MN312389, MN312388, MN312387, MN312386, MN312385, MN312384, MN312383, MN312382, MN312381, MN312380, MN312379, MN312378, MN312377, MN312376, MN312375, MN312374, MN312373, MN312372, MN312371, MN312370, MN312369, MN312368, MN312367, MN312366, MN312365, MN312364, MN312363, MN312362, MN312361, MN312360, MN312359, MN312358, MN312356, MN312355, MN312354, MN312353, MN312352, MN312351, MN312350, MN312349, MN312348, MN312347, MN312346, MN312345, MN312344, MN312343, MN312341, MN312340, MN312339, MN312338, MN312337, MN312336, MN312335, MN312334, MN312333, MN312332, MN312331, MN312329, MN312328, MN312327, MN312326, MN312325, MN312324, MN312323, MN312322, MN312321, MN312320, MN312319, MN312318, MN312317, MN312316, MN312315, MN312314, MN312313, MN312312, MN312311, MN312310, MN312308, MN312307, MN312306, MN312305, MN312303, MN312302, MN312301, MN312300, MN312299, MN312298, MN312297, MN312296, MN312295, MN312294, MN312293, MN312292, MN312291, MN312290, MN312289, MN312287, MN312286, MN312285, MN312284, MN312283, MN312282, MN312281, MN312280, MN312279, MN312278, MN312277, MN312276, MN312275, MN312274, MN312273, MN312272, MN312271, MN312270, MN312269, MN312268, MN312267, MN312266, MN312265, MN312264, MN312263, MN312262, MN312261, MN312260, MN312259, MN312258, MN312257, MN312256, MN312255, MN312254, MN312253, MN312252, MN312251, MN312250, MN312249, MN312248, MN312247, MN312246, MN312245, MN312244, MN312243, MN312242, MN312241, MN312240, MK991951, MK991950, MK991949, MK991948, MK991947, MK991946, MK991945, MK991944, MK991943, MK991942, MK991941, MK991940, MK991939, MK991938, MK991937, MK991936, MK991935, MK991934, MK991933, MK991932, MK991931,

MK991930, MK991929, MK991928, MK991927, MK991926, MK991925, MK991924, MK991923, MK991922, MK991921, MK991920, MK991919, MK991918, MK991917, MK991916, MK991915, MK991914, MK991913, MK991912, MK991911, MK991910, MK991909, MK991908, MK991907, MK991906, MK991905, MK991904, MK991903, MK991902, MK991901, MH170151, MH170150, MH170149, MH170148, MH170147, MH170146, MH170145, MH170144, MH170143, MH170142, MH170141, MH170140, MH170139, MH170138, MH170137, MH170136, MH170135, MH170134, MH170133, MH170132, MH170131, MH170130, MH170129, MH170128, MH170127, MH170126, MH170125, MH170124, MH170123, MH170122, MH170121, MH170120, MH170119, MH170118, MH170117, MH170116, MH170115, MH170114, MH170113, MH170112, MH170111, MH170110, MH170109, MH170108, MH170107, MH170106, MH170105, MH170104, MH170103, MH170102, MH170101, MH170100, MH170099, MH170098, MH170097, MH170096, MH170095, MH170094, MH170093, MH170092, MH170091, MH170090, MH170089, MH170088, MH170087, MH170086, MH170085, MH170084, MH170083, MH170082, MH170081, MH170080, MH170079, MH170078, MH170077, MH170076, MH170075, MH170074, MG333999, MG333998, MG333997, MG333996, MG256474, MG256473, MG256472, MG256471, MG256470, MG256469, MG256468, MG256467, MG256466, MG256465, MG256464, MG256463, MG256462, MG256461, MG256460, MG256459, MG256458, MG256457, MG256456, MG256455, MG256454, MG256453, MG256452, MG256451, MG256450, MG256449, MG256448, MG256447, MG256446, MG256445, MG256444, lcl|MN823620, lcl|MN823619, lcl|MN823618, lcl|MN701039, lcl|MN701038, LC469047, LC469046, LC469045, LC469044, LC469043, LC469042, LC469041, LC469040, LC469039, LC469038, LC469037, LC469036, LC469035, LC469034, LC469033, LC469032, LC469031, LC469030, LC469029, LC469028, KY783903, KY783902, KY783901, KY783900, KY783899, KY783898, KY783897, KY783896, KY783895, KY783894, KY783893, KY783892, KY783891, KY783890, KY783889, KY783888, KY783887, KY783886, KY783885, KY783884, KY783883, KY783882, KY783881, KY783880, KY783879, KY783878, KY783877, KY783876, KY783875, KY783874, KY783873, KY783872, KY783871, KY783870, KY783869, KY783868, KY783867, KY783866, KY783865, KY783864, KY783863, KY783862, KY783861, KY783860, KY783859, KY783858, KY783857, KY783856, KY783855, KT894926, KT894925, KT894924, KT894923, KT894922, KT894921, KT368821, KT346250, KT346249, KT346248, KT346247, KT346246, KT346245, KT346244, KT346243, KT346242, KT346241, KT346240, KT346239, KT346238,

KT346237, KP876546, KP876545, KP876544, KP876543, KP876542, KP876541, KP876540, KP876539, KP876538, KP876537, KP876536, KP876535, KP876534, KP876533, KP876532, KP876531, KP876530, KP876529, KP876528, KP876527, KP876526, KP876525, KP876524, KP876523, KP876522, KP876521, KP876520, KP876519, KP876517, KP876516, KP876515, KP876514, KP876513, KP876512, KP876511, KP876510, KP876509, KP876508, KP876507, KP876506, KP876505, KJ868722, KJ868721, KJ652018, KC886322, KC886321, KC779226, KC779225, AY864196, AB890000, AB889999, AB889998, AB889997, AB889996, AB889995, AB683971, AB683970, AB539080

Bat related Helicase sequences:

MK720946, lcl|EF434378, lcl|EF434377, lcl|EF434376, lcl|DQ648789, lcl|DQ648788, lcl|DQ648787, lcl|DQ648786, lcl|DQ364567, lcl|DQ249249, lcl|DQ249247, lcl|DQ249246, lcl|DQ249244, lcl|DQ249243, lcl|DQ249242, lcl|DQ249241, lcl|DQ249240, lcl|DQ249239, lcl|DQ249238, lcl|DQ249237, lcl|DQ249236, FJ588687, DQ071615, Algeria/alpha

Human SARS-CoV-2

EPI_ISL_1000947, PI_ISL_1040650, EPI_ISL_1070637, EPI_ISL_1079162, PI_ISL_1081794, EPI_ISL_1081831, EPI_ISL_1086034, EPI_ISL_1093427, EPI_ISL_1093428, EPI_ISL_1093429, EPI_ISL_1093430, EPI_ISL_1240719, EPI_ISL_1240720, EPI_ISL_1240721, EPI_ISL_1240722, EPI_ISL_1240723, EPI_ISL_1240724, EPI_ISL_1240725, EPI_ISL_1253807, EPI_ISL_1253966, EPI_ISL_402123, EPI_ISL_403962, EPI_ISL_410546, EPI_ISL_412116, EPI_ISL_412972, EPI_ISL_413565, EPI_ISL_414630, EPI_ISL_415581, EPI_ISL_416411, EPI_ISL_416498, EPI_ISL_417010, EPI_ISL_417547, EPI_ISL_418241, EPI_ISL_418242, EPI_ISL_418243, EPI_ISL_419871, EPI_ISL_420037, EPI_ISL_420134, EPI_ISL_420314, EPI_ISL_424278, EPI_ISL_428671, EPI_ISL_431102, EPI_ISL_437689, EPI_ISL_437994, EPI_ISL_447653, EPI_ISL_449872, EPI_ISL_449933, EPI_ISL_451186, EPI_ISL_454416, EPI_ISL_455479, EPI_ISL_455918, EPI_ISL_458094, EPI_ISL_471159, EPI_ISL_471160, EPI_ISL_475023, EPI_ISL_476559, EPI_ISL_477142, EPI_ISL_480243, EPI_ISL_491247, EPI_ISL_512616, EPI_ISL_526223, EPI_ISL_527891, EPI_ISL_529008, EPI_ISL_613440, EPI_ISL_644681, EPI_ISL_645044, EPI_ISL_649064, EPI_ISL_672138,

EPI_ISL_676593, EPI_ISL_693597, EPI_ISL_699147, EPI_ISL_735422, EPI_ISL_759955, EPI_ISL_766861, EPI_ISL_766862, EPI_ISL_766863, EPI_ISL_766864, EPI_ISL_766865, EPI_ISL_766866, EPI_ISL_766867, EPI_ISL_766868, EPI_ISL_766869, EPI_ISL_766870, EPI_ISL_766871, EPI_ISL_766872, EPI_ISL_766873, EPI_ISL_766874, EPI_ISL_766875, EPI_ISL_794604, EPI_ISL_860556, EPI_ISL_940753, EPI_ISL_978540.

11. Publications

11.1. Publications related to the thesis topic

Zeghbib, S., Herczeg, R., Kemenesi, G., Zana, B., Kurucz, K., Urbán, P., Madai, M., Földes, F., Papp, H., Somogyi, B., & Jakab, F. (2019). Genetic characterization of a novel picornavirus in Algerian bats: Co-evolution analysis of bat-related picornaviruses. Scientific Reports, 9(1), 15706. https://doi.org/10.1038/s41598-019-52209-2

Zeghbib, S., Somogyi, B. A., Zana, B., Kemenesi, G., Herczeg, R., Derrar, F., & Jakab, F. (2021). The Algerian Chapter of SARS-CoV-2 Pandemic: An Evolutionary, Genetic, and Epidemiological Prospect. Viruses, 13(8), 1525. https://doi.org/10.3390/v13081525

11.2. Conferences related to thesis topic

Zeghbib S. Genetic and evolutionary characterization of a novel picornavirus in Algerian *Miniopterus schreibersii* bats *5th International Congress on Infectious Diseases* Berlin, Germany, March 01-02, 2018.

Zeghbib S. Facteurs climatiques et maladies virales – Rôle de la biologie moléculaire, *L'association FIKR pour la santé, l'Environnement et le Développement en Collaboration avec la Faculté des Sciences*, M'Sila, Algeria, April 28 2016.

11.3. Publications outside the thesis topic

Kemenesi, G., Tóth, G. E., Bajusz, D., Keserű, G. M., Terhes, G., Burián, K., **Zeghbib, S.**, Somogyi, B. A., & Jakab, F. (2021). Effect of An 84-bp Deletion of the Receptor-Binding Domain on the ACE2 Binding Affinity of the SARS-CoV-2 Spike Protein: An In Silico Analysis. Genes, 12(2), 194. https://doi.org/10.3390/genes12020194

Kemenesi, G., Tóth, G. E., Mayora-Neto, M., Scott, S., Temperton, N., Wright, E., Mühlberger, E., Hume, A. J., Zana, B., Boldogh, S. A., Görföl, T., Estók, P., Lanszki, Z., Somogyi, B. A., Nagy, Á., Pereszlényi, C. I., Dudás, G., Földes, F., Kurucz, K., Madai, M., **Zeghbib, S**., Maes, P., Vanmechelen, B., Jakab, F. (2021). Reservoir host studies of Lloviu virus: First isolation, sequencing and serology in Schreiber's bats in Europe [Preprint]. Microbiology. https://doi.org/10.1101/2021.08.10.455806

Kemenesi, G., **Zeghbib, S**., Somogyi, B. A., Tóth, G. E., Bányai, K., Solymosi, N., Szabo, P. M., Szabó, I., Bálint, Á., Urbán, P., Herczeg, R., Gyenesei, A., Nagy, Á., Pereszlényi, C. I., Babinszky, G. C., Dudás, G., Terhes, G., Zöldi, V., Lovas, R., … Jakab, F. (2020). Multiple SARS-CoV-2 Introductions Shaped the Early Outbreak in Central Eastern Europe: Comparing Hungarian Data

to a Worldwide Sequence Data-Matrix. Viruses, 12(12), E1401. https://doi.org/10.3390/v12121401

Konrat, R., Papp, H., Szijártó, V., Gesell, T., Nagy, G., Madai, M., **Zeghbib, S**., Kuczmog, A., Lanszki, Z., Helyes, Z., Kemenesi, G., Jakab, F., & Nagy, E. (2020). The Anti-histamine Azelastine, Identified by Computational Drug Repurposing, Inhibits SARS-CoV-2 Infection in Reconstituted Human Nasal Tissue In Vitro (p. 2020.09.15.296228). https://doi.org/10.1101/2020.09.15.296228

Lanszki, Z., Kurucz, K., **Zeghbib, S**., Kemenesi, G., Lanszki, J., & Jakab, F. (2020). Identification of Hepatitis E Virus in the Feces of Red Foxes (Vulpes vulpes). Animals : An Open Access Journal from MDPI, 10(10), 1841. https://doi.org/10.3390/ani10101841

Lanszki, Z., Zana, B., **Zeghbib, S**., Jakab, F., Szabó, N., & Kemenesi, G. (2021). Prolonged Infection of Canine Distemper Virus in a Mixed-Breed Dog. Veterinary Sciences, 8(4), 61. https://doi.org/10.3390/vetsci8040061

Papp, H., **Zeghbib, S**., Földes, F., Banfai, K., Madai, M., Kemenesi, G., Urbán, P., Kvell, K., & Jakab, F. (2020). Crimean-Congo hemorrhagic fever virus infection triggers the upregulation of the Wnt signaling pathway inhibitor genes. Virus Genes, 56(4), 508–514. https://doi.org/10.1007/s11262-020-01759-z

Zana, B., Kemenesi, G., Buzás, D., Csorba, G., Görföl, T., Khan, F. A. A., Tahir, N. F. D. A., **Zeghbib, S.**, Madai, M., Papp, H., Földes, F., Urbán, P., Herczeg, R., Tóth, G. E., & Jakab, F. (2019). Molecular Identification of a Novel Hantavirus in Malaysian Bronze Tube-Nosed Bats (Murina aenea). Viruses, 11(10), 887. https://doi.org/10.3390/v11100887

11.4. Conferences outside the thesis topic

Zana B, Kemenesi G, Urbán P, Kurucs K, Földes F, **Zeghbib S**, Oldal M, Jakab F. A nuygati mézelö méhekre (Apis mellifera) veszélyt jelentö vírusok jelenlétének kimutatása hazai denevér guano minták metagenomikai elemzése során *Magyar Mikrobiológiai Társaság 2016. évi Nagygyülése,* Keszthely 2016.Október 19-21.